CASE FILE
COPY

PHYSICAL AND DYNAMICAL STUDIES OF METEORS

by Richard B. Southworth and Zdenek Sekanina

1. Report No. NASA CR-2316	2. Government Accession No.	3. Recipient's Catalog No.
4. Title and Subtitle PHYSICAL AND DYNAMICAL STUDIES OF METEORS		5. Report Date October 1973
		6. Performing Organization Code
7. Author(s) Richard B. Southworth and Zdenek Sekanina		8. Performing Organization Report No.
9. Performing Organization Name and Address Smithsonian Institution Astrophysical Observatory Cambridge, Massachusetts 02138		10. Work Unit No. 188-45-52-03
		11. Contract or Grant No. NAS1-11204
12. Sponsoring Agency Name and Address National Aeronautics and Space Administration Washington, DC 20546		13. Type of Report and Period Covered Contractor Report
		14. Sponsoring Agency Code

15. Supplementary Notes
This is a topical report.

16. Abstract

    Interplanetary distributions from a sample of 20,000 radar meteor observations are presented. These distributions are freed from all known selection effects with the exception of a possible bias against fragmenting meteors which has not yet been adequately assessed. These data thus represent the largest and most accurate collection of radar meteor distributions. Both general average distribution and the distribution of meteor streams with their comet and asteroid associations are presented. Sporadic space density and space density of meteor streams are presented.

17. Key Words (Suggested by Author(s)) meteor; radar observation; distributions; selection effects; space density; fragmentation; meteor streams; luminosity; recombination; diffusion; meteor masses; orbital parameters; simultaneous observation; image orthicon	18. Distribution Statement Unclassified - Unlimited

19. Security Classif. (of this report) Unclassified	20. Security Classif. (of this page) Unclassified	21. No. of Pages 108	22. Price* Domestic, $4.25 Foreign, $6.75

*For sale by the National Technical Information Service, Springfield, Virginia 22151

TABLE OF CONTENTS

PHYSICAL AND DYNAMICAL STUDIES OF METEORS

Special Progress Report

1. SUMMARY

1.1 Aims

This research focused on the interplanetary distribution of radar meteors, freed from observational bias. We sought both the general average distribution and the distribution of meteor streams with their comet and asteroid associations.

1.2 Data

The Havana, Illinois, "synoptic-year" radar observations and the Havana-Sidell simultaneous radar-television observations constituted the data. In addition to being the largest and most accurate collection, these data have two unique and crucial advantages:

A. There is an adequate sample of very slow meteors, which recombination has eliminated from all other surveys.

B. There is a reliable calibration of the meteor masses.

The only known selection effect not yet adequately assessed is a possible bias against fragmenting meteors.

1.3 Orbital Distribution

Low-velocity meteors predominate; the velocity mode in the atmosphere is under 15 km sec^{-1}, and the mode in space at 1 a.u. from the sun is under 20 km sec^{-1}. Radiants cluster to the sunward and antisun directions. Moderate eccentricities and low inclinations predominate; retrograde orbits are very rare.

1.4 Space Density

We extrapolated the orbital distribution observed at the earth to include unobservable orbits and used the resultant value to correct the space density of observed orbits. The result is meaningful between about 0.4 and 2.0 a.u., and uncertain but suggestive farther away. Meteors are concentrated to a relatively thin layer centered on the ecliptic plane. In that plane, there is a minimum of density at about 0.7 a.u., and a maximum beyond 2 a.u.

1.5 Collisions

If this space-density distribution is in equilibrium, then most meteors must end their lives in collisions with each other. Moreover, a simplified theoretical model incorporating collisions and the Poynting-Robertson effect agrees with observation. Nonetheless, collisions need further study.

1.6 Streams

With the use of the most powerful stream-search technique in existence, we found 200 new streams in the synoptic-year data and confirmed the existence of two-thirds of the 83 streams detected previously in the 1961−1965 sample of radio meteors. Some of the new streams have most uncommon orbits. A new, rich stream with a revolution period of more than 30 years has been discovered. Streams of low inclination are often detected at both nodes.

1.7 Associations with Comets and Asteroids

A number of known comet−meteor associations are confirmed, and a few new possible associations detected. The previously detected associations with the minor planet Adonis are strongly reinforced (including a major, broad stream), and several possible associations with other asteroids, meteorite Príbram, and a Prairie Network fireball are suggested.

1.8 Height-Velocity Diagram

Plots of both the individual radio meteors and the radio streams fail to exhibit the discrete-level structure known to exist for photographic meteors. Some features of the height-velocity diagram are, however, detected.

1.9 Space Density in Streams

The mean space density in streams is much below the sporadic density, but the central density may significantly exceed the sporadic density. The absolute stream-density values based on the statistical model of meteor streams and on the sporadic density estimated in this report are in an order-of-magnitude agreement with densities estimated from the cometary production rates of solid material.

2. INTRODUCTION

The Radio Meteor Project, initiated at Harvard College Observatory under the direction of Professor Fred L. Whipple, and transferred to the Smithsonian Astrophysical Observatory (SAO) in 1966, constitutes part of a broad program of meteor and meteorite research at the two observatories. Under NASA support via contract NSR 09-015-033, the project included research activities in Cambridge, Massachusetts, and data collection by an eight-station radar system near Havana, Illinois, and by an image-orthicon system at Sidell, Illinois.

Research under the current contract NAS 1-11204 is directed toward distributions of radar meteor orbits in interplanetary space. The specific tasks are the following:

A. Use of the radar/image-orthicon data to improve assessment of radar observational biases.

B. Determination of meteor orbital distributions from the synoptic-year sample, including corrections for observational biases.

C. Determination of orbital parameters of meteor streams and the density distribution of meteors in the streams.

D. Investigation of associations of meteor streams with comets and with asteroids.

This report contains results for each task and also unanticipated results on the space density of meteors and on collisions between meteors.

3. OBSERVATIONS

3.1 Radar Meteors

Multistation radar observations of meteors contain the bulk of the orbital data on meteors, nearly equaling photographic observations in accuracy while far outnumbering them. (Reliable visual or satellite orbits are still rare.) The Havana system, with more receivers and greater sensitivity than any other, acquired the largest and most reliable collection of radar meteor data. We are here directly concerned with the orbital data but must make extensive use of the data on the meteor's interaction with the atmosphere to evaluate selection effects.

3.2 Synoptic Year

The primary data used for this report are the radar meteor observations collected in Havana, Illinois, during the period known as the synoptic year. The equipment and observations are described in the Final Report of contract NSR 09-015-033.

The Havana facility was extensively refurbished in 1967 and 1968: Measurements were made of the antenna radiation patterns, and equipment was installed to calibrate transmitted and received signals. The synoptic year comprises nearly uniform coverage of all hours and alternate weeks from December 1968 to December 1969, with the Havana system in its best condition.

A satisfactory observation made with the Havana system yields the meteor's radiant, velocity, and deceleration; the location of its trajectory in the atmosphere and the distribution of electrons along the trajectory; electron-diffusion rates in the atmosphere; atmospheric-wind components; and, possibly, electron recombination rates or indications of meteor fragmentation. The meteor's orbit around the sun is deduced from the radiant and the velocity, and its mass, from the velocity and the electron distribution. The computer facilities at Langley Research Center reduced the observations.

3.3 Simultaneous Radar-Television Observations

Beginning in 1969, an image-orthicon system on loan from U.S. Naval Research Laboratory was sited at Sidell, Illinois, to observe optically some of the same meteors observed by radar from Havana. These observations are described in the Final Report of contract NSR 09-015-033, and also by Cook et al. (1972). Because we were able to use the much better known masses of optical meteors, these simultaneous observations are the best data for calibration of the masses of the radar meteors.

4. SELECTION EFFECTS

4.1 Radar Biases

The meteors we observe on radar are not, we know, a random sample of the influx to the earth; corrections for the many biases have occupied meteor astronomers for years. We have lately made several advances, large and small, in measuring these biases. All the corrections used are described in the present section.

4.2 Observational Geometry

Elford (1964) determined the probability that the Havana radar would observe a meteor as a function of radiant altitude and azimuth. His table of the response function of the six stations transmitting on the double trough and receiving on a single trough at site 3 and a double trough at other sites was not included in his 1964 report but is very similar to the tables that were. We have corrected it for the subsequent antenna calibration, as follows. The important differences between the measured antenna pattern and the design pattern that Elford used are a 6° decrease in elevation of the main beam and an increase in sidelobe sensitivity, in the measured pattern. Since sidelobe meteors are routinely rejected from the reductions, they are not considered here. We first revised Elford's radiant-sensitivity contours to delete his assumption that the electron line density is proportional to $\cos Z_R$, where Z_R is the radiant zenith distance. Next, we rotated the contours by 6° so as to center them on the measured main beam. Then we restored a proportionality between electron line density and $(\cos Z_R)^{0.75}$, which is more nearly correct for fragmenting meteors.

The weight given each meteor as a function of radiant azimuth and altitude is the reciprocal of the revised radiant sensitivity, except that radiants with sensitivities less than 10% of the maximum are omitted altogether. A further weight was then applied as a function of radiant declination; this is inversely proportional to the range of right ascension within the 10% contour. Since observations were uniformly distributed over the day, all radiants observable from Havana are now equitably represented.

4.3 Ionizing Probability

Cook et al.'s (1972) ionizing probability, derived from the simultaneous radar-television observations at Havana and Sidell, is adopted here.

Future analysis of more of the simultaneous observations may revise the ionizing probability for fast meteors, which has perforce been extrapolated from lower velocities. Such an analysis could not, however, remove the predominance of low-velocity meteors.

4.4 Diffusion

The upper bound to meteor heights observed at Havana is set by ambipolar diffusion of the ionized column (Southworth, 1973). Thus, some of the faster meteors escape observation because they are too high. Figure 4-1 shows the distribution in height for various velocity groups among 11,061 meteors from the synoptic year; it is evident that the distributions are truncated at the right for velocities above roughly 40 km sec^{-1}. Fitting a mean height distribution to the left sides of these truncated distributions, we found the fraction of meteors missed; we then derived the following empirical correction formula. Meteors with velocities v over 34 km sec^{-1} have their weights multiplied by the additional factor

$$W_D = \exp [6.56 \,(\log_{10} v - 1.53)^2] \quad . \tag{4-1}$$

This correction reaches its maximum $W_D = 2.1$ at $v = 72$.

4.5 Initial Radius

Although the initial radius of the electron column (actually the radius reached in a few milliseconds) has appeared significant to several observers of relatively bright radar meteors, it does not seem important to the synoptic-year observations (Southworth, 1973). We propose that the radii measured with two-frequency or three-frequency radars (Baggaley, 1970; Moisya et al., 1970; Kolomiets, 1971) should be understood as resulting from a combination of three processes: (1) diffusion of individual ions and electrons into the undisturbed atmosphere, as treated theoretically
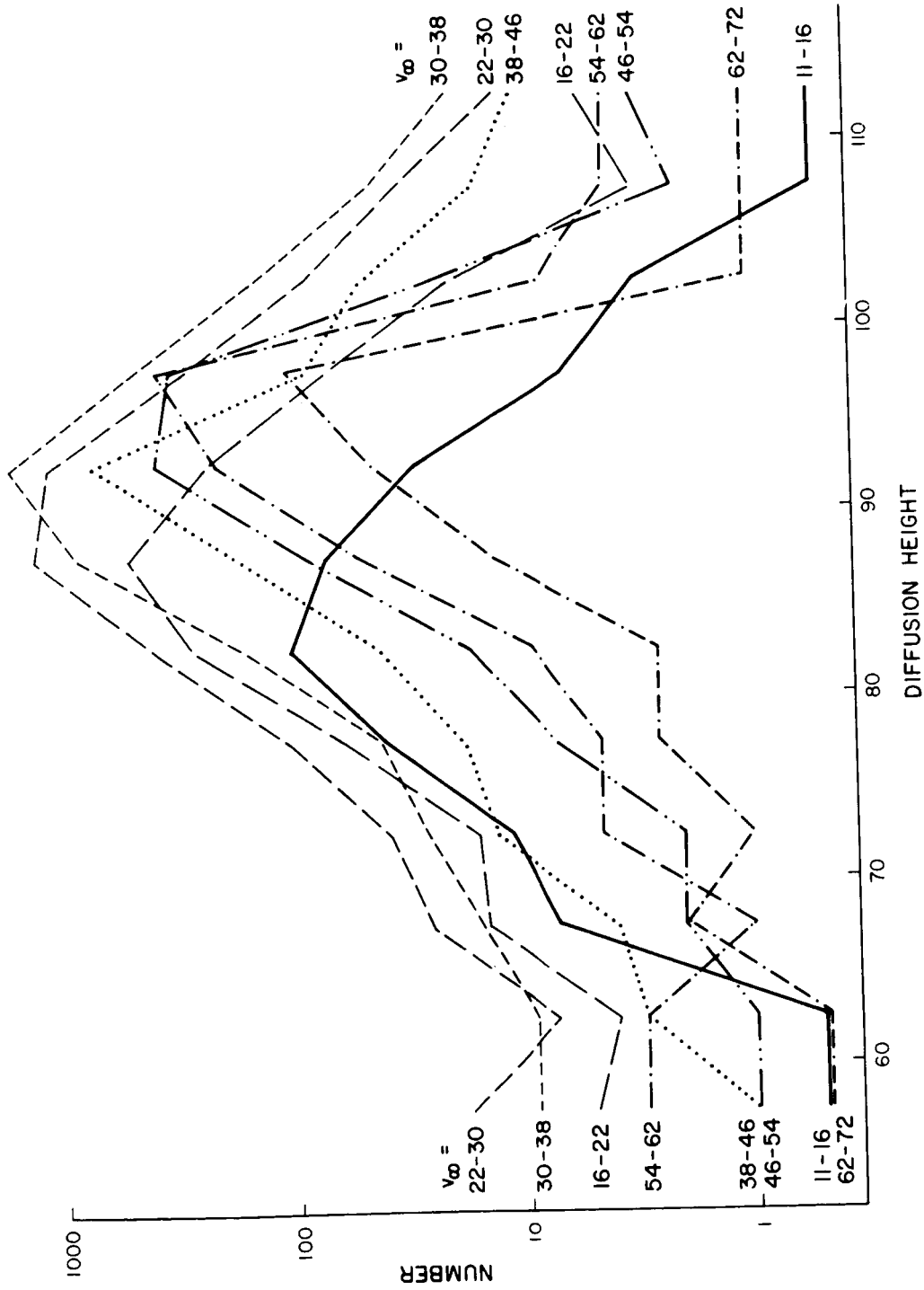
Figure 4-1. Distributions of diffusion heights at maximum ionization for 11, 061 meteors, divided into intervals of no-atmosphere velocity.

11

by Manning (1958) and Öpik (1955); (2) expansion of a hot cloud of neutral gas; and (3) lateral spread of fragments of the original meteoroid. Only the first of these has usually been considered, but the Havana-Sidell observations appear to show that (3) is quite significant for some meteors. Baggaley's conclusion that initial radius is proportional to the 0.5 power of atmospheric mean free path is inexplicable by use of (1) alone, but easily understood as (2) or as a combination of (1) and (3) or of (1), (2), and (3). For an order-of-magnitude estimate of (2), we compute the radius r_c of the cylinder in the atmosphere that contains the same amount of heat energy as the energy deposited in the atmosphere by the meteors. We find

$$r_c^2 \approx 6 \times 10^{-14} \frac{mv^2}{\rho t} \quad , \tag{4-2}$$

where m and v are the meteor's mass and velocity, respectively; ρ and t are atmospheric density and temperature, respectively; and all units are cgs. At 100-km height and 60 km sec^{-1}, the brightest synoptic-year meteors ($\sim 10^{10}$ elec cm^{-1}, mass $\sim 10^{-5}$ g at 60 km sec^{-1}) have $r_c \approx 14$ cm, which is negligible at the Havana wavelength (733 cm). However, at the transition between underdense and overdense trials (line density $\sim 10^{12}$ elec cm^{-1}), a meteor of the same height and velocity would have $r_c \approx 140$ cm and an echo attenuation

$$A \approx \exp\left[-8\pi^2\left(\frac{140}{733}\right)^2\right] = 0.06 \quad , \tag{4-3}$$

which is a severe observational bias. It is probable that process (2) has been neglected heretofore because ionizing efficiencies were believed to be higher, and masses correspondingly lower.

In view of the foregoing, we do not believe that the initial radius biases the synoptic-year data, except perhaps as the effect of fragmentation, which is separately discussed. No correction was applied.

4.6 Recombination

Southworth (1973) showed that recombination is an important limitation to surveys using less-sensitive equipment. For the synoptic year, however, recombination can

be expected to affect only the lowest bright meteors observed, and then not to attenuate them beyond observability. An empirical check comparing the height distributions for different ranges of radar magnitude showed no apparent effects of recombination. No correction was applied.

Future studies that treat individual masses will need recombination corrections to electron line densities and therefore to masses on at least some meteors. However, as explained in Sections 4.8 and 5.1, the electron line densities do not enter the weights in this report.

4.7 Fragmentation

The Havana-Sidell simultaneous observations (Cook et al., 1972) appear to show that fragmentation is sometimes associated with severe attenuations of radar echo strength. This can be easily understood as the effect of lateral spread of the particles from the mean trajectory. Simple theory leads to the expectation that the effect is most important for slow meteors, and photographic meteor studies lead to the expectation that it is important for some showers. However, there is as yet no radar analysis evaluating its importance, and no corrections have been applied.

The possible underrepresentation of fragmenting meteors is the only significant bias that we suspect to remain in the results reported here.

4.8 Mass Distribution

Although we have observed meteors covering a range of more than 10^3 in electron line density, the steep dependence of ionizing probability on velocity ensures a strong negative correlation between mass and velocity in the synoptic-year meteors. As it is not possible to select an unbiased sample from among these, we have assigned to each meteor a weight representing the number of meteors of some standard mass. This procedure implicitly assumes that the mass distribution is independent of orbital parameters over the range of masses observed at any one velocity, and we have not noticed any counterexamples in our data. Our data are not sufficient to show whether the orbital distribution is independent of mass over the whole range of masses observed.

13

However, we expect that there is some dependence of orbital distribution on mass, and our results necessarily refer to the orbital characteristics of masses that are larger at low velocity than they are at high.

On the assumption that orbital elements are independent of mass, a small mass is as good a sample of orbital elements as is a large one. Since, as just explained, we make this assumption for all meteors of the same velocity, we are also taking advantage of it to equalize, for all meteors of the same velocity, that part of the statistical weight that depends on mass. This amounts to omitting the observed total number of electrons from the weights. It has appreciably smoothed the final distributions.

We have adopted Whipple's (1967) mass distribution, specifically that the number of particles with mass $\geq m$ is

$$n = \text{constant } (m)^{-1.36} \quad . \tag{4-4}$$

The corresponding factor in the statistical weights to reduce counts to observations at equal masses is

$$f = \beta^{-1.36} \quad , \tag{4-5}$$

where β is the ionizing probability. There is certainly a suggestion in Whipple's collection of data that the slope is lower for our smaller masses. Adopting an exponent of -1.0 for masses below 10^{-5} g would increase the relative abundance of high-velocity orbits in our distributions by a factor ~ 3, but would still leave them numerically unimportant. Since the ionizing efficiency for high velocities also remains uncertain, we have not made this adjustment.

5. ORBITAL DISTRIBUTIONS

5.1 Synoptic-Year Sample

This section presents tables and graphs of the velocities, radiants, and orbits of meteors observed in the synoptic year. All graphs and tables are in three forms: (1) unweighted, (2) reduced to equal masses in the atmosphere, and (3) reduced to equal masses in space at the earth's distance from the sun. We use three forms to facilitate comparison with the great variety of other published forms. Observations from earth satellites should be compared with the second form; and observations not restricted to the ecliptic (e.g., comets), with the third form.

The tape of reduced observations contains 19,698 meteors. We omit 505 with slant ranges over 400 km because such observations are much more likely than others to be confused by wind shears or plasma resonance. Accordingly, the unweighted sample is 19,193. For the sample reduced to equal masses in the atmosphere, we omit a further 4973, which were observed outside the main lobe of the antenna pattern and which would therefore introduce large statistical noise in the results if they were given the very large and uncertain weights nominally belonging to them. Thus the atmospheric sample is 14,220. For the sample reduced to equal masses in space at 1 a.u., we omit 1622 more meteors with radiant latitudes south of the ecliptic, since we cannot get a complete sample of all southern radiants. This leaves 12,598 in the space sample.

Because we assume that in our observational dynamic range the orbital parameters are relatively independent of electron line density, the weights do not include the integrated number of electrons observed, although they do include all other mass factors; this procedure has appreciably reduced statistical noise in the results. Since the equipment parameters were nearly constant over the synoptic year, there are no corrections dependent on date of observation. All other corrections described in Section 4 are included. The space sample includes corrections for the collision probability with the earth.

15

5.2 Velocity

Figure 5-1 shows the distribution of no-atmosphere velocities: dotted lines for the unweighted sample, dashed for the atmospheric sample, and solid for the space sample. By comparison with distributions observed on less-sensitive equipment (e.g., the earlier Havana data; Hawkins, 1963), there is a considerable enhancement in the frequency of velocities under 30 km sec^{-1}. Moreover, velocities down to 11 km sec^{-1} are observed, whereas earlier surveys barely reached 15 km sec^{-1}. Recombination caused the bias against slow meteors on less-sensitive equipment (Southworth, 1973).

Corrected for ionizing efficiency and reduced to equal masses, the velocity distribution in the atmospheric sample shows the greatest concentration toward low velocities of any published distribution known to us. The mean is approximately 14.5 km sec^{-1}. However, the space sample shows that these very low velocities are less common outside the earth's gravitational field.

5.3 Radiants

Figures 5-2, 5-3, and 5-4 show the distribution of radiants with respect to celestial latitude β_R and longitude measured from the sun $\lambda_R - \lambda_\odot$ in the form of computer tabulations with superposed contours. The unweighted sample exhibits familiar features: concentration of most of the radiants to a broad band about the apex containing the "toroidal," "sun," and "antisun" clusters, and a relatively small cluster at the apex itself.

The atmospheric sample, even though smoothed, is comparatively noisy because of the high weights given a few slow meteors. Nonetheless, one sees that the sun and antisun clusters remain significant but that the remainder are more generally spread over the sky.

In the space sample, the sun and antisun clusters have split into northern and southern divisions, of which only the northern divisions can be reliably observed at Havana. The total distribution now consists of two broad concentrations, which

16
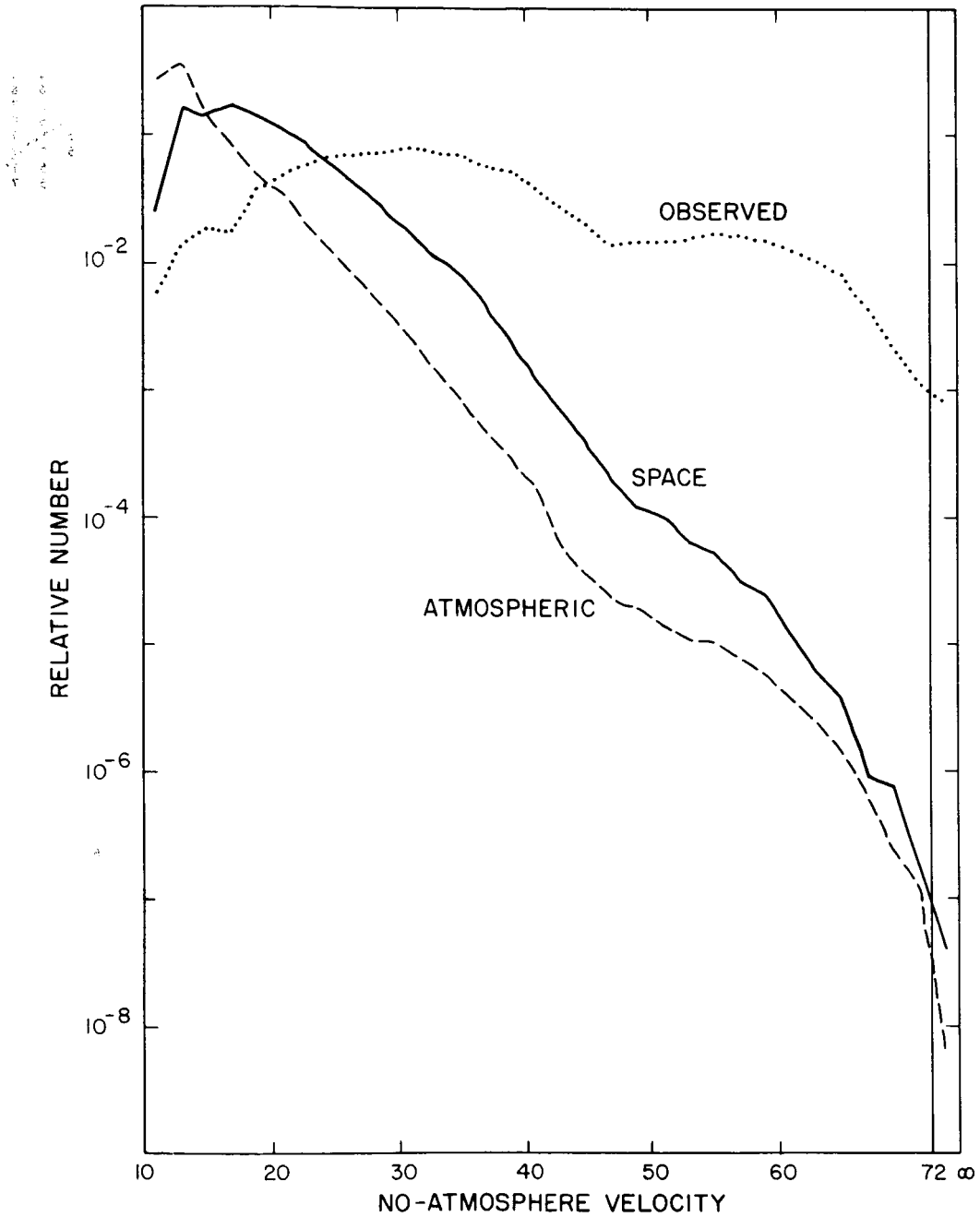
Figure 5-1. Distribution of no-atmosphere velocities. The plotted numbers are fractions of the samples within a 2-km sec^{-1} interval in velocity, or the fraction over 72 km sec^{-1}. The observed, atmospheric, and space samples are explained in the text.

17
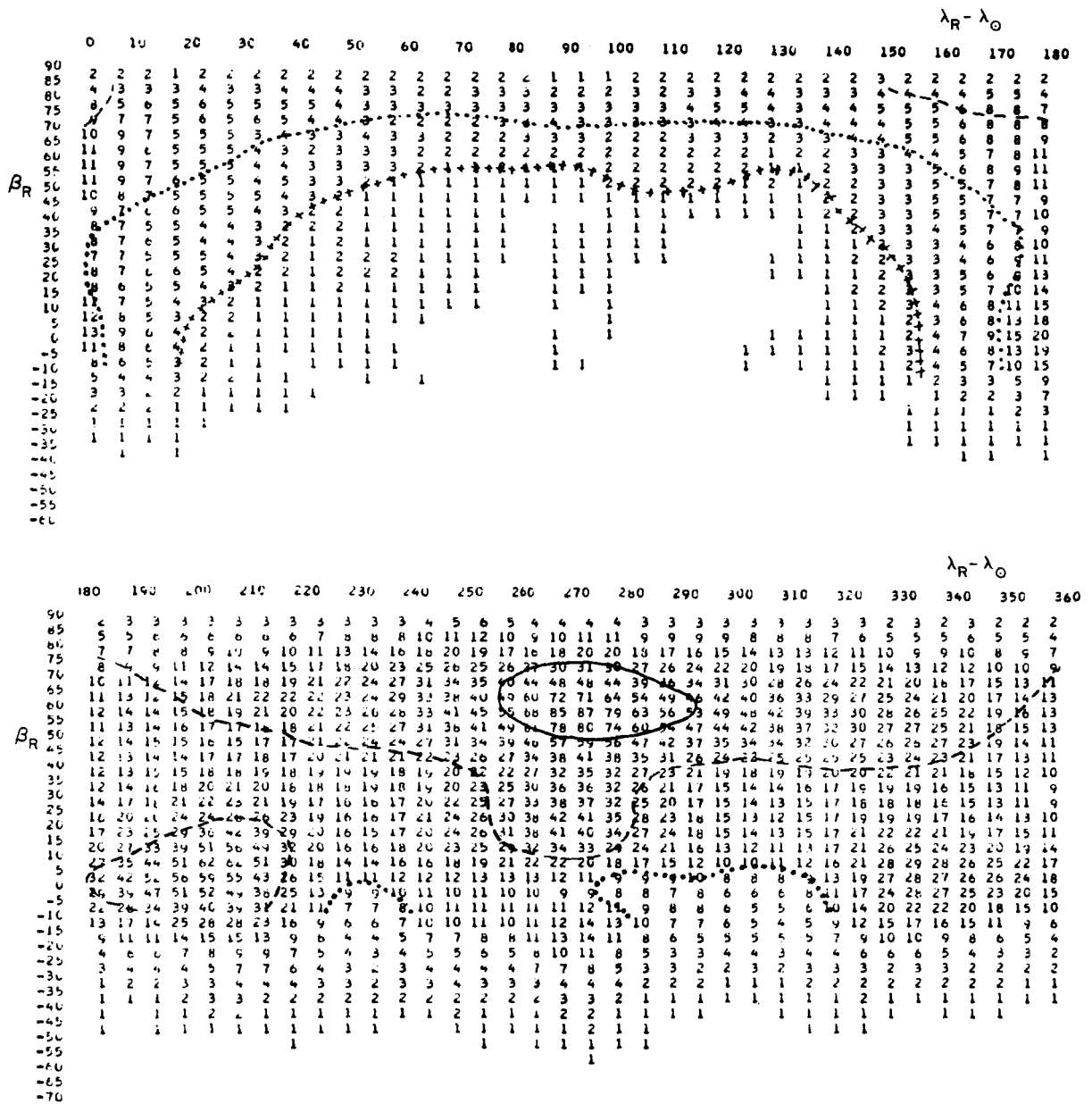
Figure 5-2. Distribution of observed radiants in latitude and longitude from the sun. The tabulated figures are the observed number within cells extending 5° in latitude and longitude, smoothed by averaging blocks of nine adjacent cells. The radiant density per square degree in a cell is equal to 0.04 sec β multiplied by the tabulated number. Contours have been drawn at 4.0 radiants per square degree (solid line), 1.2 (dashed), 0.4 (dotted), and 0.12 (crosses). Contours were not drawn in southern latitudes, where the sample is obviously incomplete. The average density of observed radiants north of the ecliptic is 0.79 per square degree.

Figure 5-3. Distribution of radiants from the atmospheric sample, as in Figure 5-2. The weights have not been normalized, so that the contours represent only relative radiant densities. On the same scale, the average radiant density north of the ecliptic is 1.40 per square degree. A few very high-weighted radiants have made this a rough distribution in spite of the smoothing. The obvious rectangular blocks of nine adjacent figures larger than their neighbors each represent one high-weighted radiant.

peak in these clusters. Moreover, the clusters have shifted away from the apex, and the relative numbers in the apex and antapex hemispheres are more nearly equal than any previously reported.

$\lambda_R - \lambda_O$

	0	10	20	30	40	50	60	70	80	90	100	110	120	130	140	150	160	170	180
90	4	2	2		1	2	2	2	1	1	1	1	1		1	1			
85											1	1			10	10	10	3	3
80	6	3	7	6	7	4	5	6	5	4	2	2	1	1	1	12	14	15	7
75	17	10	16	15	18	12	14	15	14	13	8	3	2	2	3	8	18	22	21
70	25	24	28	28	26	25	19	16	11	6	5	4	3	3	6	6	18	18	20
65	65	52	46	31	33	41	41	22	21	24	21	6	5	4	3	7	7	25	26
60	95	75	61	34	29	49	46	47	19	22	24	21	9	13	9	2	3	7	19
55	107	95	78	50	47	60	65	71	39	29	23	23	13	8	12	13	3	3	12
50	88	81	60	70	65	78	57	62	39	27	12	8	4	10	12	12	3	2	10
45	99	94	85	93	98	83	73	63	45	23	20	16	10	5	5	7	4	2	1
40	85	101	106	127	107	106	70	56	23	22	25	22	8	9	9	9	1		8
35	83	100	115	135	119	102	95	59	30	29	24	23	10	25	25	25	1	1	
30	136	149	131	143	125	135	75	68	28	38	20	19	2	24	27	27	4	1	1
25	152	137	116	131	175	165	45	45	26	44	27	36	17	32	25	21	4	1	1
20	181	185	167	152	176	160	113	53	29	37	34	45	21	16	9	5	5	2	1
15	118	128	137	129	141	113	86	26	18	86	30	43	27	21	11	1	1	1	1
10	116	121	121	92	73	52	52	23	18	11	15	19	18	12	7	1	1	1	1
5	100	86	71	38	33	31	49	9	3	8	7	10	10	10	5		1	1	1
0	61	50	38	18	22	24	18	5	3	4	4	6	5	5				1	1

$\lambda_R - \lambda_O$

	180	190	200	210	220	230	240	250	260	270	280	290	300	310	320	330	340	350	360
90	2	2	3	3	3	3	4	4	2	1	2	2	2		1	1	2	2	1
85	9	8	8	9	5	6	10	11	10	4	4	4	4	2	2	2	3	3	8
80	16	15	16	17	14	15	31	31	26	8	11	13	14	10	8	6	4	4	5
75	26	22	41	44	27	30	45	68	59	38	21	24	24	16	11	9	6	5	4
70	44	59	60	62	56	51	62	75	62	44	28	30	32	25	18	14	8	6	5
65	64	87	82	103	89	85	64	72	60	56	27	27	30	28	21	16	9	8	
60	99	98	96	98	110	97	73	56	42	38	36	23	23	28	26	19	6	9	
55	106	121	120	111	106	92	59	30	39	47	45	32	26	30	28	20	8	6	16
50	123	127	115	78	79	66	47	20	31	61	63	51	26	30	28	20		4	14
45	158	134	89	76	75	65	44	40	42	62	55	51	29	29	26	18	2		7
40	172	159	127	123	99	73	86	77	63	56	49	42	29	26	23	15		8	3
35	198	211	185	177	105	110	134	125	101	74	62	36	23	21	13		6	3	3
30	203	232	222	220	11	51	18	138	117	110	83	98	63	36	20	17	9	7	2
25	246	236	206	167	123	150	130	104	97	104	67	38	20	11	8	3	15	42	43
20	245	203	177	149	162	180	166	128	108	72	73	42	29	22	11	8	3	3	5
15	199	184	163	154	164	171	161	132	69	71	51	41	30	23	13	6	2	2	4
10	139	132	137	127	127	123	126	107	62	45	34	20	17	14	11	4	1	1	3
5																			
0	70	72	82	74	44	38	32	27	25	17	11	9	11	7	6				

Figure 5-4. Distribution of radiants from the space sample, as in Figures 5-2 and 5-3. On the scale of weights used, the average radiant density north of the ecliptic is 2.86 per square degree. The smoothing process has artificially lowered the bottom line of tabulated densities by one-third, but a real decrease also occurs at low latitudes.

5.4 Orbital Elements

Figures 5-5 to 5-10 show the distributions of the elements a, 1/a, e, q, q', and i. The observed sample differs from previous observations primarily in the added importance of low-velocity meteors, which perforce have orbits with low to moderate eccentricity, low to moderate inclinations, and perihelia and aphelia not far from the earth's orbit.
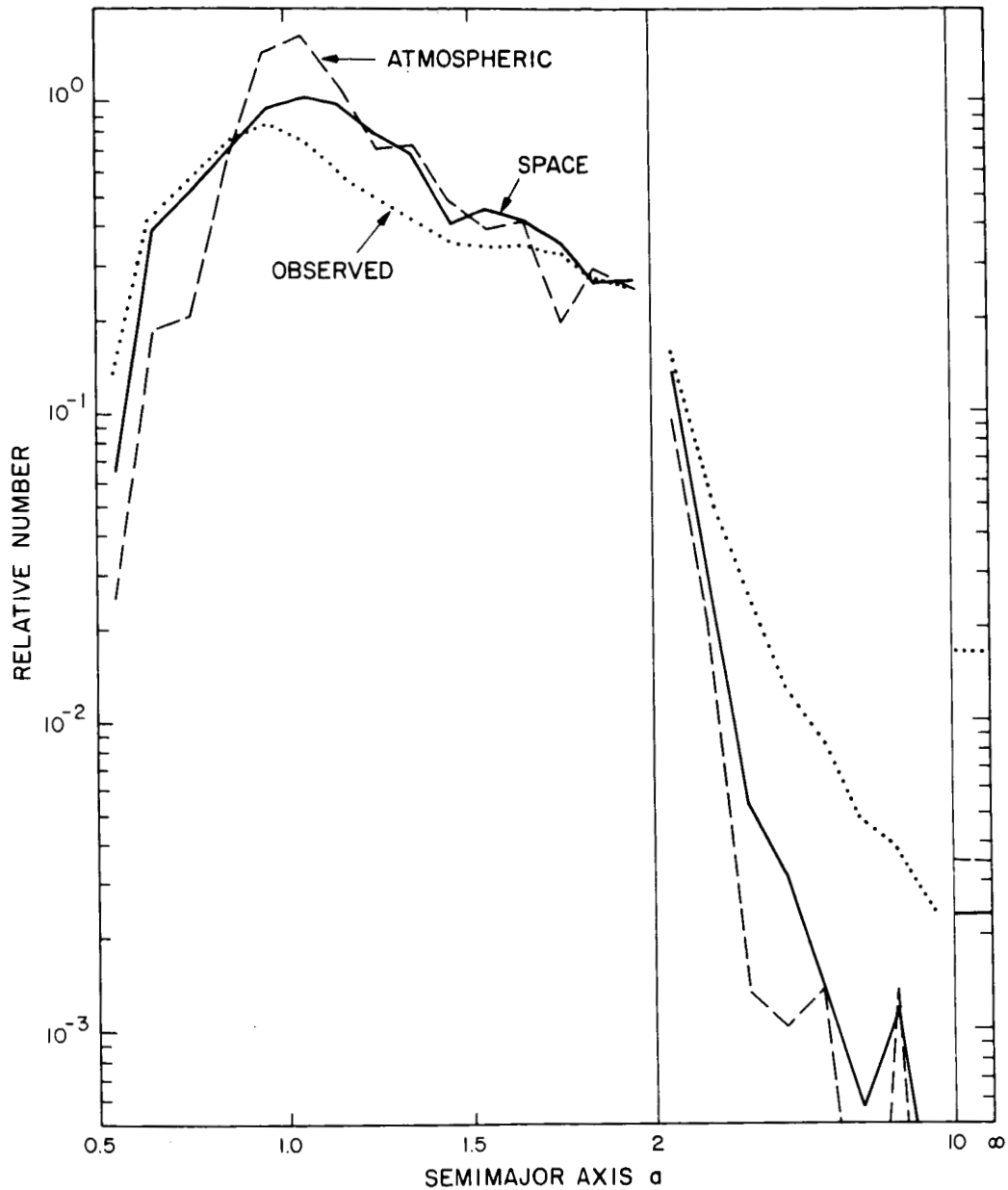
Figure 5-5. Distribution of semimajor axes a. The scale on the abscissa has been broken to permit showing details near 1 a.u. The plotted numbers are fractions of the samples per 1-a.u. interval of semimajor axis, or the fraction greater than 10 a.u.
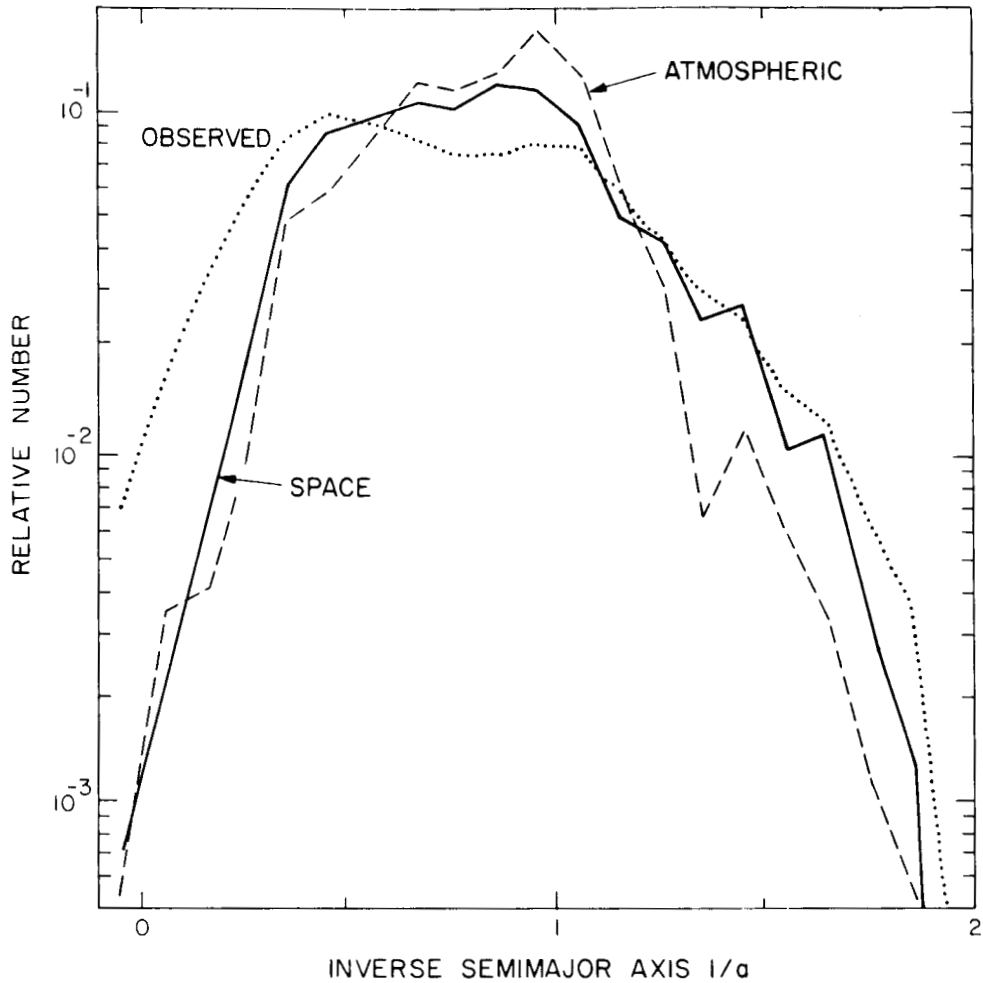
Figure 5-6. Distribution of inverse semimajor axes 1/a. The plotted numbers are the fractions of the samples within intervals of 0.1 in 1/a.

The atmospheric sample is dominated by near-circular or moderately eccentric orbits of low inclination. Other types are numerically insignificant.

The space-sample inclinations are also low, but the peak of the distribution is near 7° rather than 0°. Eccentricities, however, peak near 0.5. These are in harmony, as they must be, with the radiant distribution and with a predominance of low geocentric velocities directed approximately radially to and from the sun. The general trend of the distribution of perihelion distance is a necessary consequence of observation at the earth and of a broad spread of eccentricities. However, a rise above the trend near 0.2 and a dip below 0.1 may be indicative, respectively, of the perihelion of some significant source of the particles, or of particle removal by solar heating, or of both.

The general trend of the distribution of aphelion is also a consequence of observation at the earth, but a modest rise above the trend in the asteroid belt is very probably significant for the origin of many of these meteors (Section 7 has other evidence on the origin).
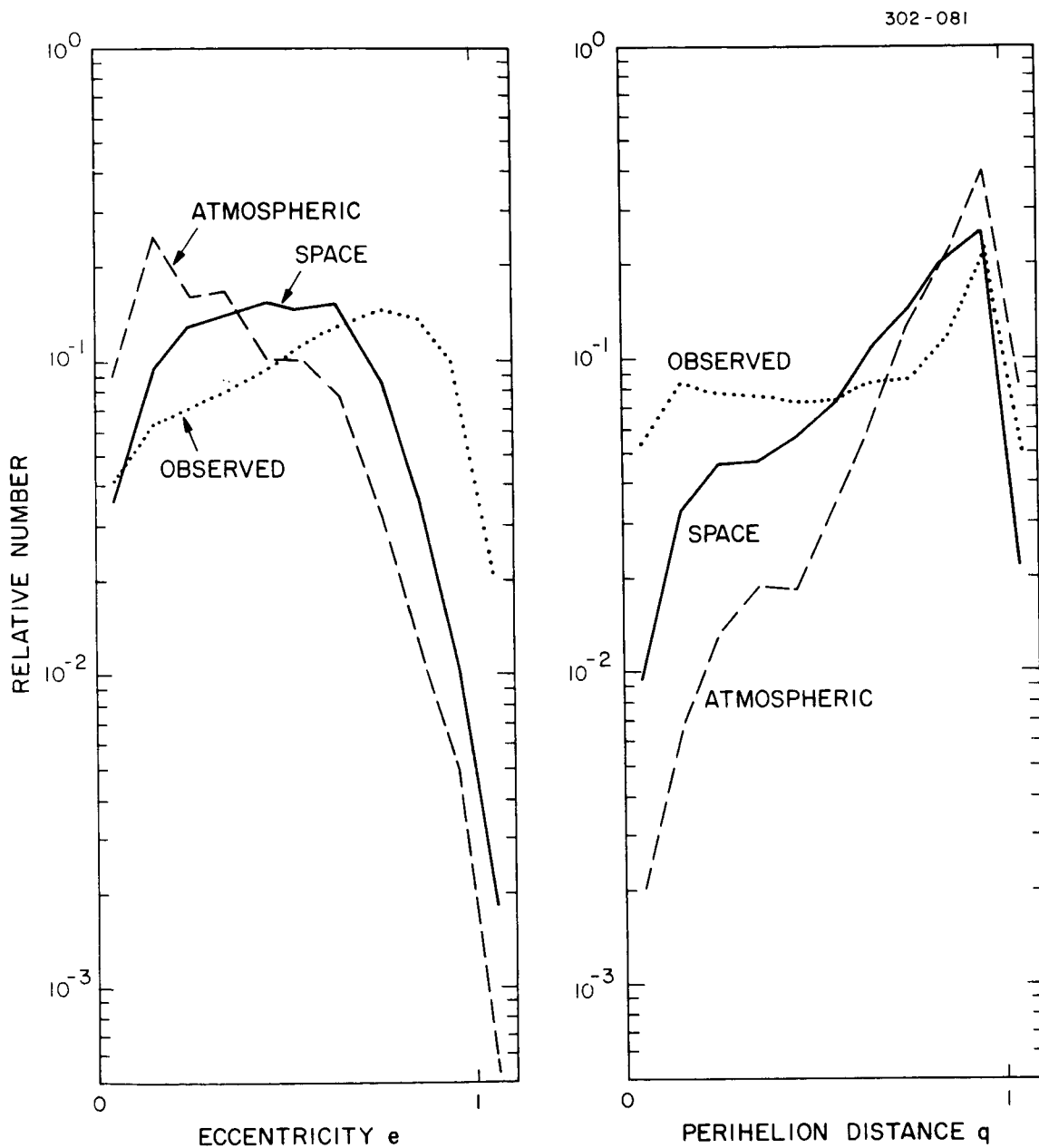
Figures 5-7 and 5-8. Distributions of eccentricity e and perihelion distance q. The plotted numbers are the fractions of the samples within intervals of 0.1 in e or q.
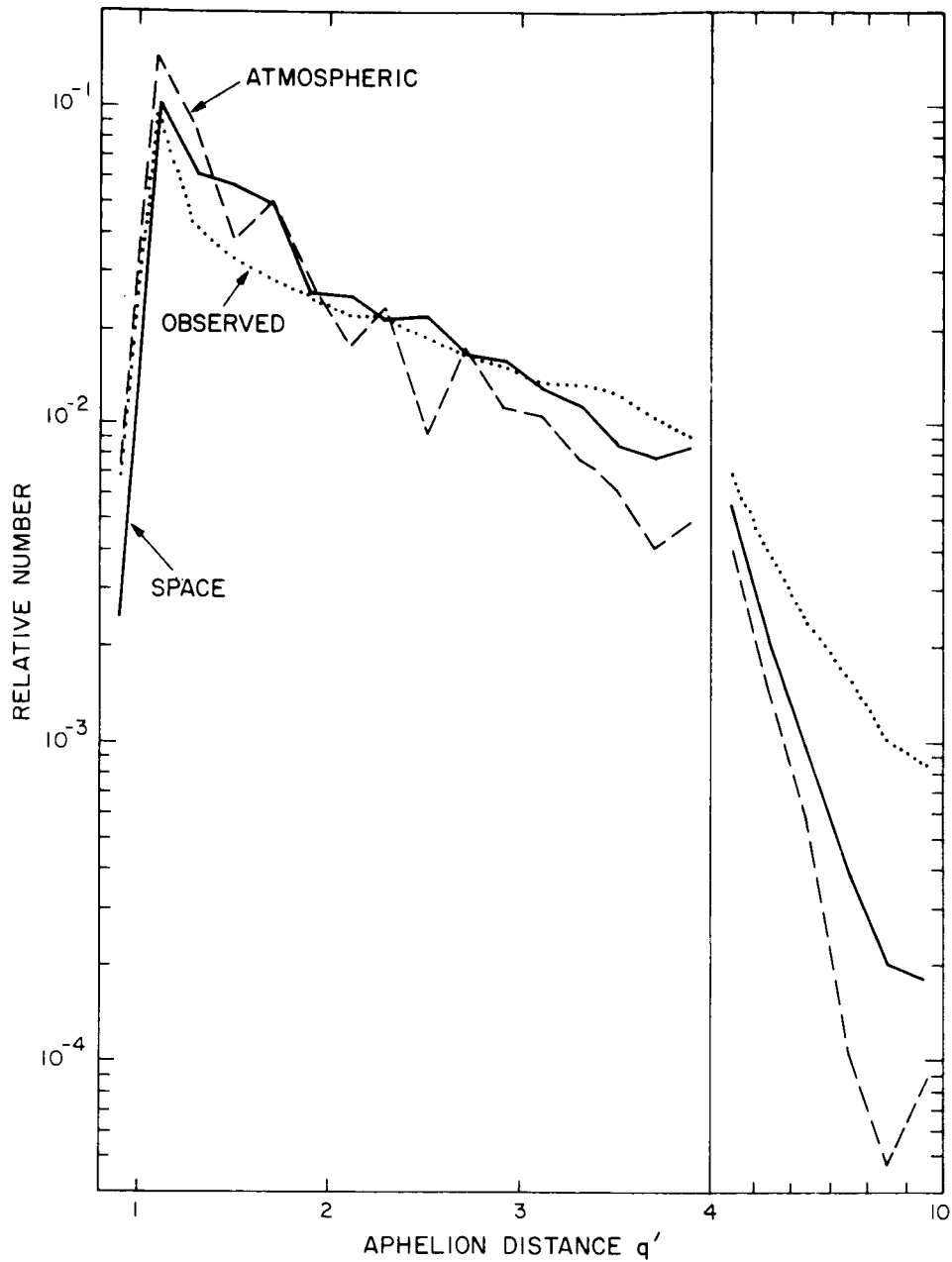
Figure 5-9. Distribution of aphelion distance q'. The scale has been broken to show more detail inside 4 a. u.; this causes an apparent sharp change in the slopes that does not actually exist. The plotted numbers are the fractions of the samples per 1-a.u. interval of aphelion distance.
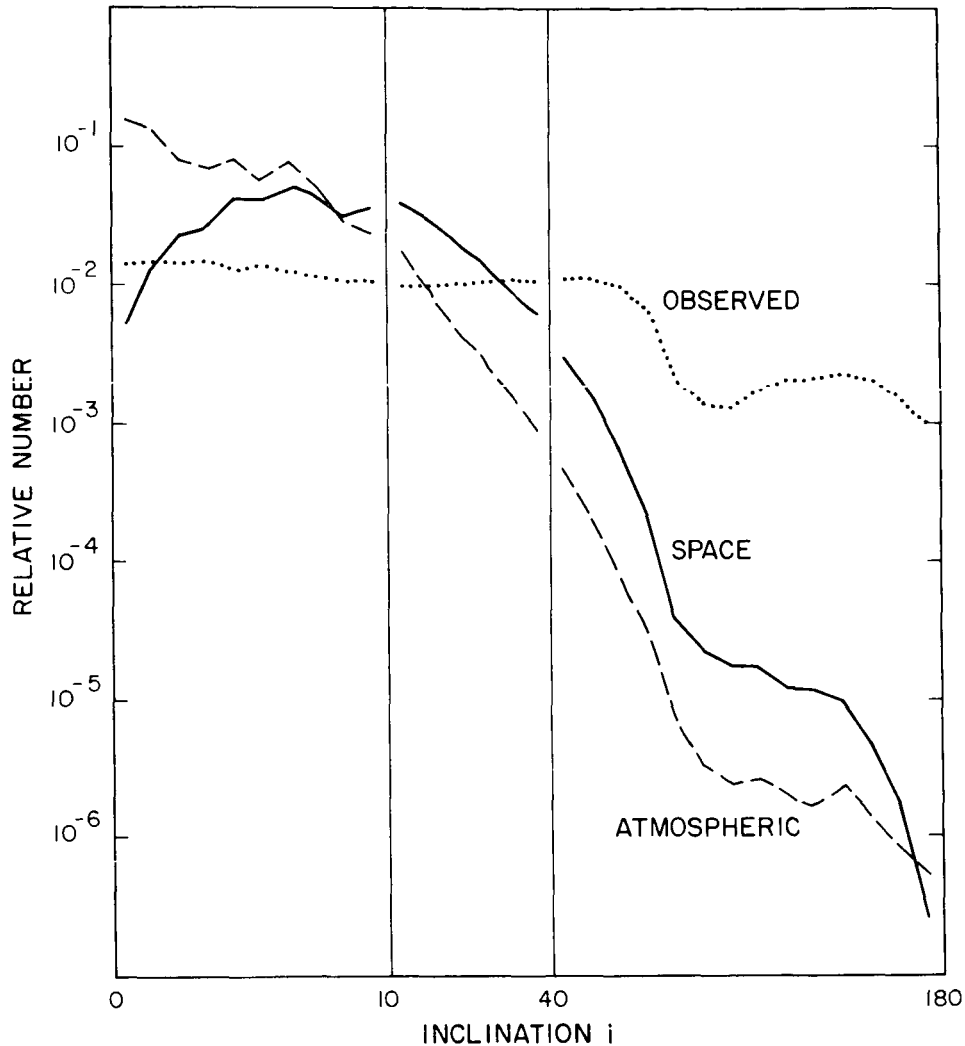
Figure 5-10. Distribution of inclinations i. The scale on the abscissa has been broken twice to permit a convenient representation. The plotted numbers are fractions of the sample per degree of inclination.

Tables 5-1 to 5-3 show relative distributions of $1/a$ versus e, $1/a$ versus i, and e versus i, respectively, for the space sample. Each table was separately scaled to a maximum entry of 800. In Table 5-1, the upper blank area would contain orbits with perihelion outside the earth's orbit, and the lower blank area would contain orbits with aphelion inside the earth's orbit. Border cells of the triangular array are only about half observable from the earth, and scattered values outside the triangle are caused by the earth's orbital eccentricity. The concentration to the top edge of the array reflects the concentration of perihelion distance toward 1.0. Tables 5-2 and 5-3 show small but definite positive correlations between $1/a$ and i and between e and i, respectively. These await interpretation, as do many other prominent features and most details of the distributions.

25

Table 5-1. Relative distribution of 1/a versus e for the space sample.

1/a	e

1/a	0.0	0.1	0.2	0.3	0.4	0.5	0.6	0.7	0.8	0.9	1.0	1.1
-0.6												5
-0.5												
-0.4												2
-0.3												2
-0.2												7
-0.1												11
0.0											37	
0.1										79	21	
0.2									221	74	6	
0.3							21	574	358	41	5	
0.4							637	557	142	33	5	
0.5					3	463	614	322	88	26	5	
0.6				2	437	800	238	159	59	20	9	
0.7			1	496	617	224	145	74	57	21	5	
0.8		1	352	569	511	216	137	99	25	35	6	
0.9		206	603	362	240	235	79	81	48	16	5	
1.0		364	436	212	70	103	87	94	54	17	6	
1.1		3	112	330	104	68	66	63	27	15	4	
1.2			23	86	219	179	42	62	55	19	6	
1.3					38	119	80	66	69	21	7	
1.4						39	161	129	80	33	7	
1.5							46	71	30	20	3	
1.6								57	97	26	9	
1.7									10	29	7	
1.8										16	4	
1.9												
2.0												

Table 5-2. Relative distribution of 1/a versus i for the space sample.

1/a	\ i = 0	10	20	30	40	50	60	70	80	90	100	110	120	130	140	150	160	170	180
-0.6																			
-0.5	4				1														
-0.4																			
-0.3			2																
-0.2				2	1														
-0.1			1	5															
0.0	1	4	4	1	1	1													
0.1	2	15	7	3	4	3	1												
0.2	18	25	26	15	6	3	2	1											
0.3	74	84	78	30	15	5	2	1											
0.4	382	304	183	60	21	7	3	1											
0.5	425	556	212	88	23	12	3	1											
0.6	573	457	302	92	25	9	3	1											
0.7	607	696	220	91	28	11	4	1											
0.8	673	433	346	81	27	11	5	1											
0.9	770	576	365	114	30	15	4	2											
1.0	516	800	297	118	46	15	9	3											
1.1	324	537	315	118	52	23	13	4											
1.2	174	292	130	78	43	27	11	5											
1.3	128	286	91	73	43	28	11	3		1									
1.4	56	113	48	96	27	30	10	2		1									
1.5	27	180	102	53	38	21	7	2		1									
1.6	55	26	8	44	12	9	6	2			1								
1.7	12	53	46	18	28	15	4	4											
1.8	1	9	5	11	9	1	4	2											
1.9			2	6	3	4	3	1											
2.0																			

27

Table 5-3. Relative distribution of e versus i for the space sample.

e	i = 0	10	20	30	40	50	60	70	80	90	100	110	120	130	140	150	160	170	180
0.0	105	230	50	15	6	1	1												
0.1	444	392	169	54	18	6	4	1											
0.2	561	491	266	97	29	11	6	2											
0.3	605	478	309	125	41	25	8	3											
0.4	417	800	307	124	52	28	10	3	1										
0.5	572	547	333	136	47	25	11	4											
0.6	516	666	310	127	52	28	12	3	1										
0.7	277	321	208	104	55	29	12	3	1										
0.8	63	86	82	79	42	19	7	5	1	1			1						
0.9	8	23	30	17	14	11	5	2	1	1									
1.0	4	5	8	2	1														
1.1																			

6. SPACE DENSITY

6.1 Observed Orbits

The space density of meteors observed at Havana from 1962 to 1965, when the radar system was much less sensitive than during the synoptic year, was computed by Southworth (1967). The only other computation of space density (Briggs, 1962) treats an equilibrium distribution of photographic meteors under the Poynting-Robertson effect. The present report follows the methods of Southworth (1967), but it uses the far superior data from the synoptic year and reaches a very different result.

The space density of the observed meteors is computed numerically in straightforward fashion. Space in the solar system is divided into bins, with divisions at intervals of 0.1 in $\log_{10} r$, of 0.1 in $\sin \beta$, and of 18° in λ, where r is the distance from the sun in astronomical units and where β and λ are heliocentric latitude and longitude, respectively. The computer follows around each orbit and computes, to a very good approximation, the time spent in every bin traversed. Adding these times (with cosmic weights) and dividing by the bin volumes gives relative space densities. Absolute space densities then follow from the local space density derived from meteor influx data.

6.2 Unobservable Orbits

Only orbits with perihelion inside the earth's orbit and aphelion outside it can be observed from earth; clearly, we need to take the unobservable orbits into account. To that end, we extrapolate the element distribution observed at the earth, as follows: We assume that a and e are independent of the angular elements i, ω, and Ω. Tables 5-2 and 5-3 show that a and e are in fact only slightly dependent on i, while regression of the nodes under planetary perturbations must have randomized ω and Ω. The two-dimensional relative distribution of 1/a and e, shown in Table 5-1, was smoothed and then approximately fitted by

$$P(1/a, e) = BE \quad ,$$

where

$$E = 75 - 131\,(e - 0.775)\,(|e - 0.775|)^{-0.6} \quad ,$$

$$\log_{10} B = \begin{cases} 0.2b & \text{if} \quad b \le 0 \quad , \\ 3b & \text{if} \quad b > 0 \quad , \end{cases}$$

$$b = 1.35 - 1/a - e \quad .$$

(6-1)

Figure 6-1 shows the areas in the $1/a - e$ plane that contain orbits reaching 1 a.u., reaching R a.u., and reaching both. The correction factor F(R) to transform observed space densities at R to total space density was computed as the numerical integral of equation (6-1) in the region reaching R, divided by the integral in the common region. Table 6-1 is the result.

Table 6-1. Correction factor for observed space densities.

$\log_{10}R$	-0.95	-0.85	-0.75	-0.65	-0.55	-0.45	-0.35	-0.25	-0.15	-0.05
$\log_{10}F$	1.41	1.35	1.22	1.06	0.90	0.73	0.57	0.39	0.21	0.06
$\log_{10}R$	0.05	0.15	0.25	0.35	0.45	0.55	0.65	0.75	0.85	0.95
$\log_{10}F$	0.21	0.64	1.04	1.40	1.72	2.03	2.34	2.66	2.98	3.24

It is evident that the correction factor F must be unreliable when it is large, since large corrections are derived from the extrapolated existence of many unobservable orbits. Although equation (6-1) was chosen as being a plausible form, as well as being an approximate fit to the observations, the bulk of the mass is in orbits with small e, for which the distribution of $1/a$ can be only poorly extrapolated. Thus, we should treat with reserve the corrected space densities beyond, say, 0.4 and 2 a.u., although the general trends beyond may still have significance.
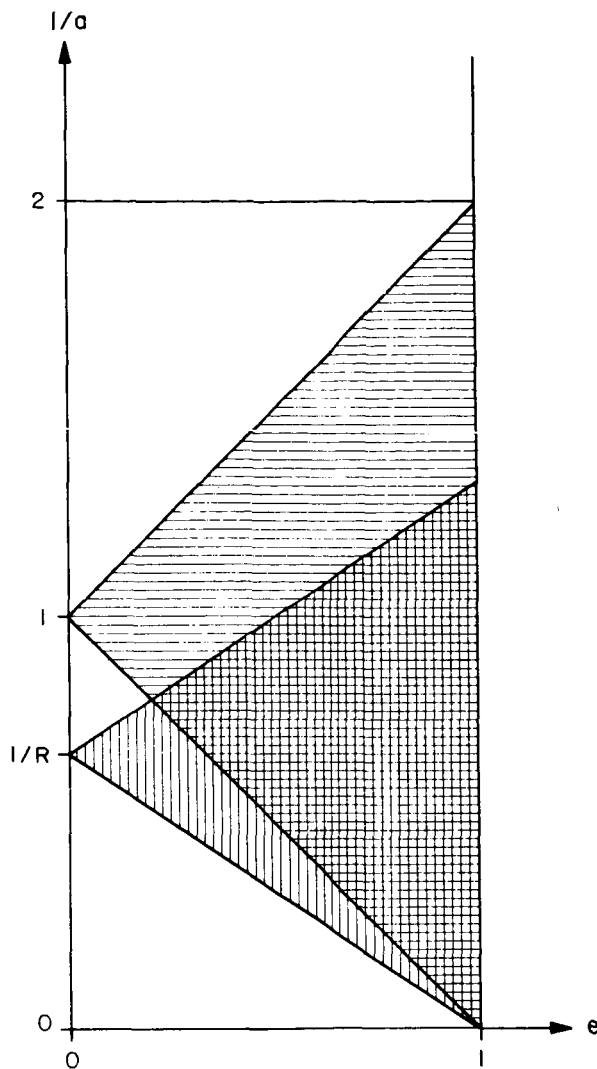
Figure 6-1. Orbits having 1/a and e in the horizontally shaded area can be observed at 1 a.u. from the sun; orbits in the vertically shaded area can be observed at R a.u.

6.3 Densities

Table 6-2 shows decimal logarithms of space density in arbitrary units, in three two-dimensional arrays.   The top section shows the distribution in r and sin β, averaged for all longitudes, and the bottom section shows the distribution in r and λ, averaged for latitudes between -30° and +30°.   Both these sections are still affected by the observational selection of meteors with nodes at the earth's orbit and also by appreciable sampling noise, but we anticipate they may be of future interest.   The

Table 6-2. Decimal logarithms of space density, in arbitrary units.

SOLAR DISTANCE

Block 1 (sin β):

sin β	.100	.126	.159	.199	.251	.316	.398	.501	.631	.794	1.000	1.259	1.585	1.995	2.512	3.162	3.981	5.012	6.310	7.943	10.00
1.0	5.295	5.255	5.093	4.902	4.784	4.634	4.336	4.024	3.718	3.342	2.956	2.904	2.999	3.190	3.325	3.412	3.448	3.636	3.820	3.804	3.878
.9	5.636	5.527	5.453	5.239	4.983	4.925	4.704	4.425	4.187	3.824	3.824	3.714	3.788	3.975	3.977	4.040	4.105	4.127	4.073	4.085	4.140
.8	5.823	5.846	5.715	5.597	5.447	5.272	5.035	4.831	4.544	4.203	4.203	4.109	4.293	4.371	4.493	4.548	4.670	4.739	4.478	4.334	4.226
.7	5.990	5.990	5.736	5.834	5.722	5.447	5.207	5.078	4.799	4.437	4.203	4.598	4.595	4.788	4.888	4.908	4.866	4.736	4.719	4.473	4.473
.6	6.277	6.336	6.110	6.064	5.816	5.567	5.452	5.300	5.146	4.792	4.792	4.719	5.043	5.138	5.206	5.253	5.245	5.150	5.035	4.964	4.964
.5	6.388	6.323	6.167	6.111	5.901	5.698	5.524	5.472	5.330	5.077	5.077	5.083	5.366	5.504	5.512	5.595	5.386	5.418	5.179	5.219	4.937
.4	6.214	6.217	6.243	6.176	5.928	5.751	5.827	5.646	5.630	5.439	5.439	5.561	5.860	5.894	5.834	5.758	5.767	5.685	5.587	5.517	5.331
.3	6.323	6.397	6.547	6.264	6.034	5.988	5.890	5.744	5.736	5.742	5.742	5.727	5.754	6.075	6.114	6.092	6.041	5.725	5.633	5.633	5.333
.2	6.534	6.462	6.547	6.330	6.305	6.151	6.009	5.959	5.968	6.037	6.037	6.004	6.181	6.229	6.298	6.350	6.212	6.189	5.915	5.633	5.645
.1	6.520	6.451	6.578	6.501	6.316	6.106	6.032	5.952	5.884	6.366	6.366	6.288	6.233	6.453	6.373	6.420	6.469	6.320	6.059	5.775	5.500
0.0	6.590	6.516	6.624	6.583	6.316	6.164	6.032	5.985	6.069	6.374	6.374	6.349	6.244	6.297	6.373	6.230	6.237	6.064	6.064	5.649	5.563
-.1	6.476	6.501	6.527	6.565	6.411	6.243	6.180	6.017	6.071	6.006	6.006	6.049	6.090	6.200	6.230	6.046	5.842	5.757	5.651	5.652	5.496
-.2	6.366	6.360	6.407	6.346	6.276	6.003	6.011	5.951	5.825	5.746	5.746	5.861	5.933	6.002	5.991	5.757	5.655	5.651	5.309	5.224	5.086
-.3	6.370	6.360	6.283	6.137	5.986	5.819	5.612	5.527	5.605	5.441	5.441	5.626	5.759	5.758	5.756	5.630	5.655	5.630	5.169	5.165	4.924
-.4	6.379	6.345	6.351	6.112	5.986	5.822	5.612	5.424	5.293	5.389	5.389	5.324	5.451	5.479	5.508	5.354	5.312	5.169	4.654	4.513	4.774
-.5	6.392	6.376	6.407	6.071	5.822	5.672	5.527	5.249	5.058	4.798	4.798	4.915	5.018	5.231	5.170	5.107	5.043	5.043	4.363	4.311	4.470
-.6	5.994	6.212	6.002	5.947	5.678	5.452	5.276	5.033	4.746	4.506	4.506	4.412	4.567	4.689	4.772	4.733	4.676	4.750	4.750	4.733	4.612
-.7	5.852	5.777	5.814	5.677	5.463	5.267	5.046	4.768	4.517	4.136	4.136	4.093	4.222	4.491	4.514	4.602	4.617	4.654	4.513	4.513	4.470
-.8	5.810	5.627	5.348	5.184	5.143	4.850	4.616	4.427	4.100	3.680	3.680	3.883	3.958	4.201	4.209	4.209	4.363	4.363	4.311	4.152	4.152
-.9	5.274	5.103	5.095	4.782	4.449	4.200	3.956	3.659	3.310	3.095	3.095	2.784	3.162	3.575	3.581	3.649	3.549	3.644	3.548	3.548	3.548

Block 2 (sin β):

sin β	.100	.126	.159	.199	.251	.316	.398	.501	.631	.794	1.000	1.259	1.585	1.995	2.512	3.162	3.981	5.012	6.310	7.943	10.00
1.0	5.205	5.145	4.954	4.756	4.575	4.347	4.146	3.942	3.727	3.599	3.570	3.474	3.430	3.449	3.491	3.512	3.564	3.579	3.610	3.643	3.643
.9	5.596	5.562	5.386	5.255	5.088	4.899	4.693	4.469	4.274	4.129	4.106	4.029	4.012	4.038	4.028	4.062	4.050	4.120	4.162	4.046	4.046
.8	5.885	5.914	5.736	5.565	5.390	5.180	4.989	4.807	4.584	4.462	4.446	4.401	4.415	4.451	4.451	4.451	4.504	4.504	4.439	4.310	4.310
.7	6.163	6.171	6.007	5.806	5.595	5.349	5.214	5.018	4.811	4.720	4.700	4.666	4.698	4.739	4.761	4.732	4.716	4.684	4.686	4.582	4.582
.6	6.295	6.307	6.122	5.961	5.787	5.580	5.433	5.224	5.088	5.026	5.015	5.023	5.047	5.132	5.150	5.115	5.081	4.954	4.795	4.795	4.795
.5	6.361	6.393	6.287	6.108	5.877	5.672	5.516	5.386	5.294	5.336	5.321	5.346	5.399	5.436	5.479	5.444	5.345	5.246	5.027	5.027	4.329
.4	6.320	6.393	6.321	6.206	6.058	5.891	5.753	5.634	5.549	5.592	5.596	5.651	5.728	5.755	5.788	5.724	5.662	5.562	5.427	5.427	5.198
.3	6.346	6.385	6.428	6.375	6.173	6.005	5.925	5.778	5.756	5.843	5.843	5.899	5.958	6.034	6.034	5.996	5.885	5.647	5.482	5.482	5.271
.2	6.346	6.490	6.522	6.499	6.381	6.221	6.082	5.992	5.961	6.066	6.066	6.094	6.160	6.253	6.242	6.205	6.122	5.914	5.845	5.845	5.570
.1	6.219	6.463	6.514	6.499	6.350	6.226	6.104	6.080	6.081	6.249	6.240	6.310	6.374	6.438	6.441	6.404	6.280	6.042	5.740	5.740	5.552
0.0	6.517	6.463	6.514	6.499	6.350	6.226	6.104	6.080	6.081	6.249	6.240	6.310	6.374	6.438	6.441	6.404	6.280	6.042	5.740	5.740	5.552

Block 3 (λ):

λ	.100	.126	.159	.199	.251	.316	.398	.501	.631	.794	1.000	1.259	1.585	1.995	2.512	3.162	3.981	5.012	6.310	7.943	10.00
0	6.331	6.234	6.347	6.145	5.994	5.867	5.660	5.695	5.516	5.706	5.651	5.602	5.707	5.699	5.725	5.689	5.511	5.520	5.137	5.279	5.279
18	6.311	6.358	6.349	6.176	5.961	5.888	5.690	5.714	5.538	5.078	5.633	5.632	5.674	5.786	5.690	5.730	5.510	5.323	5.314	4.994	4.994
36	6.165	6.442	6.382	6.156	5.978	5.891	5.711	5.728	5.578	5.620	5.634	5.654	5.687	5.781	5.746	5.766	5.505	5.229	4.963	4.969	4.310
54	6.290	6.405	6.358	6.202	6.004	5.891	5.711	5.672	5.614	5.620	5.624	5.693	5.720	5.746	5.759	5.823	5.579	5.246	5.211	4.774	4.582
72	6.302	6.412	6.282	6.239	6.055	5.860	5.729	5.646	5.617	5.561	5.538	5.738	5.747	5.739	5.798	5.823	5.596	5.226	5.228	5.360	5.360
90	6.318	6.429	6.304	6.211	6.057	5.857	5.718	5.630	5.588	5.632	5.561	5.687	5.766	5.832	5.795	5.603	5.358	5.398	5.060	5.349	5.349
108	6.239	6.373	6.317	6.208	6.010	5.857	5.724	5.630	5.588	5.680	5.569	5.690	5.705	5.869	5.870	5.653	5.689	5.409	5.132	5.207	5.207
126	6.241	6.405	6.243	6.234	5.968	5.828	5.733	5.545	5.468	5.692	5.589	5.719	5.715	5.734	5.952	5.925	5.731	5.526	5.476	5.236	5.236
144	6.377	6.322	6.252	6.151	5.978	5.868	5.714	5.531	5.495	5.049	5.632	5.709	5.779	5.716	5.932	6.033	5.747	5.618	5.469	5.307	5.307
162	6.285	6.215	6.464	6.130	5.978	5.841	5.695	5.531	5.482	5.049	5.632	5.709	5.779	5.716	5.932	6.033	5.747	5.618	5.469	5.469	5.307
180	6.203	6.215	6.288	6.073	5.829	5.841	5.695	5.455	5.482	5.610	5.646	5.759	5.787	5.817	5.932	5.854	5.747	5.761	5.577	5.221	5.221
198	6.203	6.226	6.233	5.998	5.894	5.776	5.659	5.516	5.513	5.610	5.663	5.733	5.795	5.951	5.913	5.832	5.902	5.831	5.577	4.742	4.742
216	6.233	6.231	6.038	6.002	5.902	5.776	5.640	5.542	5.529	5.656	5.663	5.685	5.833	5.913	5.918	5.832	5.879	5.619	5.346	5.024	5.024
234	6.188	6.128	6.047	5.851	5.737	5.732	5.605	5.589	5.546	5.606	5.655	5.701	5.813	5.966	5.944	5.790	5.746	5.303	5.058	5.137	5.137
252	6.159	6.108	5.982	5.834	5.717	5.717	5.651	5.508	5.583	5.634	5.653	5.704	5.845	5.888	5.888	5.664	5.715	5.246	5.085	4.954	4.954
270	6.239	6.050	5.959	5.963	5.621	5.797	5.651	5.505	5.583	5.697	5.616	5.776	5.732	5.792	5.921	5.666	5.712	5.214	5.213	5.060	5.060
288	6.195	6.018	5.956	5.925	6.014	5.716	5.626	5.479	5.550	5.679	5.589	5.734	5.705	5.790	5.812	5.687	5.565	5.328	5.134	5.062	5.062
306	6.151	5.990	5.968	6.100	6.014	5.750	5.627	5.479	5.550	5.061	5.678	5.663	5.705	5.750	5.822	5.687	5.565	5.550	5.134	5.094	5.094
324	6.283	5.933	6.036	6.234	6.045	5.750	5.686	5.546	5.541	5.061	5.692	5.661	5.738	5.738	5.756	5.736	5.620	5.532	5.175	4.798	4.798
342	6.393	5.999	6.018	6.227	6.050	5.763	5.696	5.628	5.491	5.651	5.700	5.623	5.685	5.753	5.633	5.741	5.517	5.517	5.239	4.942	4.715
360	6.393	5.999	6.018	6.227	6.050	5.763	5.696	5.628	5.491	5.651	5.700	5.623	5.685	5.753	5.633	5.741	5.517	5.517	5.239	5.169	5.169

32

central section shows the distribution in r and sin β when the observed value of ω for each orbit is replaced by a uniform distribution from 0 to 2π. Regression of the nodes must in fact smear ω nearly uniformly in the real interplanetary distribution; accordingly, we have simulated the process as our last correction for observational selection. Because the distribution is now symmetric about β = 0, this portion of the table includes only positive values of sin β.

Figure 6-2 shows the averaged density distribution, using 4×10^{-22} g cm^{-3} for the space density near the earth, as estimated in Section 7. The curves have been smoothed near r = 1 to correct bumps, which were doubtless caused by inexactness in the fit of equation (6-1) to the data. Of course, we could make cosmetic changes to (6-1), but we would make no real advance in reliability. It is not plausible that the earth should have any effect on space density that could be seen on the scale of Figure 6-2, especially at higher latitude.

Figure 6-3 shows, on two scales, the contours of space density in a plane normal to the ecliptic. The less reliable contours are dashed. The meteors are concentrated to a relatively thin layer about the ecliptic plane. There, the minimum density is 0.7 a.u. from the sun, and the maximum, between 2 and 3 a.u. from the sun.

6.4 Comparisons with Other Data

The distribution of space density just described was a considerable surprise to the authors. Nonetheless, it is in qualitative agreement with two recent results from totally different observing systems: (1) Roosen (1970) was unable to detect the earth's shadow on the gegenschein and deduced that the density of light-scattering particles must increase outward from the earth. (2) Pioneer 10 (Kinard and Soberman, 1972) detected an increase in particle density of larger particles on its way to the asteroid belt.
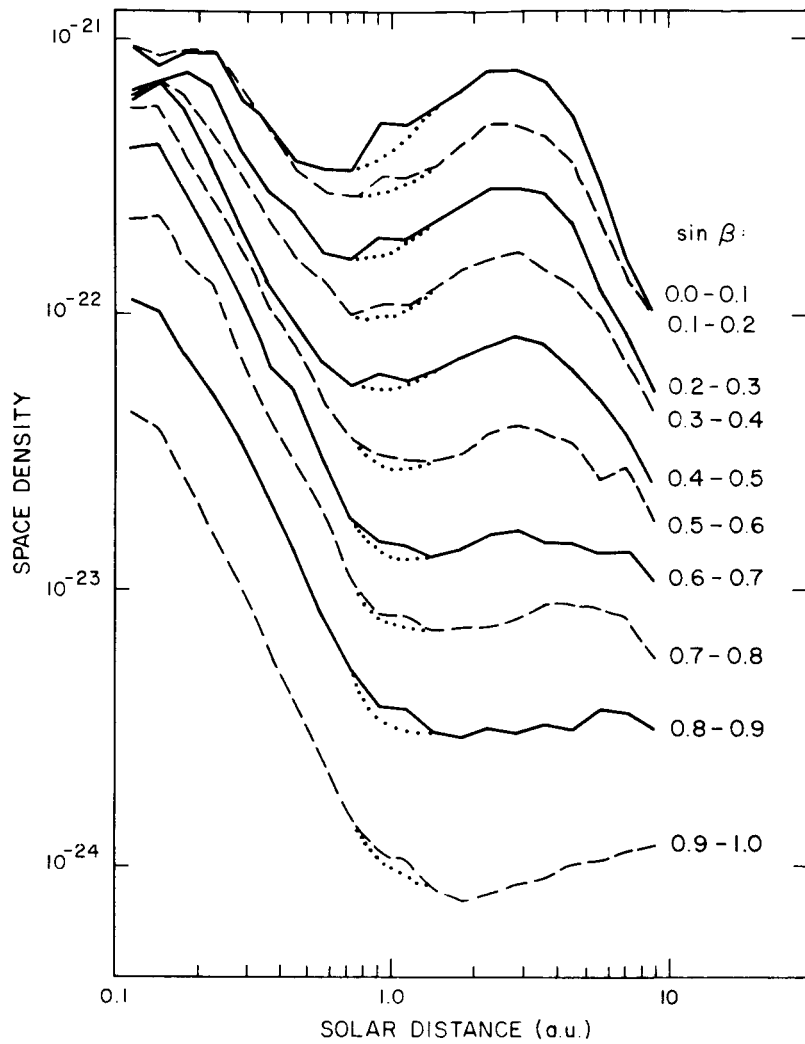
Figure 6-2. Space density of meteors, corrected for unobservable orbits. Curves are plotted for 10 ranges of heliocentric latitude β and have been smoothed near 1 a.u. in dotted lines.
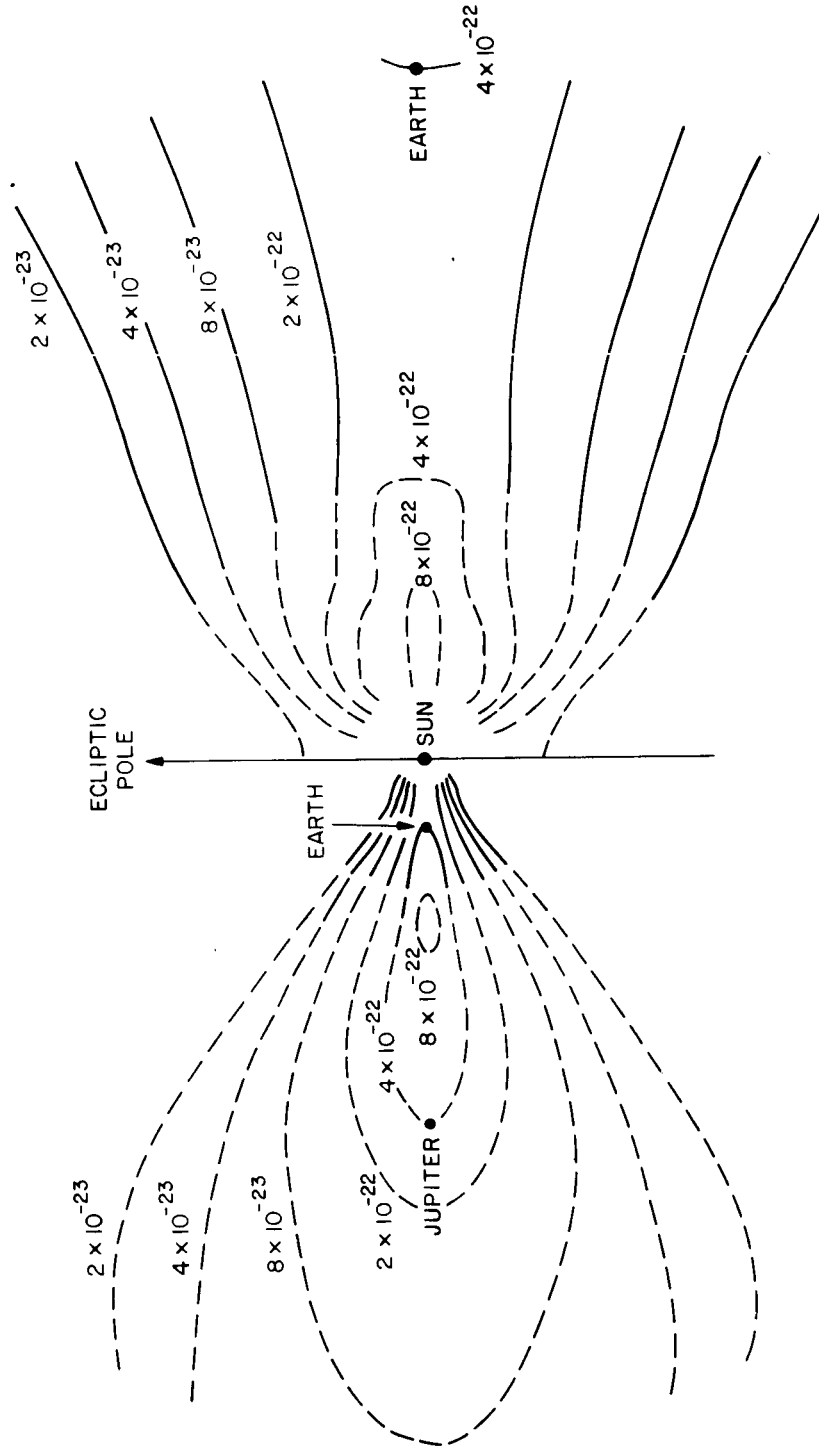
Figure 6-3. Contours of meteor space density in a plane normal to the ecliptic. The left half includes solar distances 0.4 to 10 a.u.; the right half, at tenfold scale, includes 0.1 to 1.0 a.u. The dashed contours are less reliable than the solid.

35

7. COLLISIONS IN SPACE

7.1 Significance of Collisions

The drastic revision of meteor masses and orbital distributions communicated in earlier sections of this report led to a reappraisal of the importance of collisions between meteors in space compared to other loss processes, primarily the Poynting-Robertson effect. Formerly, it had appeared that collisions were important only for retrograde orbits, for large meteoroids, and for meteoroids near the sun. Now, after revision of the masses and therefore of the total flux by means of the new ionizing efficiency, it appears that collision is at least competitive with the Poynting-Robertson effect for ordinary orbits near the earth.

The last previous estimate of radio meteor space densities (Southworth, 1967) had shown density decreasing monotonically outward from the sun, entirely in harmony with dominance of the Poynting-Robertson effect over all other loss mechanisms for meteors (except near the sun). The run of space density found in Section 6, however, can be maintained as a stationary distribution only if collisions are significant.

7.2 Theoretical Collision Model

A simple theoretical model for the distribution of space density when both collisions and the Poynting-Robertson effect are significant can be constructed as follows: Consider particles all of one size and in nearly circular orbits at small inclinations to the ecliptic. At some distance from the sun, the particles are supplied to the system at a uniform rate and then spiral in under the Poynting-Robertson effect, while preserving their respective orbital inclinations. Some of the particles at each distance from the sun undergo mutual collisions; we shall suppose that they are eliminated from the system through solar radiation pressure that blows their fragments away. The Poynting-Robertson effect reduces the radius r of each orbit at the rate

$$\left(\frac{dr}{dt}\right)_{PR} = \frac{-5 \times 10^{11}}{s \delta r} \text{ cm sec}^{-1} \quad , \tag{7-1}$$

37

where t is time and s and δ are particle radius and density in cgs units; the particles are taken to be spheres. If there were no collisions, the Poynting-Robertson effect would set up a density distribution inversely proportional to r (Southworth, 1967) because the orbital planes near the sun are more densely concentrated to the ecliptic. Thus,

$$\left(\frac{d\rho}{dr}\right)_{PR} = -\frac{\rho}{r} \quad . \tag{7-2}$$

Two particles collide if their centers approach closer than 2s, so that each particle sweeps out a volume $4\pi s^2 v \, dt$ in the time dt, where v is the mean relative velocity. Consequently, collisions diminish the space density at the rate

$$\left(\frac{d\rho}{dt}\right)_C = -\frac{\rho^2}{m} \, 4\pi s^2 v = \frac{-3\rho^2 v}{s\delta} \quad , \tag{7-3}$$

where $m = (4/3)\pi s^3 \delta$ is the particle mass.

To determine v, consider first the mean relative velocity resulting from the orbital inclinations. Since these inclinations are small, the relative velocities are primarily normal to the ecliptic, and the mean absolute velocity component is

$$v_n = 7.3 \times 10^{12} \, i \, r^{-1/2} \text{ cm sec}^{-1} \quad , \tag{7-4}$$

where r is in centimeters and i is in radians. The mean relative velocity between particles is of the order of v_n, but depends on the distribution of inclinations. For this model, it will be sufficiently realistic to assume that inclinations are distributed from 0 to I so that the space density at the ecliptic plane is uniform for each interval of inclination. It can then be readily shown that the frequency of particles with inclination i is proportional to i itself, that the mean inclination is

$$\bar{i} = (2/3) I \quad , \tag{7-5}$$

and that the mean relative velocity normal to the ecliptic is

$$v_i = \frac{64}{45} \frac{I}{i} v_n \quad .$$
(7-6)

Orbital eccentricity introduces relative velocity components parallel to the ecliptic plane, both radial from the sun and parallel to the circular velocity. The mean parallel component is approximately one-half the radial component. Since eccentricity also gives rise to collisions between particles at different mean distances from the sun, we must assume that the space density does not vary substantially between perihelion and aphelion of most of the particles. If we assume a continuous distribution of eccentricities, it has not proved possible to obtain an analytic value for the mean relative velocity caused by eccentricity, but for a single eccentricity e we find the mean component parallel to the ecliptic plane to be

$$v_e = 1.57 \frac{e}{i} v_n \quad .$$
(7-7)

For a distribution of eccentricities, the numerical coefficient in (7-7) would be larger, because the faster particles collide more frequently and are therefore more highly weighted in the mean. When the mean velocity for a distribution of inclinations is compared with the mean for a single inclination, it appears that the coefficient should be increased by roughly a factor of 2. We therefore use

$$v_e = \frac{3\bar{e}}{i} v_n \quad ,$$
(7-8)

where $\bar{e}$ is the mean eccentricity. Then for the total mean relative velocity, we have

$$v = 7.3 \times 10^{12} \, (4.6 \, \bar{i}^{-2} + 9 \, \bar{e}^{-2})^{1/2} \, r^{-1/2} \quad .$$
(7-9)

Since there is a constant rate of particle supply, there is an equilibrium density distribution. As each group of particles supplied within a small interval of time spirals in toward the sun, the density within that group traces out the general run of density with respect to distance from the sun. Combining collisional losses (7-3)

39

with orbital shrinkage (7-1), and adding the effect (7-2) of the clustering of the orbital planes, we thus find that the space density obeys

$$\frac{d\rho}{dr} = \left(\frac{d\rho}{dr}\right)_{PR} + \left(\frac{d\rho}{dt}\right)_C \left(\frac{dt}{dr}\right)_{PR} \quad . \tag{7-10}$$

Substituting (7-1), (7-2), (7-3), and (7-9) gives

$$\frac{d\rho}{dr} = -\frac{\rho}{r} + A \rho^2 r^{1/2} \quad , \tag{7-11}$$

where

$$A = 93 \left(\bar{i}^2 + 2 \bar{e}^2\right)^{1/2} \quad . \tag{7-12}$$

We now obtain the model density distribution in the ecliptic as the solution of (7-11):

$$\frac{\rho_{min}}{\rho} = 3 \left(\frac{r}{r_{min}}\right)^{-2} \left(\frac{r}{r_{min}}\right)^{3/2} \quad , \tag{7-13}$$

which has a density minimum ρ_{min} at distance r_{min} from the sun given by

$$\rho_{min} = A^{-1} r_{min} - \frac{3}{2} \tag{7-14}$$

and

$$r_{min} = \left(\frac{1}{3A \, \rho_0 \, r_0} + \frac{2}{3} r_0^{1/2}\right)^2 \quad , \tag{7-15}$$

where ρ_0 is the density at a given distance r_0 from the sun. Figure 7-1 shows the theoretical distribution (7-13).
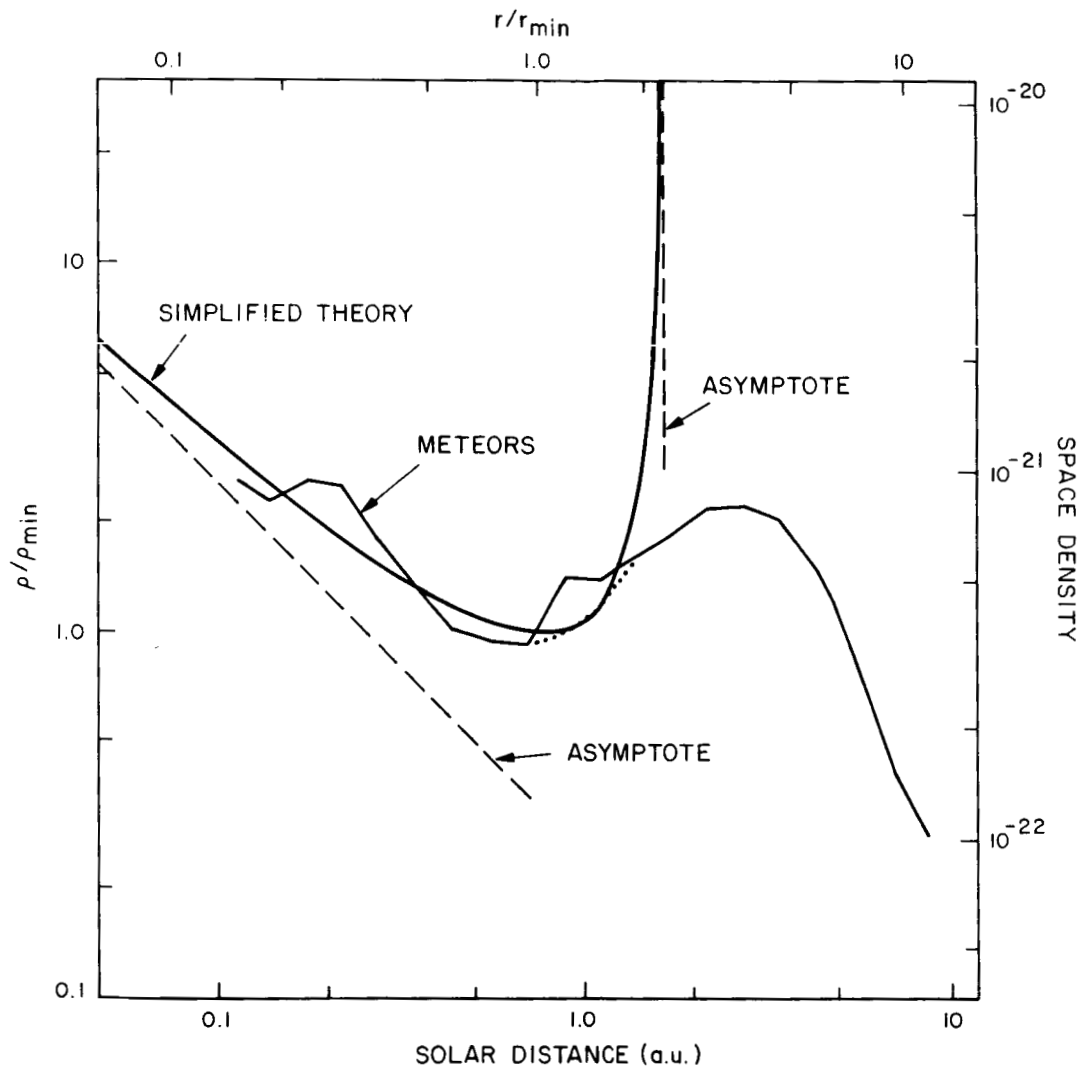
Figure 7-1. Radial distribution of space density. The model distribution given by equation (7-13) is drawn as the smooth curve labeled "Simplified Theory" referred to the top and left-hand scales. The asymptotes are dashed. The top curve of Figure 6-2, labeled "Meteors" referred to the bottom and right-hand scales, has been positioned to make an approximate fit to the model.

The model distribution (7-13) has a vertical asymptote at $r = 2.25\ r_{min}$, corresponding to dominance of collisions over the Poynting-Robertson effect; but this part of the solution must be neglected because it violates the assumption that space density does not vary steeply with distance from the sun. The model distribution is also asymptotic at small r to

$$3\,\rho r = \rho_{min}\, r_{min} \quad , \tag{7-16}$$

which corresponds to dominance of the Poynting-Robertson effect over collisions.

We note that, in this simple model, if collisions eliminate most of the particles, then the asymptotic density at small r is related to the distance of the particle supply from the sun. Substitution of (7-14) and (7-15) into (7-16) shows that if

$$\rho_{asy}\, r_{asy} \ll \rho_{sup}\, r_{sup} \quad , \tag{7-17}$$

then

$$r_{sup} = (2A\, \rho_{asy}\, r_{asy})^{-2} \quad , \tag{7-18}$$

where subscripts sup and asy, respectively, denote the point of supply and a point on the asymptote. If we relax the condition (7-17), then the right-hand side of (7-18) is an upper bound to r_{sup}.

7.3 Comparison with Observation

For an order-of-magnitude comparison of the model distribution with observation, we can take Whipple's (1967) influx distribution and a mean geocentric velocity of 9 km sec^{-1} (derived from our observed mean v_∞ of 14.5 km sec^{-1}) to estimate a total space density of small particles (smaller than meteorites) of

$$\rho_0 \approx 4 \times 10^{-22} \text{ g cm}^{-3} \tag{7-19}$$

at the earth's orbit; thus,

$$r_0 = 1.5 \times 10^{13} \text{ cm} \quad . \tag{7-20}$$

Our observed inclination and eccentricity distributions give

$$A \approx 66 \quad , \tag{7-21}$$

and substitution into (7-15) gives

$$r_{min} \approx 1.2 \times 10^{13} \text{ cm} \quad ,$$

$$\approx 0.8 \text{ a. u.} \quad . \tag{7-22}$$

Figure 7-1 also shows the space density on the ecliptic as derived in Section 6.3, positioned to match at ρ_0 and r_{min}. We concentrate our attention on the interval from 0.5 to 1.5 a. u. (and we must ignore the derived density at 0.9 a. u., as explained in Section 6). Within these limits, the fit between model and observation is better than might have been expected. In particular, the match along the r axis, given by (7-22), shows that we have been lucky in our estimates of A and ρ_0. Nonetheless, observation seems to support the approximate validity of the model in this interval.

7.4 Sources of Meteors

Comparison of the observed run of density in Figure 7-1 leads directly (if we accept the assumptions of the model and the reliability of the data analysis) to conclusions concerning where the particles are supplied. No significant number of particles enter the system in the range where the model distribution fits the observations — that is, from 0.5 to 1.5 a. u. Most of the particles enter between 1.5 and roughly 4 a. u. — that is, in the region of the asteroid belt. However, this is also the region most densely populated by short-period comets and also by particles that are captured by Jupiter from long-period orbits, so that we cannot identify the source of this supply in an easy fashion. If we take the "observed" curve in Figure 7-1 at face value, there is a further supply of particles in the neighborhood of 0.2 a. u., which tempts us to identify them with particles ejected from bright long-period comets near perihelion. However, because of the limitation on the observations, it would not be safe to place any reliance on such a source at this time from this set of data. For the same reason, we cannot safely say anything about particle sources or their absence beyond 4 a. u.

7.5 Further Research

Our recognition that collisions are very important in the evolution of meteor orbits requires us to recast the theory of orbital distribution. This is both an important

opportunity and a considerable task. The theory will need to include particle density, breaking strength, and fragment size distribution, as well as space density and flux distribution, because these are the parameters that determine the loss of most particles from the system and also the gain of collisional fragments to the system. Considerable computation will doubtless be necessary, but careful formulation is even more important. One result to be hoped is that the physical properties of individual particles can to some extent be determined from the other parameters, such as orbital distribution, that we now know to be linked with them.

The simplified model in Section 7.2 neglects differences in collision rate that depend on particle size or orbital inclination or eccentricity. One effect of these differences is a difference in the average age of particles in the system, depending on size and orbit; large particles and those in highly inclined or eccentric orbits are much younger. Now that a meaningful space density distribution is available, it may well be possible to find collisional ages for meteor streams.

At least three kinds of observational data are at hand for comparison with a theory including collisions, so that we have reason to expect that the comparisons can in fact tell us some things we should like to know, such as particle properties. First, the space density distribution is approximately as concentrated to the ecliptic plane as are the short-period comets, even though the long-period comets are the known source of both a substantial proportion of the observed large (photographic) and small (radar) meteors and almost all the observed dust input. Both Jupiter perturbations (which are independent of the physical properties of the particles) and collisions and the Poynting-Robertson effect (which depend on the physical properties) are important to the present distribution. Second, there is vast observational literature on the mass distributions of the whole cloud and of individual meteor streams. The mass distributions of new streams are important input data to a general study of collisions; the overall mass distribution is a function of the physical properties of the particles. Third, the observed distribution of masses and orbits within individual meteor streams (including the 200 new streams announced in this report) makes it possible to compare dynamical and collisional ages of the streams.

Theoretical study of collision processes is, in fact, an essential step in improving our knowledge of interplanetary density distributions, because the emprical extrapolation of the observed orbital distribution in Section 6 needs theory if it is to be improved. At the same time, we would extend our knowledge of both general space distributions and the physical properties of individual meteors. (In particular, we might find that mass distributions depend on mean distance from the sun and perhaps from the ecliptic plane.) We should also expect new results on the history of the sources of the interplanetary cloud.

8. COMPUTERIZED SEARCH FOR RADIO METEOR STREAMS

8.1 Two-Phase Computerized Stream Search in the Synoptic-Year Sample

The stream search performed by us on the sample of 19,303 radio meteor orbits from the years 1961 to 1965 was based on the statistical model of meteor streams (Sekanina, 1970a; referred to hereafter as Paper I). The model provides parameters of the distributions of meteor orbits in a stream and in the surrounding sporadic background in terms of the Southworth-Hawkins (1963) D-criterion, which tests the similarity of meteor orbits in terms of the differences in their Keplerian elements.

The search procedure starts from an initial orbit, which is assumed to be known, and iterates the elements of the stream's mean orbit by weighting them with the use of the elements of individual meteors until the orbit converges. The method is very convenient for searching for members (in a sample) of known meteor streams (see Sekanina, 1970b; Paper II) or for meteor streams associated with objects of known orbits (see Sekanina, 1973; Paper III). Searching for new streams, for which of course no orbital information is available in advance, becomes more difficult as the size of a meteor sample to search grows.

Theoretically, one should have to take the orbit of every single meteor in the sample as the initial set of elements, which for extensive samples is practically impossible, even with the aid of a powerful computer, because of the enormous number of calculations associated with the particular search procedure.

From the synoptic-year data, 19,698 radio meteor orbits have been successfully processed. This is far more than the number for which the orbit-to-orbit approach would be reasonable. Fortunately, it proved possible to use the original Southworth-Hawkins (1963) search program in the place of a preparatory search to supply the required initial orbits for further analysis by the statistical-model search program. Practical calculations have confirmed that the two computer programs complement each other excellently and have shown that the two-phase technique is the most effective stream-search method in existence, particularly for a huge sample of orbital data.

We also used the orbits of previously known meteor streams and other objects as additional initial orbits, in part to check the completeness of the list of initial stream orbits supplied by the Southworth-Hawkins search program.

8.2 Phase I: Major Source of Initial Orbits

With the synoptic-year sample of 19,698 radio meteors, the Southworth-Hawkins search program would require a computer memory capacity several times larger than that of a CDC 6400, on which this phase was carried out. It was therefore necessary to divide the whole sample into smaller sets and to search for streams in each of them. The sets had to overlap each other significantly to ensure that no stream was lost because of the dividing lines. This brought the estimated number of necessary subsets to at least 10. The longitude of perihelion and the inclination were taken as the dividing parameters, although the perihelion distance and the eccentricity were another possible pair. Only the nodal longitude and the argument of perihelion were felt to be less convenient, since for certain types of orbits, fairly large spreads in the two elements have only slight effects on the magnitude of the D-criterion.

Table 8-1 shows the division of the sample into 12 sections by inclination and longitude of perihelion. For each section, we list the number of streams detected by the Southworth-Hawkins program at two different rejection levels, D_s. The rejection levels were established in accordance with Lindblad's (1971) paper. The average number of meteors per section was about 3800, which, with Lindblad's formula (2), gives $D_s = 0.10$. We also made an independent search with $D_s = 0.08$ in an effort to increase our ability to separate streams. For low-inclination sections, the rejection levels were decreased to 0.08 and then 0.06, because the major, broad streams are well known (we used the known orbits of these streams as the initial orbits to collect their members) and because we more urgently wished to separate possible minor showers.

Table 8-1 indicates that 90 to 98% of the detected streams had no more than five members. We considered these streams as fortuitous groupings of nonrelated meteors and discarded them. By so doing, we reduced the total numbers of streams from 6019 to 502 for the higher rejection levels and from 4763 to 167 for the lower.

Table 8-1. Number of streams detected by the Southworth–Hawkins search program among the radio meteors of the synoptic year (N is the number of meteors per stream).

Range in inclination	Rejection level, D_s	Range in longitude of perihelion								Totals	
		0° – 150°		90° – 240°		180° – 330°		270° – 60°			
		N > 1	N > 5	N > 1	N > 5	N > 1	N > 5	N > 1	N > 5	N > 1	N > 5
0° – 40°	0.06	324	8	491	12	358	6	238	2	1411	28
	0.08	450	23	636	36	489	30	350	15	1925	104
25° – 65°	0.08	393	22	536	18	481	15	407	24	1817	79
	0.10	491	51	686	55	577	61	464	54	2218	221
45° – 180°	0.08	340	15	418	15	401	12	376	18	1535	60
	0.10	447	40	501	43	472	44	456	50	1876	177

The remaining 669 streams went through a second screening: rejection of streams that were multiply listed because the 12 sections overlapped (Table 8-1) and because two rejection levels were used. We discarded all the multiple entries that differed from each other by less than 0.06 (but keeping the limit somewhat flexible in individual cases). We also discarded entries that indicated a clear identity with a stream detected in Paper II or III. We refrained from being too harsh in reducing the number of stream entries because multiple entries still surviving in the list would be rejected anyway in the following phases of screening. The present phase brought the number of streams down to 285.

8.3 Phase I: Other Sources of Initial Orbits

Besides the initial orbits provided by the Southworth-Hawkins program, we used a number of orbits of previously known streams and of potentially related objects as additional initial orbits for Phase II. Specifically, the entries are as follows:

A. Orbits of the radio meteor streams detected in the 1961−1965 set of data, as published in Papers II and III.

B. Predicted orbits of twin showers (i.e., daytime branches) of low-inclination streams of Papers II and III (see below for details).

C. Orbits of periodic comets with perihelion distances $q \lesssim 1.2$ a.u., approaching the earth's orbit within a few tenths of 1 a.u.

D. Orbits of earth- and Mars-crossing asteroids (with $q \lesssim 1.2$ a.u.).

E. Orbits of meteorites and bright fireballs.

Since verification of the existence of meteor streams detected in the 1961−1965 list of orbits is one of the primary aims of this investigation, orbits A permit this to be done most easily. Also, the problem of stream associations with periodic comets, asteroids, and related bodies can be solved most directly by applying orbits C, D, and E, respectively.

Orbits B deserve special attention. As pointed out by Whipple (1940) in the case of the Taurids, a broad meteor stream moving in a low-inclination orbit meets the earth at two points: on its way to as well as on its way from the sun. It is observed

as two apparently independent but actually closely related showers. In Paper III, we suggested that such a pair be called the twin showers. If the motion of the stream is direct, one of the twin showers (preperihelion branch) must be nighttime, and the other, daytime. In Table XIV of Paper III, we listed seven pairs of twin showers, of which three had been established a long time ago   and the remaining four were detected in the 1961−1965 collection of radio orbits.

In an effort to increase the chance of discovering more twin showers to the previously known nighttime low-inclination showers, we predicted approximate orbits of the former from the 1961−1965 orbits of the latter, using a criterion based on Figure 8-1.

A stream moving in the plane of the ecliptic intersects the earth's orbit on the way to the sun at point Ω, and on the way from the sun at point Ω_*.

For some members of the stream, Ω is actually the ascending node and ω is the argument of perihelion; these meteors could cause a nighttime shower. For some other members of the stream, Ω_* is the ascending node and ω_* is the argument of perihelion; they could produce a daytime shower. Obviously, the two elements of the twin showers are related to each other by

$$\omega_* = 360° - \omega \quad ,$$

$$\Omega_* = \Omega + 2\omega \quad , \tag{8-1}$$

while for the other three elements, we have $i_* \approx i \approx 0$, $q_* \approx q$, $e_* \approx e$. The predicted elements of the twin showers served as additional initial orbits in the Phase II calculations.

8.4 Phase II: The Weighting System

The technique developed in Paper I and previously applied in Papers II and III was used in Phase II with only one minor change.
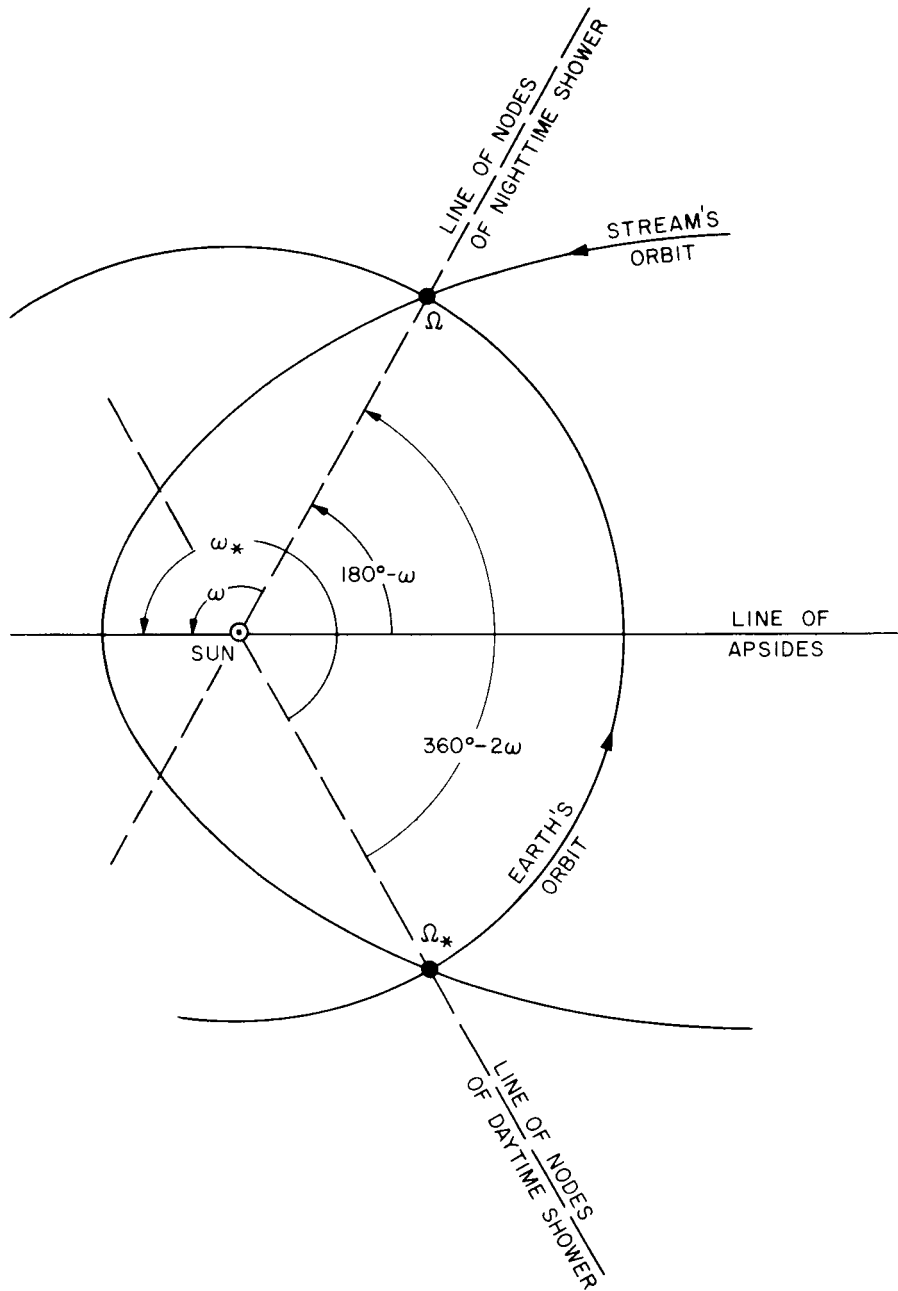
Figure 8-1. The orbits of twin showers (schematic). Here, ω and Ω are the argument of perihelion and the longitude of ascending node, respectively, of the nighttime (preperihelion) shower, and ω_* and Ω_*, the same elements of the daytime (postperihelion) shower.

The search in the synoptic year sample for meteors belonging to 40 streams detected in the 1961–1965 collection was carried out with four different weighting systems. The system used for the 1961–1965 set,

$$w = 1 - D/0.2 \quad \text{for} \quad D < 0.2 \quad ,$$
$$w = 0 \qquad\qquad \text{for} \quad D \geq 0.2 \quad , \tag{8-2}$$

was generalized to

$$w = (1 - D/D_0)^h \quad \text{for} \quad D < D_0 \quad ,$$
$$w = 0 \qquad\qquad \text{for} \quad D \geq D_0 \quad , \tag{8-3}$$

and, with use of the same initial orbits, the mean orbits of the streams were calculated for the following combinations of (D_0, h): 0.20, 1; 0.20, 2; 0.25, 1; 0.25, 2. It was found that the four resulting sets of elements were in very good agreement for a number of streams and in reasonable agreement for most streams.

There were, however, several instances where the mean orbits appeared to depend more substantially on the weighting system, and these were the key cases for deciding which of the four (D_0, h) pairs to prefer in searching for new streams.

To illustrate the following arguments, we list a few examples in Table 8-2. For high-inclination streams, the mean elements from different weighting systems compare with each other quite favorably (December Draconids and λ Draconids). At moderate and low inclinations, a high degree of consistency exists only for concentrated streams (Geminids, Southern δ Aquarids, and Monocerids).

The system with $D_0 = 0.2$ and $h = 2$ tends occasionally to give somewhat erratic results for very extended streams (Piscids, Southern Arietids, and to some extent ζ Perseids), apparently because it gives too much weight to orbits with very low D's and too little weight to those with relatively large D's.

The system with $D_0 = 0.25$ and $h = 1$, on the other hand, seems to give too much weight to orbits with large D's, which may result in suppressing dispersed,

53

Table 8-2. Comparison of mean orbits of several streams calculated with different weighting systems (D_0, h).

Stream	D_0	h	Equinox 1950.0			q (a.u.)	e	a (a.u.)	π (1950)
			ω	Ω	i				
ζ Perseids	0.20	1	60°.1	81°.2	6°.6	0.361	0.757	1.486	141°.3
	0.20	2	62.9	76.8	4.8	0.385	0.748	1.524	139.8
	0.25	1	60.1	82.7	7.6	0.364	0.751	1.465	142.8
	0.25	2	60.5	80.8	6.5	0.365	0.755	1.492	141.4
β Taurids	0.20	1	232.1	282.9	0.7	0.269	0.841	1.694	155.0
	0.20	2	53.0	102.5	0.6	0.280	0.828	1.627	155.5
	0.25	1	59.9	83.0	7.6	0.363	0.752	1.462	142.9
	0.25	2	52.3	102.0	0.3	0.274	0.834	1.653	154.3
Southern δ Aquarids	0.20	1	155.3	305.7	28.3	0.070	0.957	1.633	100.9
	0.20	2	155.4	305.4	28.6	0.067	0.960	1.669	100.8
	0.25	1	155.3	306.2	27.7	0.071	0.955	1.577	101.5
	0.25	2	155.4	305.7	28.2	0.069	0.958	1.630	101.0
Piscids	0.20	1	306.4	172.5	3.8	0.311	0.769	1.344	118.9
	0.20	2	297.0	166.3	5.6	0.368	0.779	1.667	103.2
	0.25	1	306.7	174.8	2.0	0.306	0.777	1.371	121.4
	0.25	2	306.3	172.8	3.5	0.311	0.769	1.349	119.1
λ Draconids	0.20	1	155.9	195.6	66.4	0.967	0.537	2.087	351.6
	0.20	2	157.6	195.9	66.0	0.973	0.499	1.944	353.4
	0.25	1	154.5	195.5	67.3	0.962	0.566	2.215	350.0
	0.25	2	156.0	195.7	66.6	0.967	0.530	2.060	351.7
Southern Arietids	0.20	1	122.1	18.7	2.9	0.337	0.765	1.434	140.8
	0.20	2	133.2	359.3	2.8	0.239	0.828	1.389	132.5
	0.25	1	124.6	14.2	1.9	0.315	0.780	1.433	138.7
	0.25	2	122.5	17.8	2.9	0.333	0.768	1.435	140.3
Triangulids	0.20	1	270.2	218.4	18.6	0.603	0.645	1.699	128.6
	0.20	2	275.0	215.6	16.8	0.563	0.665	1.679	130.6
	0.25	1	264.2	219.6	18.7	0.649	0.627	1.740	123.8
	0.25	2	269.6	218.6	18.3	0.606	0.647	1.718	128.2
Monocerids	0.20	1	135.4	71.9	22.3	0.155	0.977	6.626	207.3
	0.20	2	136.6	71.4	22.1	0.147	0.978	6.621	208.0
	0.25	1	135.2	72.1	22.6	0.160	0.970	5.372	207.3
	0.25	2	135.8	71.8	22.3	0.153	0.975	6.199	207.6
December Draconids	0.20	1	185.1	253.7	42.1	0.981	0.586	2.370	78.8
	0.20	2	184.5	253.6	42.8	0.983	0.589	2.393	78.1
	0.25	1	183.3	255.4	41.8	0.981	0.569	2.276	78.7
	0.25	2	184.6	254.2	42.2	0.981	0.582	2.346	78.8
Geminids	0.20	1	325.3	261.3	23.4	0.139	0.894	1.307	226.6
	0.20	2	325.3	261.9	23.1	0.139	0.893	1.301	227.2
	0.25	1	325.2	260.6	23.4	0.140	0.893	1.312	225.8
	0.25	2	325.2	261.4	23.2	0.139	0.893	1.306	226.7

low-population streams and lead relatively often to spurious convergences. Surprisingly, our calculations showed that this weighting system suppressed the β Taurid stream in favor of the ζ Perseids.

The two remaining weighting systems used give practically identical results in almost all cases. One of the very few exceptions was again the β Taurid stream, where the (0.2, 1) system gave the opposite node to that given by the other systems. The (0.25, 2) system appeared to be slightly preferable for more dispersed streams because of being somewhat faster in their delineating, and just as good as the (0.2, 1) one for more concentrated streams. Also, the quadratic form of the former approximates a Gaussian-type curve, which is the postulated stream-membership probability function, much better than does the plain linear form of the (0.2, 1) system. As a result, we found the (0.25, 2) weighting system most convenient and applied it throughout.

9. RESULTS OF THE STREAM SEARCH

9.1 List of the Detected Radio Streams

Detection of any particular stream in different samples depends on the degree of compatibility of the corresponding observing schedules. The observing schedule of the synoptic year is given in Table 9-1, for comparison with the 1961−1965 observing schedule (see Table I of Paper I).

The orbits of possible streams provided by the Southworth-Hawkins search program, plus the orbits of potential parent or related bodies, of the streams detected in the 1961−1965 sample, and of suspected twin showers, produced a total of 473 entries for Phase II of our search and resulted in detecting in the synoptic-year sample 256 streams, 200 of which were not found in the previous radio meteor sample.

The orbital elements and related parameters of the streams detected in the synoptic-year sample are listed in Table 9-2. The individual columns give the following information (all angular data are referred to the standard equinox 1950.0):

Column 1. Designation of the stream.

Column 2. Argument of perihelion ω and its mean error (degrees).

Column 3. Longitude of ascending node Ω and its mean error (degrees).

Column 4. Inclination i and its mean error (degrees).

Column 5. Perihelion distance q and its mean error (a.u.).

Column 6. Eccentricity e and its mean error.

Column 7. Semimajor axis a (a.u.) and revolution period P (years).

Column 8. Longitude of perihelion $\pi = \omega + \Omega$ (degrees) and the date of passage through the node (UT and days in 1950).

Column 9. No-atmosphere velocity V_∞ and its mean error (km sec^{-1}).

Column 10. Right ascension α_R of the corrected mean radiant from individual meteor radiants and its mean error (degrees).

Column 11. Declination δ_R of the corrected mean radiant from individual meteor radiants and its mean error (degrees).

Column 12. Right ascension α_R and sun-oriented celestial longitude $\lambda_R - \lambda_\odot$ of the corrected mean radiant from the stream's mean orbit (degrees).

Column 13. Declination δ_R and celestial latitude β_R of the corrected mean radiant from the stream's mean orbit (degrees).

Column 14. Geocentric V_G and heliocentric V_H velocity at the node (km sec^{-1}).

Column 15. The node (A — ascending; D — descending), and the type of stream (C — circumpolar, with the mean radiant permanently above the horizon at Havana; D — daytime; M — mixed, with the mean radiant never more than 10° below the horizon; N — nighttime).

Column 16. Height at maximum ionization h_{max} and its mean error (km).

Column 17. Number of meteors in the sample with D < 0.25 with respect to the mean orbit, with an asterisk to indicate that the stream was detected in the 1961—1965 sample.

9.2 Identification of Streams Detected in the 1961—1965 Sample

The D-test was used to identify in the synoptic-year sample the streams previously found in the 1961—1965 sample. With an identification threshold of $D_i = 0.2$, we were able to identify 55 of the 83 streams of the 1961—1965 sample; 1 more stream was probably detected, though with $D_i = 0.26$; and 27 streams were not found. The doubtful case is the Quadrantid shower. With the radar network idle during the period of the shower's maximum activity, the search program detected a minor stream with the mean orbit similar to that of the Quadrantids, but with the node shifted by 13° forward, thus matching the nearest operational period of the radar. Of the 27 streams apparently absent in the synoptic-year sample, positively three (January Scutids, Andromedids, and December Ursids) and probably two more (ρ Geminids and November Cepheids) could not be detected, because of gaps in the operational schedule in the critical periods. In 5 cases of the 22 remaining unidentified streams (Equuleids,

Table 9-1. Observing schedule of the Havana meteor radar during the synoptic year.

Date (CST)	Number of successfully reduced meteors	(%)	Date (CST)	Number of successfully reduced meteors	(%)
1968			1969 (cont.)		
December 2−6	498	2.53	June 16−21	701	3.56
December 14	212	1.08	June 30−July 4	977	4.96
December 16−20	269	1.37	July 14−19	1059	5.38
			July 21	3	0.01
1969			July 25−26	11	0.06
January 13−17	808	4.10	July 28−August 1	1272	6.46
January 27−31	618	3.14	August 11−15	1373	6.97
February 10−14	496	2.52	August 17−18	175	0.89
February 24	75	0.38	August 25−30	892	4.53
February 26−28	89	0.45	September 7	219	1.11
March 10−14	557	2.83	September 9−12	1239	6.29
March 17−19	25	0.13	September 18	49	0.25
March 23−28	404	2.05	September 22−26	1210	6.14
April 7−9	497	2.52	October 6−10	1369	6.95
April 11−12	39	0.20	October 14−15	44	0.22
April 17	109	0.55	October 20−24	1117	5.67
April 20−21	71	0.36	November 3−8	1124	5.70
April 24−25	133	0.67	November 14	8	0.04
May 5−9	490	2.49	November 16	39	0.20
May 19−23	573	2.91	December 12−14	157	0.80
June 2−6	694	3.52			
June 11−12	3	0.01	Total	19,698	100.00

Table 9-2. List of 256 streams detected among 19,698 radio meteors of the synoptic-year sample.

1	2	3	4	5	6	7	8	9	10	11	12	13	14	15	16	17
BETA TRIANGULIDS	198.3	286.7	4.7	.930	.503	1.871	125.0	14.3	31.0	33.0	37.4	37.1	8.5	D	83.6	32
	5.2	5.1	.6	.009	.012	2.56	JAN 7.6	.2	3.1	2.5	120.5	21.1	37.4	N	2.9	
ZETA AURIGIDS	221.0	293.2	11.1	.901	.513	1.851	154.2	16.2	83.8	58.0	83.9	58.3	11.9	D	89.3	22 *
	1.5	1.2	.6	.006	.013	2.52	JAN 13.9	.2	2.1	1.6	152.9	34.9	36.4	U	2.0	
JANUARY BOOTICS	346.4	294.2	59.9	.836	.090	.919	280.6	31.4	225.8	44.2	225.5	43.6	29.4	D	90.0	15
	8.2	.1	1.0	.014	.017	.88	JAN 14.9	.4	1.1	.5	267.3	56.9	28.5	M	1.2	
THETA CORONA BOREALIDS	43.5	294.5	74.7	.647	.250	.863	338.0	36.9	231.6	31.1	231.9	30.9	35.3	D	91.1	20
	2.9	.1	.6	.013	.017	.80	JAN 15.2	.2	.8	.5	283.6	47.7	27.7	D	.7	
LAMBDA BOOTICS	211.9	294.5	77.6	.944	.315	1.378	146.4	41.8	218.3	44.0	218.4	44.1	40.5	D	93.8	23
	2.5	.1	.7	.005	.011	1.62	JAN 15.2	.3	.6	.4	258.7	54.7	34.2	M	1.8	
CORONA BOREALIDS	114.5	294.6	78.2	.880	.219	1.127	49.1	40.7	232.8	34.6	233.4	34.4	39.3	D	92.7	32
	3.0	.1	.5	.007	.012	1.20	JAN 15.3	.2	.4	.3	283.3	51.4	31.9	D	.4	
CANIDS	70.2	114.8	1.4	.700	.770	3.045	185.0	22.5	105.5	20.2	105.7	20.3	19.8	A	90.2	11 *
	1.9	1.6	.7	.013	.010	5.31	JAN 15.5	.3	.9	1.3	169.9	-2.3	38.9	N	.8	
QUADRANTIDS	152.6	295.1	73.1	.941	.612	2.424	87.7	42.4	241.5	41.1	241.7	41.1	41.2	D	92.3	14 *
	1.3	.2	1.2	.004	.013	3.77	JAN 15.8	.5	.8	.7	289.1	60.1	37.9	M	.7	
JANUARY SAGITTARIIDS	66.6	295.3	4.3	.303	.780	1.744	1.9	28.4	283.8	-18.6	284.1	-18.7	26.3	D	84.6	14
	.9	.1	.7	.008	.014	2.30	JAN 16.0	.6	.4	.7	348.1	4.1	35.8	D	4.7	
JANUARY DRACONIDS	185.8	295.3	44.9	.979	.449	1.775	121.1	28.1	245.9	62.4	246.6	62.7	26.0	D	93.1	32
	1.5	.2	.7	.001	.011	2.36	JAN 16.0	.3	1.3	.6	254.9	79.3	36.2	U	.9	
DELTA CANCRIS	291.3	296.4	1.5	.397	.783	1.829	227.7	28.4	129.8	19.8	130.0	19.9	26.4	D	88.1	37 *
	1.5	1.6	.6	.009	.013	2.47	JAN 17.1	.4	1.1	.6	190.8	1.5	36.2	N	1.1	
JANUARY CANCRIDS	271.4	300.2	3.7	.576	.684	1.823	211.6	23.5	125.1	24.9	125.4	24.9	20.9	D	86.8	25
	1.5	1.5	.8	.009	.015	2.46	JAN 20.8	.3	1.1	1.1	181.6	5.3	36.2	N	1.2	
PSI LEONIDS	304.9	303.2	2.9	.295	.807	1.528	248.1	30.4	143.2	16.9	143.4	16.9	28.4	D	87.8	38
	1.3	1.3	.6	.009	.010	1.89	JAN 23.8	.4	.8	.5	197.0	2.3	34.8	N	.9	
XI SAGITTARIIDS	46.9	304.9	1.1	.285	.736	1.080	351.8	26.6	283.2	-21.9	283.7	-21.9	24.4	D	85.1	26
	1.8	1.4	.7	.010	.016	1.12	JAN 25.4	.6	1.0	.6	337.8	.9	31.0	D	2.6	
JANUARY AQUARIDS	106.3	305.3	6.7	.748	.504	1.508	51.6	17.7	309.8	-2.0	310.2	-2.3	14.0	D	78.8	14
	1.5	1.9	.9	.009	.015	1.85	JAN 25.8	.3	1.6	2.3	6.7	15.5	34.8	D	1.6	
CAPRICORNIDS-SAGITTARIIDS	69.8	309.1	6.2	.415	.758	1.712	18.9	27.3	298.9	-14.2	299.2	-14.3	25.1	D	84.3	29 *
	1.4	1.3	.6	.009	.012	2.24	JAN 29.6	.3	.9	.6	349.3	6.3	35.7	D	1.6	

60

Table 9-2. (Cont.)

1	2	3	4	5	6	7	8	9	10	11	12	13	14	15	16	17
H DRACGNIDS	215.5 1.4	309.3 .3	27.0 .7	.916 .005	.572 .013	2.143 3.14	164.8 JAN 29.7	21.8 .3	174.5 6.3	76.8 .7	169.1 165.6	78.4 62.1	18.7 37.3	D U	90.7 1.0	24
IOTA DRACONICS	244.3 4.9	309.9 .3	37.1 .9	.912 .009	.146 .015	1.068 1.10	194.2 JAN 30.3	22.7 .4	228.8 1.9	58.1 .9	228.8 233.7	58.5 69.8	19.9 31.2	D U	93.3 2.2	17
PSI CYGNIDS	152.0 2.0	310.2 .2	30.4 .5	.940 .006	.623 .014	2.492 3.93	102.2 JAN 30.6	22.9 .2	297.8 1.2	51.4 1.4	298.1 16.4	51.4 69.4	20.2 38.0	D U	87.9 1.3	10
ALPHA LEONIDS	143.2 2.2	130.7 2.3	3.7 .7	.198 .012	.801 .016	.993 .99	273.9 JAN 31.1	29.3 .6	159.2 1.0	6.2 .6	158.6 207.1	6.4 -2.4	27.2 29.9	A N	84.1 1.2	29 *
LAMBDA CAPRICORNICS	108.0 1.5	313.5 1.5	1.5 .8	.702 .010	.716 .013	2.473 3.89	61.5 FEB 2.9	21.4 .3	323.7 1.4	-11.3 1.4	324.0 9.1	-11.4 2.7	18.5 37.9	D D	83.7 1.8	16
DELTA LEONIDS	91.3 1.6	133.8 1.8	6.4 .7	.580 .010	.676 .012	1.788 2.39	225.1 FEB 3.2	23.5 .2	135.2 1.2	7.5 1.0	135.4 181.9	7.4 -9.1	20.9 36.1	A N	85.6 1.2	37 *
EPSILCN AQUARIDS	84.8 1.5	315.1 1.7	8.8 .8	.529 .010	.741 .013	2.044 2.92	39.9 FEB 4.5	25.4 .3	310.2 1.3	-6.8 1.0	310.5 356.0	-6.8 11.1	23.1 36.9	D D	84.3 1.8	25
FEBRUARY DRACCNIDS	189.8 1.1	318.9 .9	31.7 .5	.978 .002	.569 .008	2.270 3.42	148.7 FEB 8.2	22.8 .2	259.8 3.0	74.4 .6	260.6 146.6	75.1 80.9	20.0 37.6	D U	90.8 1.1	56
XI CYGNIDS	136.3 5.2	321.5 4.5	3.7 .7	.969 .005	.075 .012	1.047 1.07	97.8 FEB 10.8	11.4 .1	316.2 10.4	45.0 3.7	319.1 23.8	45.3 56.7	2.4 30.8	D M	80.6 1.0	20
KAPPA GEMINIDS	222.6 7.1	322.5 5.0	.8 .6	.942 .010	.156 .018	1.116 1.18	185.1 FEB 11.8	11.6 .1	113.0 7.2	23.9 4.4	119.7 153.7	27.6 6.8	3.7 31.9	D N	79.2 1.0	22
RHO LEONIDS	84.7 1.6	162.3 1.8	.5 .5	.618 .011	.711 .013	2.138 3.13	247.0 MAR 3.4	23.5 .3	160.9 1.2	7.3 .8	161.3 177.8	7.1 -.8	20.9 37.0	A N	86.5 .9	29
MU LECNIDS	226.0 2.9	343.2 3.0	5.8 .5	.878 .012	.556 .016	1.978 2.78	209.2 MAR 4.3	16.4 .3	145.0 2.0	32.1 1.4	145.9 154.3	31.5 16.8	12.3 36.7	D N	83.6 .7	23
PI VIRGINIDS	303.9 1.0	347.9 1.0	2.9 .5	.289 .007	.839 .007	1.792 2.40	291.8 MAR 9.0	31.9 .3	184.1 .6	.5 .4	184.4 196.0	.4 2.1	30.1 35.8	D N	88.5 .8	60 *
NORTHERN ETA VIRGINICS	281.8 1.1	349.3 .6	11.3 .7	.501 .008	.703 .013	1.690 2.20	271.1 MAR 10.4	25.8 .4	182.2 .6	13.8 .8	182.3 187.3	13.6 13.4	23.5 35.4	D N	81.4 1.1	26 *
LEONICS-URSIDS	241.8 1.9	349.5 .1	8.5 1.2	.814 .010	.518 .018	1.691 2.20	231.3 MAR 10.6	17.7 .3	166.6 1.8	28.1 2.6	166.5 166.7	28.3 20.7	13.9 35.5	D N	83.2 .7	10
SOUTHERN ETA VIRGINICS	101.8 1.1	170.4 0.0	2.6 .9	.499 .009	.706 .011	1.697 2.21	272.2 MAR 11.5	25.3 .4	175.2 .6	-1.5 1.0	175.4 105.9	-1.4 -3.1	22.9 35.5	A N	85.6 2.0	16 *

Table 9-2. (Cont.)

1	2	3	4	5	6	7	8	9	10	11	12	13	14	15	16	17
MARCH HERCULIDS	346.3 4.8	350.6 .1	66.1 .8	.835 .010	.091 .013	.918 .88	336.9 MAR 11.7	33.6 .4	261.0 .5	31.8 .3	261.3 266.5	31.5 54.6	31.9 28.4	D N	89.4 .5	14
CHI HERCULIDS	274.6 3.4	350.8 .2	49.9 .9	.802 .007	.227 .015	1.039 1.06	265.4 MAR 11.9	28.3 .4	243.5 1.3	40.6 .5	243.5 236.6	40.1 59.7	26.1 30.2	D M	89.6 .4	14
SOUTHERN VIRGINIDS	310.6 1.2	355.3 1.2	6.4 .5	.288 .008	.759 .010	1.196 1.31	305.9 MAR 16.4	28.4 .3	196.0 .8	-1.0 .4	196.0 199.9	-1.2 5.2	26.2 32.1	D N	86.8 1.0	63 *
MARCH VIRGINICS	256.4 3.0	1.9 3.6	2.4 .8	.853 .011	.238 .018	1.119 1.18	258.3 MAR 23.0	13.2 .2	180.7 3.6	11.5 2.8	180.7 174.4	10.7 10.1	7.3 31.3	D N	80.5 1.5	19
MARCH LYRIDS	19.2 3.9	4.5 .2	62.4 .8	.732 .014	.161 .018	.873 .82	23.7 MAR 25.7	31.6 .4	275.5 .9	31.5 .4	275.8 274.1	31.4 54.7	29.7 27.4	D D	89.9 1.4	17
HERCULIDS-LYRIDS	183.2 8.2	4.7 .3	66.2 1.1	.984 .007	.069 .013	1.057 1.09	187.9 MAR 25.9	34.6 .4	272.3 .7	34.6 .6	271.7 268.0	35.2 58.6	33.3 31.0	D N	90.7 1.3	15
TAU DRACONIDS	169.0 1.3	5.8 .9	33.0 .6	.988 .002	.542 .012	2.156 3.17	174.8 MAR 27.0	23.1 .3	286.4 2.5	69.1 .6	285.5 29.8	69.7 83.5	20.2 37.0	D U	88.5 .8	40 *
PI DRACCNIDS	135.7 2.8	11.0 1.9	15.2 .8	.960 .004	.162 .012	1.146 1.23	146.7 APR 1.2	14.2 .2	318.0 5.0	65.2 1.0	317.8 11.8	66.8 71.5	8.7 31.6	D U	81.6 .9	20 *
NORTHERN VIRGINIDS	310.3 1.5	11.9 1.6	4.8 .5	.278 .008	.785 .011	1.295 1.47	322.2 APR 2.1	29.5 .3	210.5 .8	-8.4 .5	210.4 199.4	-8.5 3.6	27.4 32.7	D N	84.3 1.2	63 *
LIBRICS	326.7 1.8	15.2 1.9	5.8 .6	.191 .009	.794 .014	.926 .89	341.9 APR 5.5	28.3 .6	224.3 .7	-12.8 .4	223.2 209.3	-12.6 3.8	26.0 28.0	D N	85.4 1.1	38 *
LAMBDA AURIGICS	162.4 3.7	16.6 2.9	2.6 .6	.983 .003	.227 .013	1.272 1.43	179.0 APR 6.9	11.8 .1	80.5 5.5	40.0 4.1	81.3 66.9	46.5 23.3	3.8 33.0	D M	82.1 .9	35
APRIL VIRGINICS	291.5 1.4	17.5 .1	15.3 1.1	.434 .011	.711 .013	1.501 1.84	309.0 APR 7.8	27.1 .4	213.1 1.0	3.6 1.1	213.2 192.3	3.4 15.8	24.8 34.3	D N	89.0 1.0	12 *
NU HERCULIDS	305.6 3.2	18.1 .2	65.8 .5	.751 .013	.189 .016	.926 .89	323.7 APR 8.4	33.6 .2	271.2 .7	30.0 .3	271.2 253.6	30.0 53.4	31.9 28.5	D N	89.0 1.1	18
ALPHA VIRGINICS	106.7 1.2	198.4 1.3	1.5 .5	.477 .008	.691 .010	1.541 1.91	305.1 APR 8.7	25.0 .3	203.6 .8	-11.7 .6	203.9 188.0	-11.8 -1.7	22.7 34.5	A N	86.7 1.0	61 *
EPSILCN LYRIDS	11.2 7.4	18.4 .8	44.5 1.0	.865 .016	.077 .018	.938 .91	29.6 APR 8.7	24.6 .4	280.6 1.2	42.4 .5	280.3 269.8	42.1 64.9	22.1 28.5	D M	89.1 1.1	10
APRIL CYGNIDS	139.8 .9	18.5 .1	66.4 .6	.898 .004	.768 .012	3.863 7.59	158.3 APR 8.8	40.4 .3	303.3 .7	44.4 .5	303.4 307.3	44.6 61.7	39.0 39.3	D M	95.1 .5	30

62

Table 9-2. (Cont.)

1	2	3	4	5	6	7	8	9	10	11	12	13	14	15	16	17
MARCH ANDROMEDIDS	144.6	18.6	13.9	.928	.605	2.350	163.2	17.3	31.8	56.7	32.9	58.1	13.2	D	86.8	26
	1.7	1.4	.9	.006	.009	3.60	APR 8.9	.3	3.1	1.9	35.0	41.7	37.4	U	1.0	*
Q DRACONIDS	172.6	19.9	48.1	.997	.578	2.359	192.5	30.3	281.2	57.6	280.8	57.8	28.2	D	89.7	15
	1.7	.4	1.0	.001	.009	3.62	APR 10.3	.5	1.5	.9	284.9	79.9	37.4	U	.7	
GAMMA VIRGINICS	240.8	25.2	.5	.829	.517	1.717	266.0	16.9	188.7	-2.1	188.9	-2.5	13.0	D	85.1	10
	1.7	1.9	1.0	.009	.024	2.25	APR 15.7	.3	1.9	2.1	164.0	1.2	35.3	N	2.1	
THETA LIBRIDS	332.0	27.9	2.7	.101	.920	1.269	359.9	36.3	236.3	-18.4	235.6	-18.7	34.2	D	92.7	20
	1.9	2.1	.9	.009	.009	1.43	APR 18.4	.7	2.7	.4	209.7	1.0	31.8	N	1.2	
APRIL URSIDS	183.5	28.2	9.4	.993	.473	1.885	211.7	14.2	149.3	54.9	152.3	58.8	8.6	D	84.0	21
	3.3	2.7	.9	.003	.013	2.59	APR 18.7	.2	5.9	3.0	101.1	43.5	36.2	U	1.0	*
G DRACONIDS	188.7	31.4	33.0	.997	.591	2.438	220.1	23.4	248.4	65.3	248.4	65.5	20.6	D	90.4	25
	1.7	1.6	.7	.002	.011	3.81	APR 22.0	.3	2.6	.8	145.5	81.2	37.5	U	1.2	
ETA TAURIDS	131.3	34.8	1.2	.877	.588	2.130	166.1	16.3	58.3	23.6	58.8	23.9	12.0	D	83.9	42
	1.3	1.3	.6	.006	.008	3.11	APR 25.5	.2	1.1	1.7	26.9	3.5	36.7	D	.7	
ALPHA AURIGIDS	148.2	37.4	5.8	.950	.372	1.514	185.6	13.4	82.8	50.2	78.6	51.1	7.4	D	84.4	46
	3.1	3.1	.5	.008	.012	1.86	APR 28.2	.2	3.4	2.0	44.5	28.0	34.7	U	.8	
R DRACONIDS	148.6	46.4	25.7	.981	.147	1.150	195.0	17.7	291.8	65.3	291.5	67.4	13.8	D	82.9	17
	6.3	1.3	.8	.008	.014	1.23	MAY 7.4	.3	4.3	.9	329.2	81.6	31.6	U	1.1	
GAMMA PEGASIDS	25.6	47.1	42.0	.108	.889	.967	72.7	34.8	1.6	17.7	1.7	17.5	33.0	D	91.2	16
	.7	.1	.8	.006	.007	.95	MAY 8.2	.6	.8	.5	321.6	15.3	28.5	D	.6	
MAY PISCIDS	35.9	47.3	29.1	.147	.896	1.412	83.2	35.8	11.9	19.0	12.1	19.0	34.1	D	92.8	18
	.9	.1	.8	.006	.006	1.68	MAY 8.4	.4	.6	.3	331.3	12.7	33.4	D	.6	
EPSILON ARIETIDS	90.0	47.4	2.8	.592	.708	2.026	137.4	23.2	43.6	20.9	44.0	21.0	20.6	D	86.7	25
	1.4	1.2	.7	.010	.012	2.88	MAY 8.5	.3	.9	1.0	.3	4.1	36.3	D	1.1	
OMICRON CETIDS	213.9	227.9	32.6	.122	.925	1.623	81.8	38.1	21.5	-4.0	21.9	-3.9	36.6	A	90.9	11
	1.2	1.0	1.0	.006	.006	2.07	MAY 9.0	.5	.7	.6	330.9	-12.1	34.7	D	.7	*
MAY ARIETIDS	60.8	54.3	3.4	.363	.763	1.528	115.1	27.4	36.5	17.8	36.8	17.9	25.2	D	88.6	56
	1.3	1.4	.5	.008	.010	1.89	MAY 15.6	.3	.9	.5	346.0	3.2	34.1	D	.5	
SOUTHERN MAY OPHIUCHIDS	130.0	237.1	3.5	.264	.824	1.502	7.1	30.9	254.0	-25.0	254.3	-25.1	29.0	A	90.1	22
	2.1	2.4	.6	.012	.016	1.84	MAY 18.5	.7	1.5	.5	198.7	-2.4	33.8	N	.8	*
NORTHERN MAY OPHIUCHIDS	308.3	57.6	13.5	.283	.807	1.464	5.9	30.7	256.2	-12.8	256.4	-13.1	28.7	D	88.1	30
	1.8	1.7	.7	.011	.014	1.77	MAY 19.0	.5	1.0	.5	199.0	9.7	33.6	N	1.3	*

63

Table 9-2. (Cont.)

1	2	3	4	5	6	7	8	9	10	11	12	13	14	15	16	17
EPSILON AQUILIDS	318.3 / 1.2	58.8 / .2	59.6 / .7	.354 / .010	.594 / .013	.873 / .82	17.1 / MAY 20.3	32.6 / .3	284.1 / .8	15.5 / .6	284.3 / 228.8	15.5 / 38.1	30.8 / 27.0	D / N	87.6 / 2.3	17
MAY URSIDS	169.7 / 1.5	58.9 / 1.0	23.3 / .5	1.004 / .002	.461 / .011	1.863 / 2.54	228.6 / MAY 20.4	18.3 / .2	232.8 / 4.3	75.5 / 1.0	232.7 / 63.5	76.7 / 74.9	14.6 / 35.8	D / U	90.8 / 1.0	35 *
MAY LYRIDS	228.1 / 3.3	59.0 / .2	47.2 / 1.0	.954 / .007	.205 / .015	1.201 / 1.32	287.1 / MAY 20.5	27.1 / .4	285.4 / .8	46.6 / .6	285.1 / 240.1	46.4 / 68.3	24.9 / 31.9	D / M	77.0 / 6.1	16
MAY DRACONIDS	185.2 / 1.0	60.5 / 1.0	29.6 / .5	1.009 / .001	.665 / .011	3.008 / 5.22	245.7 / MAY 22.1	22.2 / .3	239.5 / 1.6	64.5 / .7	239.9 / 114.5	64.6 / 77.5	19.3 / 38.2	D / U	88.9 / 1.0	29
MAY CASSIOPEIDS	90.5 / 2.6	68.1 / 1.6	17.1 / .6	.812 / .009	.261 / .014	1.099 / 1.15	158.6 / MAY 30.0	15.9 / .2	31.0 / 3.8	66.7 / .8	32.4 / 350.9	66.5 / 49.1	11.5 / 30.5	D / U	85.6 / .9	30
CHI SCORPIIDS	261.4 / 1.3	72.9 / 1.8	4.1 / .7	.663 / .009	.687 / .011	2.116 / 3.08	334.3 / JUN 4.0	22.3 / .2	247.2 / 1.4	-14.9 / 1.0	247.4 / 175.2	-15.2 / 6.5	19.6 / 36.5	D / N	86.8 / 1.3	32 *
JUNE CAMELOPARDALIDS	126.4 / 1.1	74.8 / .3	27.9 / .5	.845 / .006	.699 / .012	2.807 / 4.70	201.2 / JUN 6.0	24.1 / .3	71.7 / 1.9	72.7 / .7	72.3 / 7.2	72.8 / 49.8	21.5 / 37.8	D / C	92.8 / 1.3	23
ARIETIDS	25.9 / .8	76.9 / .9	25.0 / .6	.085 / .004	.938 / .005	1.376 / 1.61	102.8 / JUN 8.1	37.6 / .6	39.1 / .7	23.8 / .3	39.5 / 327.6	23.6 / 7.8	35.7 / 32.2	D / D	92.5 / .6	48 *
PSI AURIGIDS	126.1 / 1.0	78.7 / 1.2	10.7 / .7	.852 / .006	.646 / .011	2.406 / 3.73	204.8 / JUN 10.0	18.7 / .2	102.2 / 1.4	47.7 / 1.4	102.3 / 20.3	48.1 / 25.0	15.2 / 37.1	D / M	85.4 / 1.0	27
JUNE AURIGIDS	110.2 / 2.0	80.0 / 2.5	2.0 / .6	.829 / .009	.390 / .014	1.358 / 1.58	190.2 / JUN 11.4	15.0 / .2	92.0 / 2.1	29.2 / 1.8	92.4 / 12.1	29.6 / 6.2	10.2 / 33.1	D / D	83.2 / .9	34
ZETA PERSEIDS	60.5 / 1.4	80.8 / 1.6	6.5 / .5	.365 / .009	.755 / .011	1.492 / 1.82	141.3 / JUN 12.2	27.3 / .3	63.3 / 1.1	27.1 / .5	63.7 / 345.9	27.4 / 6.1	25.1 / 33.8	D / D	86.9 / 1.6	56 *
M DRACONIDS	161.5 / 9.2	85.3 / .1	32.9 / 1.0	1.005 / .004	.067 / .015	1.077 / 1.12	246.8 / JUN 16.9	20.1 / .4	300.1 / 2.3	62.5 / .9	299.5 / 277.1	64.1 / 77.6	17.0 / 30.6	D / U	88.1 / 1.1	13
OPHIUCHIDS	279.3 / 1.4	85.5 / 1.6	.3 / .6	.503 / .011	.774 / .014	2.224 / 3.32	4.8 / JUN 17.1	26.5 / .4	269.5 / 1.1	-22.8 / .7	269.1 / 184.0	-23.1 / .3	24.3 / 36.6	D / N	87.9 / .8	28 *
JUNE LYRIDS	224.1 / 1.5	85.5 / .2	45.3 / .8	.912 / .007	.556 / .021	2.054 / 2.94	309.6 / JUN 17.1	29.1 / .3	281.9 / 1.3	43.6 / .9	281.5 / 205.6	43.8 / 66.4	27.1 / 36.3	D / M	88.0 / 2.6	11
JUNE CYGNIDS	192.8 / 5.3	85.6 / .1	55.3 / .8	1.005 / .004	.114 / .012	1.134 / 1.21	278.4 / JUN 17.2	30.0 / .4	314.8 / .9	54.0 / .5	314.0 / 265.7	54.3 / 65.8	28.2 / 31.3	D / U	91.1 / .5	24
JUNE AQUILIDS	329.5 / .6	85.8 / .7	39.3 / .6	.114 / .004	.916 / .005	1.348 / 1.57	55.3 / JUN 17.5	37.9 / .4	297.1 / .6	-7.1 / .5	297.6 / 212.4	-7.2 / 13.6	36.3 / 32.5	D / N	91.2 / .7	35

Table 9-2. (Cont.)

1	2	3	4	5	6	7	8	9	10	11	12	13	14	15	16	17
SCORPIIDS-SAGITTARIIDS	113.8 / 1.4	270.4 / 1.5	2.5 / .6	.384 / .010	.799 / .011	1.908 / 2.64	24.2 / 22.3 JUN	28.8 / .3	282.2 / 1.1	-25.2 / .5	282.5 / 190.9	-25.2 / -2.2	26.8 / 35.7	A / N	86.5 / 1.9	31 / *
ALPHA DRACONIDS	168.0 / 1.6	90.5 / 1.5	21.7 / .5	1.000 / .002	.596 / .008	2.479 / 3.90	258.5 / 22.4 JUN	18.7 / .2	207.4 / 2.6	64.0 / .9	208.6 / 62.3	65.9 / 66.2	15.1 / 37.4	D / U	88.6 / 1.1	54
SIGMA CAPRICORNIDS	309.4 / 1.6	92.3 / 1.9	8.2 / .5	.332 / .007	.707 / .013	1.133 / 1.21	41.7 / 24.3 JUN	25.5 / .4	292.4 / 1.1	-13.6 / .5	292.4 / 99.6	-14.1 / 7.7	23.2 / 30.7	D / N	85.9 / 1.3	45 / *
JUNE SCUTIDS	278.8 / 1.1	94.9 / 1.5	15.7 / .6	.599 / .006	.560 / .011	1.361 / 1.59	13.7 / 27.0 JUN	21.7 / .3	280.7 / 1.0	1.0 / .8	281.1 / 187.3	.9 / 23.9	18.9 / 32.9	D / N	84.5 / 1.2	32 / *
THETA AURIGIDS	83.6 / 1.5	95.3 / 1.9	4.4 / .4	.631 / .009	.521 / .011	1.315 / 1.51	178.9 / 27.4 JUN	19.2 / .2	92.6 / 1.5	31.4 / .8	93.0 / 357.3	31.4 / 8.0	15.8 / 32.7	D / D	85.2 / .5	41
TAURIDS-ARIETIDS	16.2 / 1.4	98.6 / 1.3	9.9 / .8	.060 / .006	.927 / .008	.820 / .74	114.8 / 30.9 JUN	32.5 / .7	52.7 / 1.9	22.1 / .7	54.3 / 318.7	22.6 / 3.1	30.1 / 24.6	D / D	90.1 / .9	27
MU SAGITTARIIDS	263.3 / 2.0	98.7 / 2.2	1.5 / .4	.665 / .013	.642 / .014	1.858 / 2.53	2.0 / 31.0 JUN	21.1 / .2	274.3 / 1.4	-20.7 / .7	274.8 / 175.8	-20.9 / 2.5	18.3 / 35.6	D / N	81.9 / 1.4	30
AQUARIDS-AQUILIDS	326.7 / .7	99.0 / .6	43.1 / .7	.152 / .004	.867 / .006	1.143 / 1.22	65.7 / 1.3 JUL	35.6 / .4	310.1 / .6	.5 / .5	310.5 / 214.1	.5 / 18.1	33.8 / 30.7	D / N	91.0 / .6	38
CHI SAGITTARIIDS	108.4 / 1.3	279.5 / .1	3.9 / 1.0	.430 / .009	.783 / .014	1.981 / 2.79	27.9 / 1.8 JUL	27.7 / .4	289.7 / .7	-26.1 / .9	290.0 / 188.4	-26.1 / -3.9	25.6 / 36.0	A / N	82.2 / 3.0	11
P DRACONIDS	162.4 / 2.0	99.7 / .3	20.7 / .6	1.003 / .002	.322 / .016	1.479 / 1.80	262.1 / 2.0 JUL	16.6 / .2	227.3 / 4.5	70.6 / 1.2	226.4 / 43.0	71.5 / 74.0	12.4 / 33.9	D / U	85.1 / 2.2	19
BOOTIDS-DRACONIDS	184.0 / 1.5	99.8 / .2	21.3 / 1.1	1.014 / .001	.596 / .019	2.511 / 3.98	283.8 / 2.1 JUL	18.3 / .4	233.7 / 3.1	52.2 / 1.8	233.8 / 100.3	52.8 / 67.7	14.7 / 37.3	D / U	89.8 / 1.6	12
J DRACONIDS	186.2 / 1.8	99.8 / .1	38.0 / .6	1.012 / .001	.416 / .016	1.733 / 2.28	286.0 / 2.1 JUL	24.3 / .2	280.9 / 1.9	63.8 / .8	280.5 / 233.9	63.9 / 84.9	21.7 / 35.2	D / U	92.1 / 1.5	21
EPSILON CEPHEIDS	5.8 / 8.7	99.8 / .1	58.0 / 1.1	.892 / .012	.069 / .015	.958 / .94	105.6 / 2.1 JUL	30.0 / .4	331.5 / 1.1	55.6 / .4	332.8 / 270.8	55.8 / 59.4	28.0 / 28.4	D / U	89.5 / 1.0	14
BETA ANDROMEDIDS	8.9 / .9	99.8 / .1	58.7 / 1.2	.139 / .006	.768 / .011	.601 / .47	108.7 / 2.1 JUL	28.2 / .3	13.4 / 2.1	36.4 / .9	13.6 / 288.1	36.9 / 28.4	26.0 / 16.1	D / D	85.9 / 1.0	13
LACERTIDS	192.7 / 9.0	99.9 / .1	75.6 / .6	.995 / .005	.113 / .013	1.122 / 1.19	292.6 / 2.2 JUL	38.3 / .3	336.8 / .8	50.7 / .5	336.2 / 268.1	51.4 / 54.8	37.2 / 31.4	D / U	88.6 / 2.8	21
OMEGA DRACONIDS	168.5 / 3.7	100.0 / 1.3	21.2 / .5	1.004 / .002	.133 / .010	1.159 / 1.25	268.5 / 2.3 JUL	15.9 / .2	266.3 / 3.3	68.9 / 1.1	266.2 / 11.1	69.0 / 86.4	11.4 / 31.5	D / U	85.5 / 1.5	48

65

Table 9-2. (Cont.)

1	2	3	4	5	6	7	8	9	10	11	12	13	14	15	16	17
CYGNIDS-DRACONIDS	218.4 4.1	100.0 .1	36.8 .6	.975 .007	.190 .014	1.203 1.32	318.4 JUL 2.3	22.4 .3	295.2 1.4	56.6 1.0	293.7 229.5	56.6 75.1	19.7 31.9	D U	86.1 2.5	24
KAPPA PERSEIDS	34.5 .7	100.0 .1	65.0 1.0	.198 .006	.793 .009	.959 .94	134.5 JUL 2.3	36.7 .4	44.2 1.3	44.7 .4	44.6 315.5	44.7 26.5	35.1 28.3	D M	90.9 .6	18
BETA TAURIDS	52.3 .8	102.0 .8	.3 .6	.274 .007	.834 .007	1.653 2.13	154.3 JUL 4.4	31.0 .4	83.9 .7	23.6 .4	84.1 342.6	23.5 .2	29.0 34.5	D D	89.8 .6	41 *
KAPPA AURIGIDS	73.0 .9	104.1 1.2	6.4 .7	.457 .006	.747 .011	1.809 2.43	177.1 JUL 6.6	26.5 .4	96.5 1.1	30.2 .8	96.9 351.9	30.2 6.9	24.2 35.3	D D	87.4 .9	32
TAU CAPRICORNIDS	311.2 1.5	109.5 1.7	4.5 .6	.272 .008	.792 .011	1.310 1.50	60.7 JUL 12.3	29.0 .3	310.6 1.1	-14.7 .4	310.4 199.4	-14.7 3.5	26.9 32.6	D N	88.8 .8	40
UPSILON DRACONIDS	168.3 1.1	112.5 .2	44.0 .7	1.008 .002	.557 .014	2.276 3.43	280.8 JUL 15.4	28.0 .3	283.2 2.7	74.0 .6	283.2 313.9	74.3 81.1	25.8 36.8	D U	92.4 1.3	19
SIGMA CASSIOPEIDS	31.5 4.4	112.5 .1	74.9 .7	.693 .010	.215 .013	.883 .83	144.0 JUL 15.4	36.1 .3	1.8 1.2	55.8 .5	2.5 279.5	55.7 48.4	34.2 26.7	D U	93.7 1.1	22
JULY CEPHEIDS	165.3 6.9	112.6 .2	56.5 .7	1.000 .004	.106 .010	1.118 1.18	277.9 JUL 15.5	30.5 .3	334.3 1.0	64.3 .6	333.5 274.0	65.1 65.1	28.7 31.2	D U	91.7 .8	31
JULY CASSIOPEIDS	47.7 7.7	112.6 .2	73.7 .7	.940 .009	.062 .011	1.003 1.00	160.3 JUL 15.5	36.7 .3	351.7 .6	56.8 .4	353.5 273.9	56.4 52.1	34.7 28.6	D U	92.7 .6	34
RHO DRACONIDS	198.3 3.3	112.7 .2	34.5 .9	1.006 .003	.131 .009	1.158 1.25	311.0 JUL 15.6	21.1 .4	298.9 1.5	64.7 .7	297.8 252.9	65.1 78.6	18.1 31.4	D U	90.3 1.0	21
KAPPA CASSIOPEIDS	83.7 2.2	113.1 .2	54.8 .8	.807 .008	.232 .011	1.052 1.08	196.8 JUL 16.1	29.9 .3	6.4 2.3	71.1 .6	6.1 299.2	71.5 58.9	27.8 29.9	D U	92.6 .7	25
CASSIOPEIDS	136.5 1.5	113.2 .2	76.1 .4	.939 .005	.375 .010	1.563 1.84	249.7 JUL 16.2	40.8 .2	1.9 .7	64.3 .4	2.0 287.8	64.6 55.4	39.3 34.0	D U	93.1 .5	46
J CEPHEIDS	45.5 6.1	113.4 .2	34.7 1.0	.875 .010	.093 .012	.965 .95	158.9 JUL 16.4	20.6 .4	330.4 2.5	72.4 1.0	331.1 289.7	72.5 68.9	17.4 28.5	D U	86.7 1.5	12
JULY DRACONIDS	155.4 1.3	113.6 .4	28.6 .9	.980 .004	.621 .013	2.586 4.16	269.0 JUL 16.6	22.0 .3	209.8 3.5	70.7 1.0	209.0 27.0	71.1 68.5	19.0 37.5	D U	90.6 1.3	18 *
ZETA URSIDS	148.3 4.6	113.7 2.8	7.4 .5	.992 .005	.108 .010	1.112 1.17	262.0 JUL 16.7	12.1 .1	205.4 5.0	57.4 2.0	198.8 40.4	62.2 60.6	4.6 31.0	D U	79.0 2.2	43
PSI CASSIOPEIDS	121.2 1.0	113.7 .2	72.1 .7	.821 .006	.660 .012	2.418 3.76	234.9 JUL 16.7	41.7 .3	28.3 1.4	71.0 .4	28.4 307.7	71.3 53.9	40.3 37.1	D U	94.4 1.1	25

66

Table 9-2. (Cont.)

1	2	3	4	5	6	7	8	9	10	11	12	13	14	15	16	17
CANES VENATICIDS	160.9 / 3.5	114.5 / 3.3	10.5 / .6	.973 / .008	.647 / .009	2.760 / 4.59	275.4 / JUL 17.5	16.3 / .3	191.3 / 2.7	33.3 / 1.7	119.3 / 57.4	35.9 / 36.2	11.7 / 38.2	D / D	85.6 / 1.0	30
OMICRON DRACONIDS	192.2 / .9	114.7 / .9	46.2 / 1.1	1.006 / .001	.768 / .018	4.329 / 9.01	306.9 / JUL 17.7	30.5 / .5	284.7 / 2.0	60.9 / .6	234.8 / 212.7	61.2 / 81.6	28.5 / 39.2	D / U	89.2 / 1.5	14
PI AQUARIDS	332.8 / 1.1	123.9 / 1.1	28.9 / .7	.095 / .007	.930 / .007	1.354 / 1.58	96.7 / JUL 27.4	37.4 / .8	333.9 / .5	-.4 / .6	334.8 / 212.6	-.3 / 9.5	35.3 / 31.9	D / N	91.8 / 1.2	31
SOUTHERN DELTA AQUARIDS	155.4 / .5	305.7 / .4	28.2 / .4	.069 / .003	.958 / .003	1.630 / 2.08	101.1 / JUL 29.3	40.0 / .4	341.8 / .4	-15.9 / .2	342.3 / 212.1	-15.5 / -7.4	38.2 / 33.9	A / N	93.4 / .6	70 / *
A CEPHEIDS	190.2 / 4.7	125.9 / .2	50.2 / .7	1.005 / .002	.104 / .010	1.121 / 1.19	316.1 / JUL 29.5	27.8 / .3	330.3 / 1.4	69.1 / .5	328.8 / 268.1	69.3 / 68.6	25.7 / 31.2	D / U	93.6 / 1.0	34
CEPHEIDS-DRACONIDS	170.3 / 1.1	126.1 / .2	50.7 / .8	1.009 / .001	.472 / .011	1.912 / 2.64	296.8 / JUL 29.7	30.6 / .3	304.5 / 2.7	75.2 / .5	305.1 / 287.8	75.5 / 75.9	28.6 / 35.8	D / U	95.5 / 1.1	24
OMICRON CEPHEIDS	16.0 / 3.9	126.3 / .2	55.7 / .6	.805 / .008	.124 / .010	.919 / .88	142.3 / JUL 29.9	29.0 / .2	355.9 / 1.1	67.3 / .4	356.5 / 275.3	67.1 / 58.7	26.6 / 27.6	D / U	90.5 / .7	42
IOTA CEPHEIDS	174.4 / 3.1	127.0 / .2	60.7 / .6	1.004 / .002	.229 / .010	1.302 / 1.49	301.4 / JUL 30.6	33.3 / .3	342.4 / 1.3	69.9 / .6	340.7 / 273.6	70.3 / 65.2	31.6 / 32.9	D / U	95.0 / 1.1	39
B CASSIOPEIDS	133.8 / 1.1	127.0 / .2	71.9 / .6	.910 / .005	.506 / .015	1.842 / 2.50	260.8 / JUL 30.6	40.2 / .3	25.0 / 1.9	74.6 / .5	24.9 / 297.0	74.9 / 57.4	38.8 / 35.6	D / U	96.5 / 1.1	22
GAMMA CEPHEIDS	127.7 / 2.1	127.2 / .2	52.9 / .6	.930 / .006	.271 / .012	1.277 / 1.44	254.9 / JUL 30.8	30.1 / .3	2.5 / 4.3	80.3 / .6	358.7 / 301.2	81.1 / 65.2	28.0 / 32.5	D / U	95.1 / 1.3	40
B CEPHEIDS	128.7 / 1.3	127.7 / .2	55.9 / .6	.896 / .006	.449 / .010	1.626 / 2.07	256.4 / JUL 31.3	32.9 / .3	35.4 / 5.6	83.4 / .5	32.9 / 311.5	84.2 / 63.0	31.1 / 34.7	D / U	95.1 / 1.2	34
IOTA CASSIOPEIDS	72.5 / 2.0	127.8 / .2	67.1 / .6	.671 / .008	.359 / .013	1.047 / 1.07	200.3 / JUL 31.4	35.3 / .3	44.5 / 1.7	70.1 / .3	45.6 / 300.5	70.1 / 50.0	33.4 / 29.8	D / U	93.4 / 1.1	26
MU CANCRIDS	71.0 / 1.1	128.0 / 1.2	2.1 / .5	.443 / .008	.742 / .009	1.720 / 2.26	199.0 / JUL 31.7	26.5 / .3	121.7 / 1.0	22.4 / .5	122.0 / 351.3	22.5 / 2.3	24.3 / 35.0	D / D	90.2 / .5	43
D CAMELOPARDALIDS	81.6 / 1.4	128.4 / .2	36.4 / .7	.631 / .008	.497 / .012	1.255 / 1.41	210.0 / AUG 1.1	26.1 / .3	118.0 / 1.6	67.4 / .7	119.1 / 337.1	67.3 / 45.4	23.6 / 32.2	D / U	91.8 / 1.0	32
E DRACONIDS	102.7 / 1.9	128.9 / .2	30.6 / .6	.805 / .008	.363 / .012	1.263 / 1.42	231.6 / AUG 1.6	21.9 / .2	146.1 / 2.7	74.6 / .9	146.2 / 344.2	74.5 / 55.6	18.9 / 32.3	D / U	92.9 / 1.0	30
L DRACONIDS	131.9 / 1.0	129.0 / .2	72.8 / .6	.868 / .006	.769 / .014	3.761 / 7.29	260.9 / AUG 1.7	30.5 / .3	166.4 / 2.8	75.9 / .7	166.1 / 349.3	75.9 / 60.1	28.5 / 38.9	D / U	92.8 / 1.9	16

67

Table 9-2. (Cont.)

1	2	3	4	5	6	7	8	9	10	11	12	13	14	15	16	17
AUGUST LYNCIDS	95.0 / 1.2	129.9 / 1.5	13.9 / .7	.631 / .009	.707 / .010	2.153 / 3.16	224.9 / AUG 2.6	24.2 / .2	139.1 / 1.1	36.6 / 1.2	139.5 / .6	36.4 / 19.7	21.7 / 36.5	D / D	87.3 / .7	30
AQUARIDS-CAPRICORNIDS	293.1 / 1.1	134.9 / 1.1	1.3 / .4	.387 / .008	.802 / .008	1.950 / 2.72	68.0 / AUG 7.9	28.5 / .2	327.1 / .7	-11.8 / .5	327.5 / 190.7	-11.9 / 1.1	26.5 / 35.9	D / N	87.4 / .9	45 *
ALPHA CAPRICCRNIDS	267.9 / 1.2	136.6 / 1.3	6.1 / .5	.620 / .009	.677 / .011	1.920 / 2.66	44.5 / AUG 9.6	22.5 / .2	314.8 / .9	-7.1 / .9	315.2 / 178.9	-7.3 / 9.3	19.7 / 35.8	D / N	81.7 / 1.1	44 *
SOUTHERN IOTA AQUARICS	319.1 / 1.5	137.3 / 1.7	4.4 / .4	.249 / .007	.762 / .011	1.045 / 1.07	96.4 / AUG 10.4	26.8 / .4	343.0 / .8	-3.2 / .5	342.5 / 205.2	-3.7 / 3.5	24.5 / 29.4	D / N	87.6 / 1.2	65 *
BETA CEPHEIDS	182.2 / 2.8	139.2 / .2	55.1 / .6	1.007 / .002	.258 / .013	1.358 / 1.58	321.4 / AUG 12.3	31.1 / .3	333.3 / 2.1	74.2 / .6	331.5 / 270.2	74.8 / 69.2	29.2 / 33.3	D / U	96.7 / 1.5	25 *
C DRACONIDS	171.7 / 4.4	139.3 / .2	33.8 / .6	1.003 / .003	.103 / .013	1.119 / 1.18	311.0 / AUG 12.4	20.8 / .3	295.1 / 3.7	75.1 / .7	292.8 / 281.9	75.6 / 78.5	17.7 / 31.2	D / U	91.2 / 1.1	35
AUGUST CASSICPEIDS	34.6 / 6.4	139.6 / .2	62.9 / .7	.898 / .009	.071 / .011	.967 / .95	174.2 / AUG 12.8	32.3 / .3	10.8 / 1.2	70.9 / .4	13.2 / 275.3	71.3 / 57.1	30.3 / 28.6	D / U	94.4 / .7	39
GAMMA CYGNIDS	238.8 / 1.0	139.7 / .4	27.1 / .7	.880 / .006	.378 / .013	1.414 / 1.68	18.5 / AUG 12.9	20.1 / .2	303.2 / .5	42.7 / 1.4	303.2 / 184.1	42.7 / 60.1	17.0 / 33.5	D / M	87.1 / .7	17
PERSEIDS	152.5 / .9	139.7 / .2	110.2 / .7	.960 / .003	.881 / .014	8.040 / 22.80	292.2 / AUG 12.9	58.4 / .2	44.8 / .7	59.2 / .4	45.2 / 282.2	59.2 / 40.1	57.5 / 40.5	D / U	97.2 / .7	8
GAMMA CASSIOPEIDS	349.7 / 2.5	139.8 / .4	67.9 / .6	.582 / .011	.275 / .015	.802 / .72	129.5 / AUG 13.0	32.6 / .2	15.3 / 1.5	61.9 / .4	15.4 / 266.0	62.0 / 49.5	30.7 / 25.3	D / U	92.6 / 1.2	15
L CEPHEIDS	299.0 / 6.4	140.2 / .6	51.4 / .5	.897 / .008	.089 / .010	.985 / .98	79.2 / AUG 13.4	27.7 / .2	347.7 / 1.3	70.1 / .5	346.5 / 259.8	68.9 / 62.8	25.3 / 28.9	D / U	93.4 / .9	49
AUGUST CEPHEIDS	22.2 / 4.7	140.2 / .2	49.4 / .7	.859 / .008	.091 / .010	.945 / .92	162.4 / AUG 13.4	26.6 / .3	358.8 / 1.5	75.4 / .5	.8 / 277.0	75.5 / 62.5	24.1 / 28.2	D / U	95.1 / .9	35
AUGUST DRACONIDS	183.1 / .8	140.8 / .3	38.5 / .5	1.010 / .001	.636 / .009	2.776 / 4.63	323.9 / AUG 14.0	25.9 / .2	271.3 / 1.3	65.0 / .5	271.3 / 152.7	65.3 / 88.6	23.6 / 37.9	D / U	91.0 / .7	60
AUGUST CANCRIDS	262.0 / 1.6	321.1 / 1.8	2.1 / .5	.569 / .010	.627 / .013	1.527 / 1.89	223.1 / AUG 14.3	22.3 / .2	138.9 / 1.1	12.5 / .8	139.2 / 356.6	12.6 / -3.1	19.6 / 34.2	A / D	87.3 / 1.3	40
PHI DRACONIDS	185.6 / 1.6	141.2 / .3	30.4 / .4	1.007 / .001	.335 / .010	1.515 / 1.86	326.8 / AUG 14.4	20.5 / .2	272.4 / 1.9	64.9 / .7	272.5 / 165.1	65.1 / 88.2	17.3 / 34.2	D / U	87.4 / 1.1	54
AUGUST UMIDS	137.0 / 1.1	141.3 / .2	35.1 / .5	.922 / .004	.483 / .008	1.782 / 2.38	278.3 / AUG 14.5	24.3 / .2	199.6 / 2.0	72.7 / .6	198.6 / 352.1	72.9 / 66.1	21.7 / 35.5	D / U	89.7 / 1.2	47

68

Table 9-2. (Cont.)

1	2	3	4	5	6	7	8	9	10	11	12	13	14	15	16	17
E CAMELOPARDALIDS	65.3 2.2	141.4 .2	39.2 .7	.679 .008	.309 .012	.982 .97	206.7 AUG 14.6	24.0 .3	115.1 3.9	77.2 .6	117.3 313.6	77.4 54.9	21.3 28.9	D U	91.6 .9	31
AUGUST URSIDS	101.5 1.1	141.5 .3	36.5 .7	.759 .006	.458 .010	1.400 1.66	243.0 AUG 14.7	25.5 .3	154.3 1.4	69.4 .7	155.2 340.7	69.4 53.1	23.0 33.4	D U	89.3 .9	34
NORTHERN DELTA AQUARIDS	323.2 1.1	141.7 1.0	19.2 .5	.169 .006	.866 .008	1.259 1.41	104.9 AUG 14.9	32.9 .5	345.7 .6	4.8 .5	345.0 207.3	4.8 9.9	31.1 31.9	D N	84.6 1.2	45 *
AUGUST CAMELOPARDALIDS	131.0 .9	142.0 .3	54.8 .7	.893 .005	.524 .011	1.875 2.57	273.0 AUG 15.3	33.3 .3	139.5 7.5	84.1 .5	143.5 317.3	84.8 63.2	31.4 35.7	D U	95.5 .9	33
EPSILCN URSICS	108.6 4.8	146.8 3.4	7.6 .6	.949 .007	.104 .011	1.059 1.09	255.4 AUG 20.2	12.2 .1	192.1 3.7	54.9 2.0	184.9 6.5	55.5 50.8	5.1 30.2	D U	81.0 1.8	42
MU DRACONIDS	177.0 3.4	147.3 1.5	13.2 .6	1.001 .003	.183 .012	1.225 1.36	324.3 AUG 20.8	13.5 .2	250.2 3.0	52.4 1.7	248.9 73.6	53.8 73.7	7.7 32.3	D U	81.6 1.8	43
BETA URSIDS	59.0 5.6	148.5 2.5	6.4 .7	.860 .014	.111 .018	.968 .95	207.5 AUG 22.0	12.0 .2	155.7 4.7	56.1 2.6	156.9 344.7	57.3 43.4	4.7 28.9	D U	81.6 1.1	21
GAMMA LEONIDS	87.3 1.0	151.8 1.2	7.0 .6	.571 .008	.710 .008	1.969 2.76	239.1 AUG 25.4	24.5 .3	155.5 .9	20.1 .9	155.9 358.6	20.0 9.3	22.0 36.1	D D	89.9 .9	46
NORTHERN IOTA AQUARICS	307.4 1.4	152.4 1.7	5.2 .4	.302 .009	.777 .011	1.356 1.58	99.8 AUG 26.0	28.2 .3	349.5 1.0	.3 .6	349.6 198.1	.2 .3	26.1 33.0	D N	87.1 .6	54 *
CASSICPEIDS-CEPHEIDS	179.1 9.9	153.6 .2	63.7 .8	.997 .005	.077 .013	1.080 1.12	332.7 AUG 27.3	33.5 .3	22.0 2.6	77.3 .6	17.4 271.5	77.4 60.4	31.9 30.9	D U	93.3 1.3	15
A CASSIOPEIDS	256.9 5.8	153.8 .2	62.9 .9	.966 .007	.076 .012	1.045 1.07	50.7 AUG 27.5	32.9 .3	12.0 2.4	73.8 .4	12.3 263.6	73.4 58.8	30.9 29.8	D U	94.5 1.0	24
XI LECNIDS	238.4 .8	334.2 .1	2.5 .8	.330 .007	.793 .008	1.598 2.02	212.6 AUG 27.9	29.4 .3	141.2 .4	13.1 .7	141.4 345.4	13.0 -2.0	27.4 34.6	A D	93.6 1.0	25
OMEGA CASSIOPEIDS	9.0 3.8	154.5 .2	65.6 .7	.774 .009	.139 .011	.899 .85	163.5 AUG 28.2	32.9 .3	38.8 1.9	73.5 .4	39.1 273.4	73.4 53.9	30.9 27.4	D U	98.8 1.1	36
E URSIDS	108.6 1.4	155.3 .3	48.0 1.2	.778 .007	.511 .014	1.590 2.00	263.9 AUG 29.0	30.6 .5	163.3 2.2	70.6 .9	164.2 329.3	70.8 56.2	28.6 34.6	D U	94.6 1.6	14
F CAMELOPARDALIDS	64.2 2.0	155.9 .2	43.3 .8	.715 .008	.260 .011	.967 .95	220.1 AUG 29.7	25.2 .3	135.0 3.2	78.4 .8	137.3 310.0	78.5 57.7	22.6 28.8	D U	96.0 1.0	26
XI DRACCNIDS	181.4 1.2	161.9 1.0	32.3 .4	1.004 .001	.609 .010	2.565 4.11	343.3 SEP 4.9	23.0 .2	265.2 1.6	59.8 .5	265.4 87.8	60.3 83.4	20.3 37.7	D U	89.2 .8	49

69

Table 9-2. (Cont.)

1	2	3	4	5	6	7	8	9	10	11	12	13	14	15	16	17
SEPTEMBER LYRIDS	208.0 3.5	163.1 2.7	11.2 .6	.984 .004	.161 .010	1.173 1.27	11.1 SEP 6.1	12.9 .2	281.6 2.3	45.8 1.8	284.3 135.0	47.0 69.1	6.6 31.9	D M	79.0 2.5	44
ALPHA TRIANGULIDS	345.9 .9	165.7 .3	38.7 1.0	.087 .007	.870 .012	.669 .55	151.6 SEP 8.8	29.2 1.0	30.4 1.9	29.5 1.7	31.1 233.5	29.4 15.7	26.6 19.4	D N	88.3 .9	13
TAU LEONIDS	273.2 1.0	345.8 1.0	.9 .7	.616 .007	.698 .008	2.037 2.91	259.0 SEP 8.9	23.3 .2	167.8 .9	3.9 1.0	168.2 1.9	3.7 -1.3	20.7 36.4	A D	88.2 .7	30
D CEPHEIDS	181.3 1.0	166.5 .3	62.7 .7	1.006 .001	.571 .012	2.342 3.58	347.8 SEP 9.6	37.0 .3	327.2 5.6	83.7 .4	324.6 270.7	84.5 69.3	35.3 37.2	D U	95.2 .9	30
C CASSICPEIDS	217.2 3.4	166.6 .3	69.5 1.1	.972 .006	.194 .014	1.206 1.32	23.8 SEP 9.7	36.8 .4	29.2 2.8	76.6 .5	29.4 261.4	76.9 58.1	35.2 32.1	D U	94.4 .8	16
RHO CEPHEIDS	257.0 5.2	166.7 .2	50.6 .6	.924 .009	.122 .013	1.053 1.08	63.7 SEP 9.8	27.9 .3	356.1 2.9	78.2 .7	354.6 253.9	77.9 64.8	25.6 30.2	D U	94.4 1.0	32
CASSICPEIDS- CAMELOPARDALIDS	347.0 1.4	166.9 .2	59.0 .6	.463 .007	.379 .011	.745 .64	153.9 SEP 10.0	29.0 .2	47.1 1.7	68.7 .4	46.7 261.1	68.9 48.7	26.8 23.7	D U	92.4 1.0	31
CEPHEIDS	347.1 3.8	167.8 .2	61.8 .5	.866 .007	.080 .008	.941 .91	154.9 SEP 10.9	31.8 .2	51.9 2.0	78.9 .3	52.2 269.6	78.9 57.1	29.8 28.4	D U	97.0 .8	48
BETA UMIDS	127.8 3.1	168.3 .4	32.8 .7	.947 .007	.175 .012	1.148 1.23	296.1 SEP 11.4	20.9 .3	221.5 2.8	74.9 .9	219.4 322.9	74.8 72.1	17.8 31.5	D U	89.3 .8	23
C CAMELOPARDALIDS	7.2 1.6	168.4 .2	50.3 .6	.543 .008	.303 .011	.779 .69	175.6 SEP 11.5	26.1 .2	79.0 3.2	76.5 .4	78.9 277.4	77.2 53.9	23.6 24.8	D U	93.5 1.0	40
RHO URSIDS	66.9 1.9	168.4 .2	56.1 .8	.636 .009	.363 .013	.999 1.00	235.3 SEP 11.5	31.1 .3	143.1 1.8	70.1 .6	144.0 308.0	70.0 51.5	29.1 29.4	D U	97.3 2.3	23
B CAMELOPARDALIDS	14.3 1.9	168.4 .1	62.9 .6	.611 .008	.252 .011	.817 .74	182.7 SEP 11.5	31.2 .2	81.1 2.2	74.8 .3	81.8 278.2	75.1 51.8	29.1 25.8	D U	94.1 .9	47
H CAMELOPARDALIDS	135.1 4.2	168.5 .3	70.1 .8	.955 .006	.201 .015	1.195 1.31	303.6 SEP 11.7	37.1 .3	92.0 4.2	80.1 .4	95.6 283.2	80.6 57.2	35.5 32.0	D U	97.2 1.2	23
ALPHA CAMELOPARDALIDS	9.3 1.5	168.6 .2	58.9 .6	.397 .008	.442 .012	.712 .60	177.9 SEP 11.8	28.9 .2	86.8 2.9	68.6 .4	87.7 280.2	69.3 45.9	26.5 22.4	D U	92.0 .6	38
SEPTEMBER URSIDS	133.4 .4	168.8 .2	48.4 .3	.857 .002	.916 .006	10.248 32.81	302.2 SEP 12.0	34.5 .1	196.4 .4	62.1 .3	196.7 344.4	62.0 59.7	32.8 40.9	D U	94.1 .4	65
DRACONIDS-UMICS	97.4 2.8	169.0 .9	20.4 .5	.907 .007	.135 .010	1.049 1.07	266.4 SEP 12.2	15.9 .2	210.7 1.7	67.0 1.0	205.8 339.9	67.1 65.9	11.4 30.1	D U	85.8 .9	49

70

Table 9-2. (Cont.)

1	2	3	4	5	6	7	8	9	10	11	12	13	14	15	16	17
ETA DRACONIDS	165.7 1.5	169.0 .2	31.9 .7	.993 .002	.465 .011	1.856 2.53	334.7 SEP 12.2	22.1 .3	246.3 2.0	63.8 .8	246.2 13.8	64.1 79.8	19.2 35.9	D U	87.5 .7	33 *
EPSILON UMIDS	170.0 1.7	169.2 .2	49.7 .7	.998 .002	.430 .013	1.753 2.32	339.2 SEP 12.4	30.0 .3	258.9 4.2	80.3 .7	256.7 289.3	80.7 75.5	28.0 35.5	D U	87.7 2.1	25
SEPTEMBER DRACONIDS	180.9 .9	169.8 .7	49.1 .5	1.003 0.000	.604 .009	2.532 4.03	350.7 SEP 13.0	30.8 .2	275.9 2.2	75.7 .4	275.4 272.7	76.3 80.1	28.9 37.6	D U	95.6 1.0	54
PISCIDS	306.3 .9	172.8 1.0	3.5 .4	.311 .006	.769 .007	1.349 1.57	119.1 SEP 16.1	27.8 .2	8.5 .6	6.9 .4	8.5 197.7	6.9 3.0	25.6 33.1	D N	87.6 .4	93 *
SEPTEMBER CEPHEIDS	248.6 3.6	173.8 .9	33.8 .6	.925 .007	.151 .012	1.089 1.14	62.4 SEP 17.1	21.0 .2	316.7 2.3	73.4 .8	322.0 230.2	73.3 71.6	17.8 30.7	D U	88.1 .8	41
ARIETIDS-PISCIDS	333.6 1.3	177.6 1.3	3.6 .5	.091 .006	.926 .006	1.238 1.38	151.2 SEP 21.0	35.7 .5	26.5 .7	12.2 .3	26.4 211.3	12.3 1.3	33.7 31.7	D N	89.5 .6	46
GAMMA PISCIDS	247.8 1.5	178.8 1.6	7.6 .7	.741 .009	.716 .011	2.606 4.21	66.6 SEP 22.2	20.9 .2	342.3 .9	7.7 1.1	342.4 168.1	8.0 14.3	18.0 37.8	D N	91.1 1.1	35 *
GAMMA ARIETIDS	336.8 1.2	178.8 .4	22.9 .6	.068 .006	.947 .007	1.283 1.45	155.6 SEP 22.2	37.9 .8	27.5 1.1	18.3 .5	27.8 213.5	18.4 6.5	36.3 32.3	D N	88.5 1.1	17
ETA PERSEIDS	335.6 1.2	179.2 .1	57.6 .9	.267 .007	.625 .011	.712 .60	154.8 SEP 22.6	29.7 .3	43.9 1.7	54.9 .7	43.7 239.8	55.0 36.4	27.7 22.7	D U	92.5 .6	17
XI CEPHEIDS	225.8 1.3	179.3 .3	43.0 .6	.904 .005	.471 .011	1.711 2.24	45.1 SEP 22.7	27.4 .3	327.6 1.3	67.0 .7	327.9 209.2	67.2 68.1	25.2 35.4	D U	91.2 1.0	32
RHO PISCIDS	326.6 .7	179.5 .2	17.1 .7	.146 .006	.876 .007	1.174 1.27	146.1 SEP 22.9	33.0 .6	23.1 .4	18.7 .6	23.6 209.2	18.7 8.2	31.2 31.4	D N	88.6 .6	22
KAPPA CEPHEIDS	203.7 1.0	179.5 .2	52.3 .5	.972 .002	.543 .008	2.124 3.10	23.2 SEP 22.9	32.0 .2	316.5 2.0	76.7 .4	316.1 237.0	77.0 72.9	30.1 36.8	D U	94.5 .6	45
F CEPHEIDS	259.8 2.3	179.7 .2	36.0 .7	.817 .009	.293 .013	1.155 1.24	79.5 SEP 23.1	22.9 .3	341.3 1.5	65.8 .7	342.0 212.4	65.7 62.5	20.2 31.6	D U	91.8 1.3	22
SEPTEMBER CASSIOPEIDS	298.5 2.0	179.8 .1	64.3 .5	.712 .008	.251 .010	.951 .93	118.3 SEP 23.2	33.2 .2	43.6 1.8	73.2 .4	43.5 249.9	73.3 53.1	31.3 28.6	D U	93.8 .7	35
D CASSIOPEIDS	236.6 1.2	180.0 .1	67.4 .5	.855 .007	.488 .011	1.669 2.16	56.6 SEP 23.4	38.2 .3	16.5 1.1	72.9 .6	16.2 238.6	73.0 57.5	36.6 35.2	D U	95.3 .9	12
H CEPHEIDS	219.7 5.8	180.7 .3	54.3 .8	.970 .009	.137 .016	1.124 1.19	40.4 SEP 24.1	30.0 .4	20.2 11.6	85.5 .7	10.5 260.0	86.1 65.6	28.0 31.4	D U	95.1 1.1	18

71

Table 9-2. (Cont.)

1	2	3	4	5	6	7	8	9	10	11	12	13	14	15	16	17
GAMMA UMIDS	148.7 1.4	181.2 .5	36.1 .9	.967 .004	.308 .013	1.396 1.65	329.9 SEP 24.7	23.2 .4	228.6 1.9	69.1 .9	229.0 330.8	69.1 74.6	20.4 33.7	D U	88.0 1.0	18
D URSIDS	129.2 1.0	181.5 .3	51.0 .8	.854 .006	.669 .011	2.582 4.15	310.7 SEP 25.0	33.4 .4	198.0 .9	63.0 .7	198.5 331.3	62.9 61.0	31.5 37.8	D U	92.0 .9	23
CAMELCPARDALICS	8.9 3.3	182.0 .2	66.8 .4	.824 .007	.104 .008	.919 .88	190.9 SEP 25.5	33.8 .2	102.5 1.8	77.4 .2	103.5 273.0	77.2 54.0	31.8 28.0	D U	97.7 .6	70
SEPTEMBER CAMELOPARDALIDS	354.9 1.9	182.0 .2	67.8 .5	.665 .007	.205 .009	.837 .77	176.9 SEP 25.5	33.4 .2	93.3 1.6	74.5 .2	93.9 269.7	74.6 51.2	31.4 26.5	D U	95.7 .8	57
SEPTEMBER UMICS	158.3 1.0	182.3 .2	58.6 .7	.971 .003	.712 .013	3.374 6.20	340.6 SEP 25.8	36.4 .3	211.8 1.9	76.2 .6	212.2 304.2	76.3 70.3	34.8 38.8	D U	94.8 .7	27
A CAMELOPARDALIDS	66.9 4.6	182.4 .1	59.1 .5	.882 .008	.106 .010	.987 .98	249.3 SEP 25.9	31.3 .2	136.2 2.7	79.8 .4	138.2 283.0	79.2 58.4	29.1 29.0	D U	95.7 .7	52
D DRACONIDS	144.1 1.1	182.5 .2	61.5 .7	.934 .004	.546 .012	2.058 2.95	326.6 SEP 26.0	36.5 .3	186.7 1.9	74.8 .5	187.9 303.6	75.0 64.2	34.9 36.6	D U	93.2 2.1	34
DELTA PISCIDS	93.6 1.5	11.6 1.7	.7 .5	.566 .010	.693 .012	1.843 2.50	105.2 OCT 5.2	23.1 .3	12.5 1.1	4.2 .8	12.8 181.9	4.4 -1.0	20.5 35.9	A N	86.3 .6	45
OCTOBER ANDROMEDIDS	274.5 .8	193.8 .2	16.3 .7	.554 .007	.710 .013	1.908 2.64	108.3 OCT 7.5	25.1 .4	8.8 .4	26.7 .9	9.2 185.6	26.8 20.9	22.7 36.1	D N	89.8 .9	25
OCTOBER CEPHEIDS	208.0 1.7	193.9 .2	44.9 .5	.963 .004	.391 .012	1.581 1.99	41.9 OCT 7.6	27.6 .3	304.4 3.4	78.3 .5	304.7 231.4	78.7 74.5	25.3 34.9	D U	85.0 3.9	33
G CEPHEIDS	236.2 1.8	193.9 .2	52.3 .7	.867 .008	.421 .013	1.496 1.83	70.1 OCT 7.6	31.2 .3	.2 2.7	77.3 .7	.3 227.0	77.5 63.5	29.2 34.4	D U	92.2 2.1	21
OCTOBER DRACCNIDS	187.6 1.0	194.5 .2	49.2 .6	.994 .001	.553 .008	2.221 3.31	22.1 OCT 8.2	30.7 .3	268.8 2.2	77.7 .5	268.3 257.3	78.0 78.5	28.6 37.1	D U	93.3 1.0	44 *
K CAMELOPARDALIDS	319.4 1.8	195.0 .2	67.7 .8	.495 .009	.404 .013	.831 .76	154.4 OCT 8.7	33.8 .3	73.0 2.3	68.6 .4	73.4 246.5	68.8 45.8	31.9 26.5	D U	95.4 1.0	16
THETA DRACONICS	143.6 2.7	195.1 1.4	28.1 .6	.956 .006	.240 .011	1.257 1.41	338.7 OCT 8.8	19.4 .2	234.8 1.7	61.4 1.0	234.3 347.0	61.2 73.7	16.0 32.8	D U	88.6 .9	33
SEXTANTIDS	212.3 1.0	15.1 .1	31.1 1.0	.172 .009	.816 .011	.936 .91	227.4 OCT 8.8	31.6 .7	156.5 .9	-8.3 .8	156.8 326.6	-8.3 -16.7	29.7 28.5	A D	88.3 1.8	9
L CAMELOPARDALIDS	208.8 2.6	195.3 .2	67.1 .6	.971 .004	.237 .011	1.272 1.43	44.1 OCT 9.0	36.4 .3	116.8 3.4	82.4 .4	118.3 261.3	83.1 60.3	34.8 33.0	D U	98.0 1.6	32

Table 9-2. (Cont.)

1	2	3	4	5	6	7	8	9	10	11	12	13	14	15	16	17
DELTA URSIDS	121.6 / 1.5	195.4 / .2	65.4 / .8	.827 / .009	.563 / .010	1.892 / 2.60	317.0 / OCT 9.1	38.5 / .3	184.9 / 1.1	63.0 / .6	185.4 / 309.8	62.9 / 56.5	37.0 / 36.2	D / U	97.4 / 1.9	17
J CAMELOPARDALIDS	349.8 / 1.5	195.7 / .3	60.1 / .8	.285 / .009	.564 / .014	.655 / .53	185.5 / CCT 9.4	28.9 / .3	97.4 / 2.7	63.1 / .5	97.7 / 258.8	63.6 / 40.3	26.6 / 20.3	D / U	92.7 / 1.7	12
LAMBDA DRACONIDS	156.0 / 1.1	195.7 / .2	66.6 / .7	.967 / .003	.530 / .013	2.060 / 2.96	351.7 / OCT 9.4	38.7 / .3	186.4 / 1.9	74.6 / .4	186.6 / 290.7	74.7 / 63.8	37.2 / 36.7	D / U	95.0 / .7	16
A URSIDS	33.4 / 2.6	195.8 / .1	55.8 / .6	.596 / .010	.288 / .014	.837 / .77	229.2 / OCT 9.5	29.2 / .3	159.5 / 1.8	67.4 / .7	160.2 / 291.0	67.2 / 52.5	26.9 / 26.4	D / U	93.1 / .8	31 *
N DRACONIDS	55.1 / 4.8	196.0 / .2	31.3 / .8	.812 / .012	.144 / .015	.948 / .92	251.1 / OCT 9.7	19.7 / .3	202.7 / 1.5	68.9 / 1.5	199.7 / 306.5	68.9 / 64.7	16.3 / 28.6	D / U	91.1 / 1.5	32
G CAMELCPRDALIDS	337.3 / 4.8	196.1 / .2	42.1 / .8	.761 / .010	.149 / .012	.895 / .85	173.4 / OCT 9.8	23.7 / .3	116.5 / 11.7	83.1 / .6	135.1 / 261.9	84.8 / 62.6	20.7 / 27.5	D / U	95.6 / .9	22
DRACONICS- CAMELOPARDALIDS	25.8 / 5.4	196.1 / .1	65.8 / .4	.833 / .008	.106 / .010	.931 / .90	221.9 / OCT 9.8	33.6 / .2	139.5 / 1.7	74.6 / .3	141.7 / 276.0	73.7 / 54.2	31.5 / 28.1	D / U	96.8 / .7	25
C URSIDS	129.9 / 2.3	196.1 / .2	71.7 / .7	.920 / .006	.276 / .012	1.270 / 1.43	326.0 / OCT 9.8	38.5 / .3	162.3 / 1.3	71.2 / .5	163.1 / 287.8	71.0 / 56.1	37.0 / 32.9	D / U	93.2 / 1.2	58
SOUTHERN ARIETIDS	122.5 / .9	17.8 / 1.0	2.9 / .5	.333 / .006	.768 / .007	1.435 / 1.72	140.3 / OCT 11.5	27.8 / .2	32.3 / .7	10.2 / .4	32.4 / 1.96.0	10.4 / -2.5	25.6 / 33.9	A / N	87.0 / .8	26
PSI VIRGINIDS	258.1 / 1.5	21.0 / 1.7	2.4 / .6	.525 / .008	.652 / .015	1.510 / 1.86	279.1 / OCT 14.7	23.5 / .3	192.3 / 1.1	-8.7 / .8	192.6 / 354.0	-8.8 / -3.1	21.0 / 34.4	A / D	88.8 / .9	83 *
ORIONIDS	87.0 / .8	27.1 / .1	164.4 / .8	.562 / .006	.854 / .012	3.850 / 7.55	114.1 / OCT 20.9	65.3 / .2	94.6 / .4	16.1 / .3	94.9 / 247.6	16.1 / -7.3	64.6 / 39.3	A / N	96.8 / .7	29
M CEPHEIDS	237.8 / 2.0	207.4 / .2	25.0 / .9	.892 / .006	.287 / .013	1.251 / 1.40	85.2 / OCT 21.2	18.5 / .3	336.3 / 2.8	67.7 / 1.4	338.5 / 187.9	68.2 / 65.0	14.9 / 32.7	D / U	91.1 / 1.1	17 *
E CEPHEIDS	263.4 / 3.2	207.5 / .2	32.7 / .6	.849 / .009	.206 / .014	1.070 / 1.11	110.9 / OCT 21.3	21.0 / .3	341.6 / 8.3	80.0 / .7	351.6 / 219.4	80.8 / 66.2	17.8 / 30.7	D / U	92.2 / 1.2	19
BETA CAMELOPARDALIDS	333.5 / 2.0	208.2 / .3	58.2 / .7	.331 / .009	.546 / .015	.729 / .62	181.7 / OCT 22.0	29.9 / .3	91.7 / 3.4	63.9 / .5	91.5 / 242.7	64.1 / 40.7	27.7 / 23.6	D / U	96.3 / 1.8	26
B URSIDS	42.0 / 3.0	209.1 / .2	61.7 / .6	.696 / .009	.215 / .012	.886 / .83	251.1 / OCT 22.9	32.0 / .3	171.8 / 1.2	64.7 / .5	171.9 / 286.8	64.4 / 53.4	29.8 / 27.6	D / U	96.5 / 1.2	13
TAU URSIDS	.2 / 1.8	209.4 / .3	64.5 / .8	.407 / .009	.422 / .013	.703 / .59	209.6 / OCT 23.2	30.7 / .3	142.6 / 2.2	63.1 / .6	143.2 / 271.5	63.2 / 45.4	28.7 / 22.6	D / U	91.5 / .8	31

Table 9-2. (Cont.)

1	2	3	4	5	6	7	8	9	10	11	12	13	14	15	16	17
OCTOBER URSIDS	332.0	209.8	67.3	.875	.080	.950	181.8	34.5	153.9	71.9	150.8	71.8	32.4	D	96.7	35
	7.3	.2	.7	.009	.011	.93	OCT 23.6	.3	1.5	.4	268.0	54.2	28.5	C	1.1	
PSI DRACONIDS	183.0	209.9	40.0	.992	.568	2.294	32.9	26.4	267.1	69.2	267.1	69.4	24.1	D	93.2	43
	1.0	.2	.6	.001	.008	3.47	OCT 23.7	.3	1.6	.5	259.7	87.0	37.4	C	.7	
B DRACONIDS	227.0	210.0	59.0	.950	.152	1.120	77.0	32.2	161.1	80.2	162.4	81.0	30.3	D	96.7	36
	4.5	.2	.6	.006	.012	1.19	OCT 23.8	.3	2.7	.5	258.9	62.5	31.6	C	.8	
OCTOBER UMIDS	244.8	210.1	40.8	.939	.123	1.070	94.9	24.0	236.7	83.1	230.0	85.6	21.3	D	91.0	38
	4.5	.9	.6	.006	.010	1.11	OCT 23.9	.3	6.9	.5	248.1	69.7	30.7	C	1.1	
ALPHA URSIDS	88.5	210.1	65.3	.883	.123	1.007	298.6	34.2	173.2	68.0	174.5	67.5	32.5	D	95.0	32
	4.7	.2	.5	.008	.011	1.01	OCT 23.9	.2	1.0	.4	283.4	56.4	30.0	C	.9	
A DRACONIDS	175.3	210.1	69.0	.988	.228	1.279	25.4	37.3	169.5	73.6	171.1	73.8	35.8	D	93.6	38
	2.4	.2	.4	.001	.012	1.45	OCT 23.9	.2	1.1	.4	273.1	59.7	33.2	C	.5	
OCTOBER HERCULIDS	161.1	211.0	31.2	.971	.676	2.995	12.1	23.4	255.3	50.4	255.3	50.7	20.8	D	81.6	33
	1.1	.8	.6	.002	.009	5.18	OCT 24.8	.2	1.0	.9	26.7	72.5	38.6	C	2.8	
TAURIDS	293.6	217.2	0.0	.398	.750	1.596	150.8	26.8	46.3	17.4	46.5	17.5	24.6	D	88.5	81
	.7	.8	.4	.005	.006	2.02	OCT 31.0	.2	.6	.4	191.8	0.0	35.0	N	.6	*
TRIANGULIDS	269.6	218.6	18.3	.606	.647	1.718	128.2	23.7	30.4	40.7	30.7	40.8	21.1	D	86.8	25
	1.2	1.0	.7	.009	.012	2.25	NOV 1.4	.3	.9	1.2	184.8	26.5	35.6	M	.7	*
C CEPHEIDS	236.5	218.9	32.4	.831	.562	1.899	95.4	24.4	1.6	66.8	1.9	67.1	21.8	D	91.1	31
	1.2	.9	.7	.006	.011	2.62	NOV 1.7	.3	1.6	1.0	185.3	57.1	36.3	C	.6	
GAMMA TAURIDS	143.6	39.3	17.5	.140	.912	1.585	182.9	36.4	65.2	13.7	65.4	13.8	34.7	A	88.7	32
	1.5	1.7	.6	.008	.008	2.00	NOV 2.1	.5	1.0	.3	206.6	-7.6	34.7	N	.9	
KAPPA DRACONICS	1.8	219.9	43.5	.767	.132	.884	221.7	24.2	189.0	71.4	188.2	71.4	21.5	D	93.8	34
	3.8	1.1	.6	.009	.011	.83	NOV 2.7	.3	1.4	.8	273.4	62.6	27.7	C	.9	
EPSILON DRACONIDS	203.5	221.1	33.5	.959	.591	2.344	64.6	23.9	308.3	69.4	309.0	69.9	21.2	D	92.4	18
	1.4	.1	.9	.004	.016	3.59	NOV 3.9	.4	3.3	.9	169.6	75.4	37.6	C	1.1	
NOVEMBER ORIONIDS	161.4	41.1	41.5	.045	.964	1.226	202.6	40.4	78.6	14.2	78.7	14.5	38.8	A	92.8	7
	1.5	.3	1.2	.002	.007	1.36	NOV 4.0	1.6	1.9	.3	217.7	-8.5	32.0	N	1.4	
PHI TAURIDS	326.1	221.4	19.6	.132	.910	1.467	187.5	36.1	66.4	30.3	67.3	30.1	34.2	D	90.8	32
	.8	.2	.7	.006	.008	1.78	NOV 4.2	.8	.6	.5	208.9	8.2	33.4	N	.7	
IOTA AURIGIDS	336.3	221.6	30.5	.085	.921	1.076	197.9	36.2	75.5	33.2	76.4	32.8	34.0	D	91.3	25
	.8	.4	.7	.005	.008	1.12	NOV 4.4	.9	1.2	.8	216.8	9.9	29.6	N	.6	

74

Table 9-2. (Cont.)

1	2	3	4	5	6	7	8	9	10	11	12	13	14	15	16	17
K CEPHEIDS	212.6	221.8	51.7	.921	.840	5.770	74.4	34.6	326.4	82.3	328.5	82.8	32.7	D	97.5	9
	1.2	.2	.9	.005	.017	13.86	NOV 4.6	.5	7.5	.6	210.5	69.4	40.4	U	2.8	
DRACONIDS-URSIDS	197.4	223.4	47.4	.973	.557	2.196	60.8	30.0	260.9	78.3	261.5	79.0	27.9	D	95.0	52
	.9	.2	.6	.002	.008	3.25	NOV 6.2	.3	2.9	.5	234.0	77.3	37.3	U	.6	*
NOVEMBER DRACCNIDS	348.5	223.4	61.2	.804	.111	.905	211.9	31.7	174.0	67.8	172.9	67.7	29.6	D	92.7	33
	4.8	.2	.6	.010	.012	.86	NOV 6.2	.3	1.0	.6	269.1	56.1	28.1	D	.7	
IOTA VIRGINICS	60.7	223.6	10.1	.329	.816	1.790	284.3	30.9	209.6	-3.5	209.8	-3.6	29.0	D	88.1	8
	.7	.2	1.0	.010	.010	2.39	NOV 6.4	.6	.5	.8	345.4	8.0	35.9	D	1.0	
F DRACONIDS	186.1	223.9	67.8	.985	.191	1.217	50.0	36.6	180.7	69.4	181.3	69.7	35.1	D	94.3	29
	2.9	.2	.6	.002	.012	1.34	NOV 6.7	.3	1.2	.4	269.6	59.7	32.7	U	.8	
NOVEMBER CAMELOPARDALIDS	227.6	224.1	58.4	.908	.340	1.376	91.7	33.4	164.3	81.5	164.8	82.0	31.6	D	94.4	27
	1.7	.3	.7	.006	.014	1.61	NOV 6.9	.3	4.7	.6	243.3	63.4	33.9	U	1.0	
SIGMA TAURIDS	294.4	250.9	.1	.376	.782	1.729	185.3	28.3	82.2	23.4	82.6	23.4	26.2	D	88.5	15
	1.0	.1	.6	.011	.015	2.27	DEC 3.4	.7	.5	.6	192.3	.1	35.7	N	1.9	
MONOCERIDS	135.8	71.8	22.3	.153	.975	6.199	207.6	41.6	93.8	14.4	94.4	14.5	40.0	A	93.2	30
	1.0	.9	.6	.006	.005	15.43	DEC 4.3	.4	.6	.4	202.5	-8.9	40.2	N	.6	*
K DRACONIDS	187.4	253.1	57.6	.981	.385	1.594	80.5	33.7	216.9	65.5	217.1	65.6	31.9	D	92.4	20
	1.7	.4	.8	.001	.011	2.01	DEC 5.6	.4	1.3	.6	264.8	69.2	35.3	U	1.0	
DECEMBER DRACCNIDS	184.0	253.5	42.7	.982	.579	2.335	77.5	27.9	256.3	68.9	256.2	69.1	25.7	D	89.4	35
	1.2	.2	.6	.001	.011	3.57	DEC 6.0	.3	1.8	.6	254.2	84.2	37.7	U	.6	*
MU GEMINIDS	129.4	74.6	1.1	.258	.829	1.510	204.0	31.1	94.2	22.4	94.3	22.6	29.2	A	89.7	43
	1.4	1.6	.6	.009	.011	1.86	DEC 7.1	.5	1.0	.4	199.4	-.8	34.5	N	.8	*
CHI ORIONIDS	278.7	257.5	.2	.515	.711	1.783	176.2	24.6	81.5	23.4	81.8	23.5	22.2	D	88.7	47
	1.1	1.0	.4	.007	.010	2.38	DEC 9.9	.2	.8	.5	185.0	.3	36.0	N	.7	*
GAMMA CAMELOPARDALIDS	224.3	259.0	23.4	.882	.557	1.992	123.3	20.5	29.9	72.4	32.8	73.3	17.3	D	86.1	34
	1.3	1.1	.6	.005	.010	2.81	DEC 11.4	.2	3.9	1.2	166.2	54.8	36.9	U	1.3	*
GEMINIDS	325.2	261.4	23.2	.139	.893	1.306	226.6	35.6	113.2	32.2	113.4	32.2	34.0	D	91.6	118
	.3	.3	.3	.002	.002	1.49	DEC 13.7	.2	.3	.1	208.6	10.4	33.4	N	.4	*
DECEMBER LYNCIDS	285.3	262.8	30.0	.475	.699	1.578	188.1	28.9	104.2	53.2	104.4	53.2	26.9	D	88.7	20
	.9	.3	.7	.008	.014	1.98	DEC 15.1	.5	1.1	.7	197.1	30.2	35.1	U	1.9	
DELTA DRACONICS	201.9	265.9	28.1	.956	.550	2.127	107.8	21.3	315.3	76.4	315.7	78.2	18.2	D	89.6	27
	1.3	.7	.8	.003	.011	3.10	DEC 18.2	.4	5.6	.8	154.6	72.7	37.3	U	.9	*

75

X Piscids, April Draconids, κ Cygnids, and β Cetids), the search revealed streams that must have been classified as new, but that differed significantly from the corresponding 1961–1965 streams in only one element other than the nodal longitude.

Of the remaining 17 streams of the 1961–1965 sample missing in the synoptic-year sample, 11 were found to be "absorbed" by one of the 55 identified streams (X Capricornids, σ Leonids, May Librids, May Herculids, ν Librids, Taurids-Perseids, γ Aquarids, α Cygnids, δ Cygnids, X Draconids, and October Camelopardalids); 2 by the sporadic background (June Draconids and φ Andromedids); 1 by a new stream (π Cepheids); and in 3 cases, no or only a few possibly associated meteors were found (Lyrids, η Aquarids, and Halleyids).

9.3 New Streams: Toroidal Group, Short- and Long-Period Streams, Twin Showers, and the "Cyclid" System

A great number of the new streams belong to the so-called toroidal group (Hawkins, 1963). They have direct but high-inclination orbits with low to moderate eccentricities. For example, we find 10 streams with i > 70°, of which all have q > 0.6 a.u., but only 3 have semimajor axes significantly larger than 1 a.u. Their radiants lie at high northern latitudes, mostly in the constellations of Draco, Ursa Major, Camelopardalis, Cassiopeia, Cepheus, and Ursa Minor. The traditional system of stream designation used in Paper III proved insufficient to provide names for all the new streams in that area of the sky so heavily populated by radiants. We therefore expanded the previous system of designation by adding capital letters before the name of the radiant's constellation wherever the original system proved inadequate. Also, streams coming from the constellation of Ursa Minor have been called Umids to distinguish them from streams from Ursa Major, which are called Ursids.

There are only two retrograde streams in the sample, the Orionids and the Perseids. The latter were not classified as a detected stream in the 1961–1965 sample, since only two probable members were found there.

A total of 26 streams have their perihelia less than 0.2 a.u. from the sun, and 9 streams less than 0.1 a.u. from the sun, the record being 0.045 a.u. for the November Orionids.

Nine streams have semimajor axes shorter than 0.8 a.u., and three shorter than
0.7 a.u. Two of these, the J Camelopardalids and β Andromedids, actually cross the
earth's orbit almost at their aphelion points (aphelion distances 1.02 and 1.06 a.u.,
respectively).

On the other hand, there are 12 streams in the sample with semimajor axes of
3 a.u. or longer. Surprisingly, neither the Perseid stream, nor the Orionid, nor the
Monocerid holds the record. Rather, a new, very rich stream with q = 0.86 a.u.,
inclination almost 50°, and revolution period of more than 30 years, appears to be
the most extended, not only in the synoptic-year sample, but probably among all radio
streams known so far. It is called the September Ursids, and it is associated with
neither a known comet nor a photographic stream.

We now know 14 pairs of twin showers with confidence and 4 more pairs possibly
related. Two of the seven pairs listed in Paper III as detected in the 1961–1965 sample
were not found in the synoptic-year sample: the Orionid-Halleyid pair because of the
absence of the Halleyid stream; and the σ Capricornid-χ Capricornid pair because of
the absence of the χ Capricornid stream. The ε Arietids replaced the χ Piscids as the
twin shower loosely associated with the Triangulids. The new list of detected twin
showers is in Table 9-3; the D values for the uncertain cases are in parentheses.

Nine of the new streams have inclinations less than 10° and eccentricities less
than 0.4. We find that there is a fairly close relationship among most of them in
terms of D despite an apparent variety in their orbits (Table 9-4). A similar relation-
ship detected by Southworth and Hawkins (1963) among orbits of this type of photo-
graphic meteors led the two authors to call such a "stream" the Cyclids and interpret
it as a result of a high probability that meteors in these orbits meet the earth.

9.4 Distribution of Radiants

The computer plots of radiants of the 19,698 radio meteors of the synoptic-year
sample are exhibited in Figures 9-1 and 9-2. Figure 9-1 is a plot of the ecliptical
coordinates, longitude λ versus latitude β, in Hammer's equal-area projection.

Figure 9-2 is a plot, in the same projection, of the sun-oriented ecliptical longitude $\lambda - \lambda_\odot$ versus latitude β. Except for a few details, the plots are almost identical with the corresponding plots of the individual meteor radiants from the 1961–1965 sample (see Figures 4a and 4b of Paper III).

Table 9-3. Twin showers detected during the synoptic year.

Twin showers		D	$\bar{i}$
Preperihelion	Postperihelion		
Southern Arietids	ζ Perseids	0.108	5°
Scorpiids-Sagittariids	Capricornids-Sagittariids	0.119	4°
Χ Orionids	κ Aurigids	0.135	3°
Southern η Virginids	ψ Virginids	0.136	2°
δ Leonids	August Lyncids	0.144	10°
January Cancrids	August Cancrids	0.148	3°
ρ Leonids	τ Leonids	0.150	1°
Ophiuchids	January Sagittariids	0.150	2°
Piscids	May Arietids	0.154	3°
Taurids	β Taurids	0.157	0°
μ Geminids	ξ Leonids	0.164	2°
γ Piscids	λ Capricornids	0.182	5°
Librids	ξ Sagittariids	0.198	3°
σ Taurids	μ Cancrids	0.202	1°
δ Cancrids	γ Leonids	(0.285)	4°
α Capricornids	ε Aquarids	(0.288)	7°
ζ Aurigids	March Andromedids	(0.320)	12°
Triangulids	ε Arietids	(0.388)	11°

The mean radiants of the detected streams (both new and known from the previous sample) are plotted in Figures 9-3 and 9-4. They show much the same pattern as the plots of individual radiants. At least, there is much better agreement between Figures 9-2 and 9-4 than between Figures 4b and 5b of Paper III. This is of course

due to the fact that the present search was much more complete than the former. Although we have not yet been able to determine the population and dispersion coefficients of the streams found in the synoptic-year sample, we can estimate that the total number of meteors in the detected streams is of the order of 6000, or approximately 30%, as compared to 1400 or 7.5% in the 1961–1965 sample.

Table 9-4. The Cyclid system of streams in the synoptic year (the numbers are D values in units of 0.001).

Stream	ξ Cygnids	κ Geminids	March Virginids	λ Aurigids	α Aurigids	June Aurigids	ζ Ursids	ε Ursids	β Ursids
ξ Cygnids	0	188	370	254	442	493	272	266	260
κ Geminids	188	0	266	93	238	267	229	216	165
March Virginids	370	266	0	324	404	387	269	244	252
λ Aurigids	254	93	324	0	164	236	322	306	252
α Aurigids	442	238	404	164	0	149	424	466	379
June Aurigids	493	267	387	236	149	0	449	427	309
ζ Ursids	272	229	269	322	424	449	0	87	182
ε Ursids	266	216	244	306	466	427	87	0	127
β Ursids	260	165	252	252	379	309	182	127	0

9.5 Comparison with Cook's Working List of Meteor Streams

Of Cook's (1972) working list, 16 streams were closely matched by radio streams from the synoptic-year sample (D ≲ 0.1), and 18 more streams were probably identified (D ≲ 0.2). However, we were not able to separate the northern and the southern branches of the Taurids and the X Orionids. Because the radar system did not operate early in January, we found only a remote branch of the Quadrantids. The remaining 21 streams of Cook's list, many of them either retrograde in motion or nearly parabolic or ones in southern hemisphere, were not found in the synoptic-year sample.
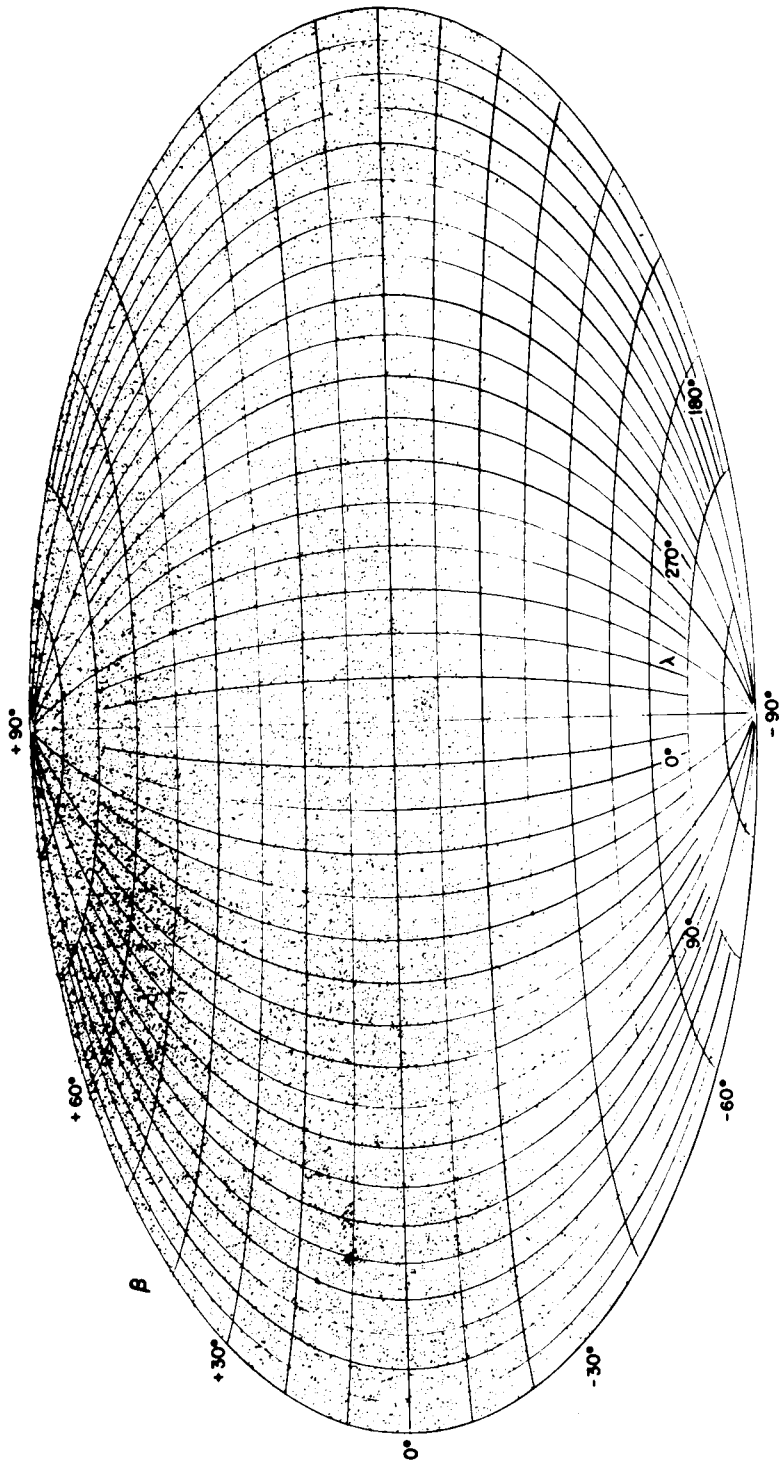
Figure 9-1. Computer plot of the ecliptical coordinates λ and β of 19,698 individual radio meteor radiants of the synoptic year in Hammer's equal-area projection.
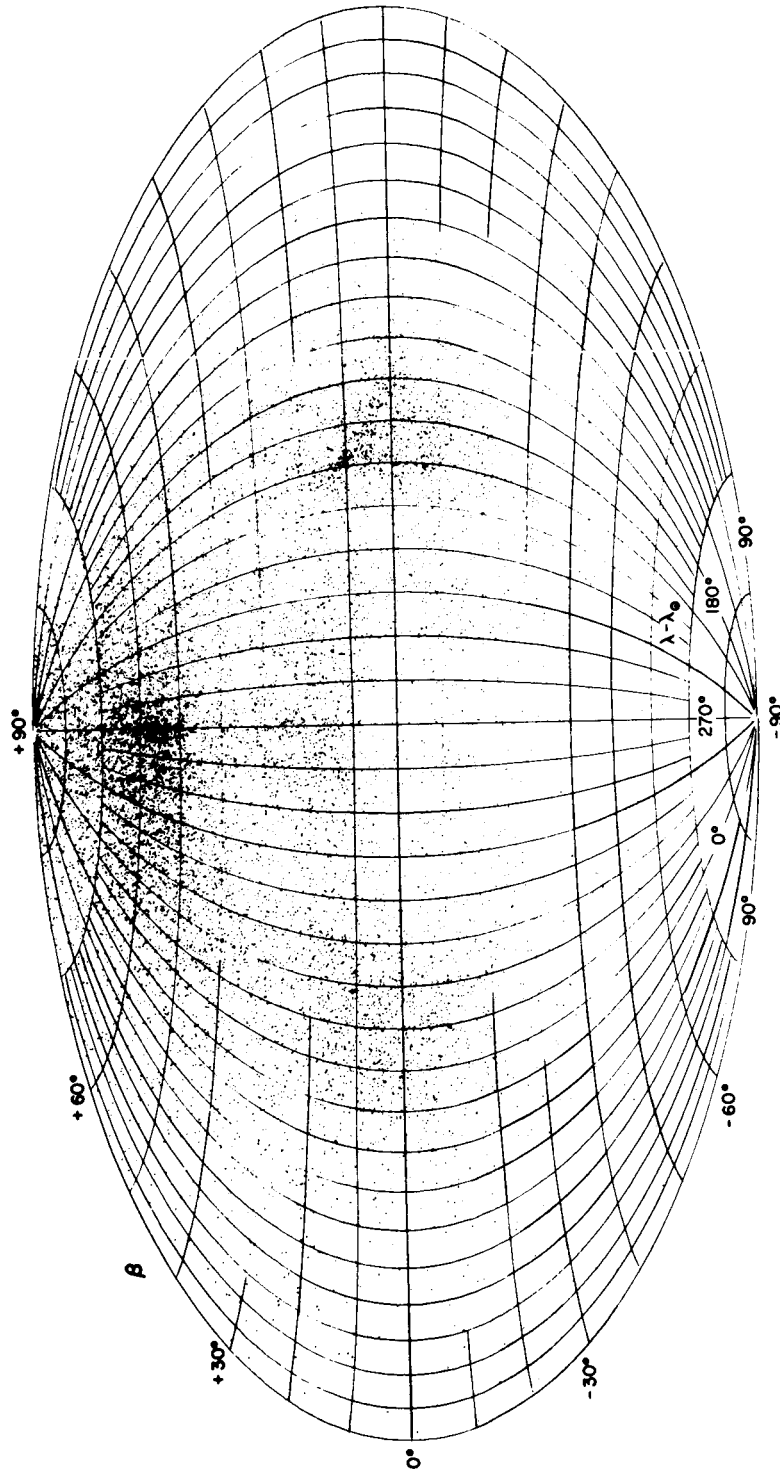
Figure 9-2. Computer plot of the sun-oriented ecliptical coordinates $\lambda - \lambda_\odot$ and β of 19, 698 individual radio meteor radiants of the synoptic year in Hammer's equal-area projection.
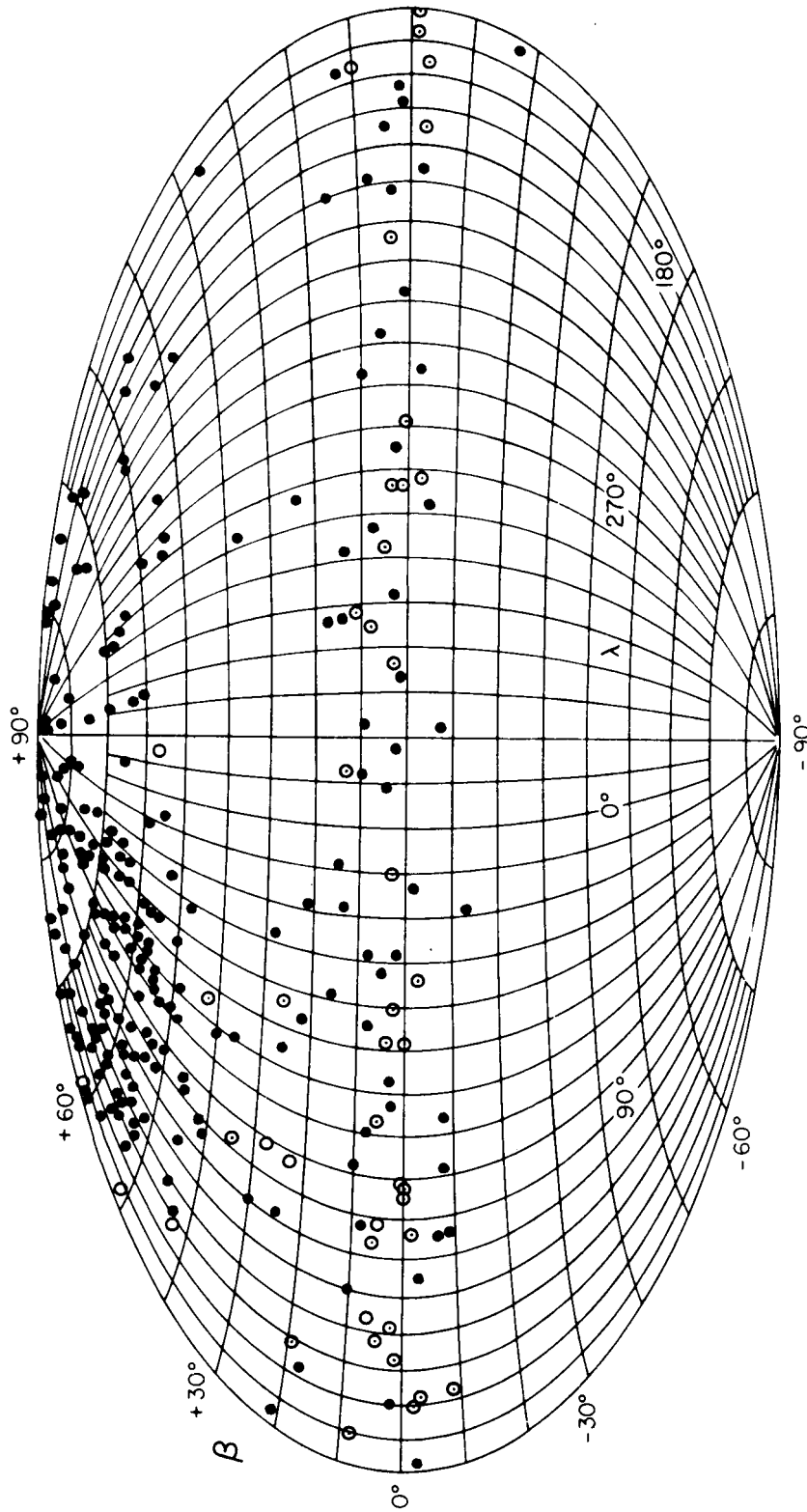
Figure 9-3. Ecliptical coordinates λ and β of the mean radiants of 256 radio meteor streams in Hammer's equal-area projection. Open circles stand for the Cyclid-type streams; circled points, for twin showers.
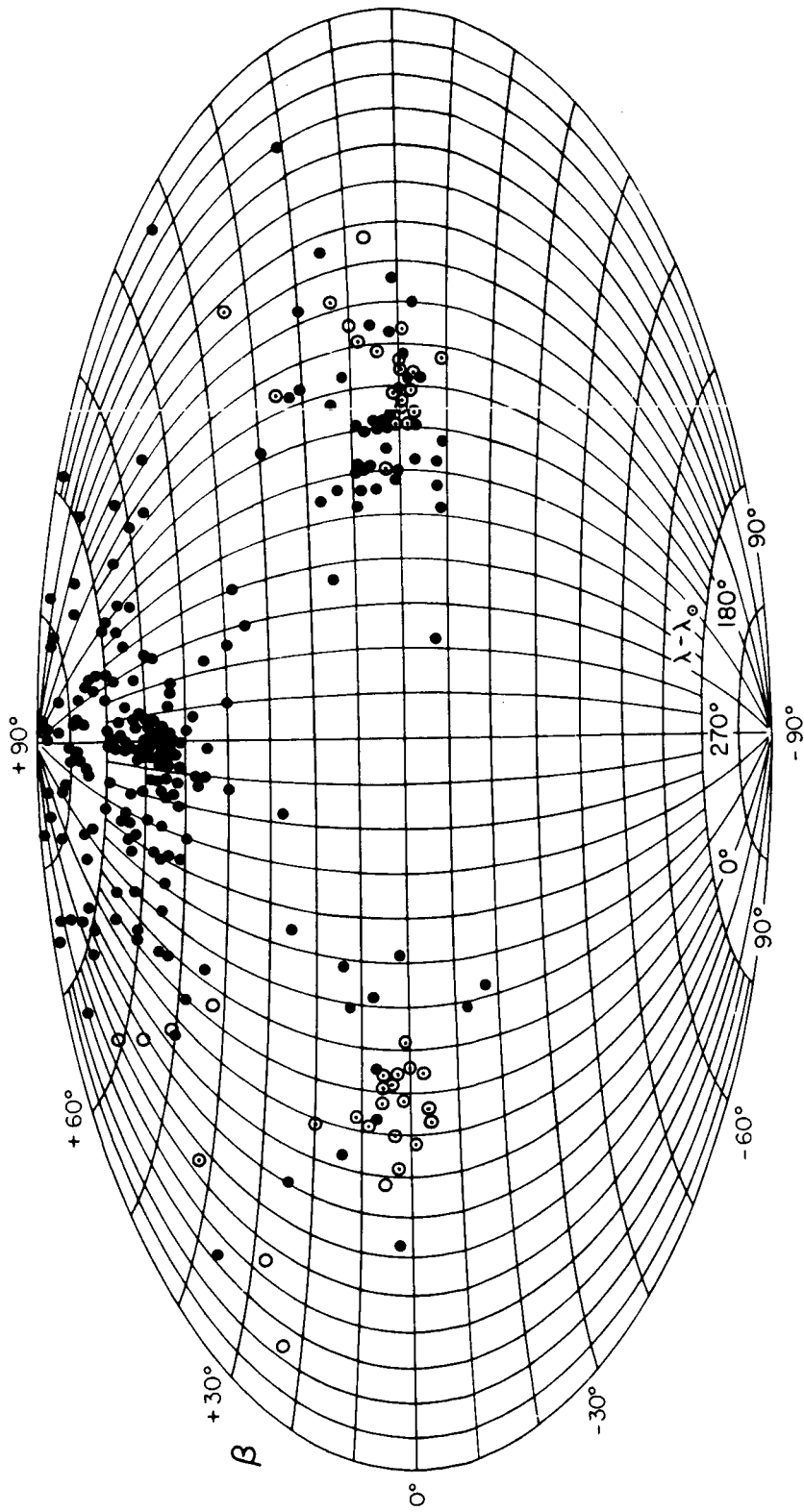
Figure 9-4. Sun-oriented ecliptical coordinates $\lambda - \lambda_\odot$ and β of the mean radiants of 256 radio meteor streams in Hammer's equal-area projection. See Figure 9-3 for the symbols used.

10.   COMET−METEOR AND ASTEROID−METEOR ASSOCIATIONS

10.1 Associations with Periodic Comets

Table 10-1 lists the detected associations between the meteor streams of the
synoptic-year sample and the potential parent objects within D = 0.3.

We find that the following periodic comets are likely to have associated streams
in the synoptic-year sample: Encke, Pons-Winnecke, Giacobini-Zinner, Halley,
Schwassmann-Wachmann 3, Swift-Tuttle, and Mellish.   Possible associations have
also been found for some other comets (Honda-Mrkos-Pajdušáková, Gale, Helfenzrieder,
Blanpain, and Lexell), but these are suspected to be fortuitous, because of the comets'
orbit instabilities in some cases or because of relatively loose relationships in others.

10.2 Adonis Meteor Streams

Among the asteroid−meteor associations, the most obvious one is again the case
of Adonis.   The σ Capricornids, a prominent stream in the 1961−1965 sample, were
found to match the asteroid's orbit less satisfactorily in the synoptic-year sample,
partly because of smaller perihelion distance and partly because of higher inclination.
However, it seems increasingly likely that the Scorpiids-Sagittariids, a very broad
stream undoubtedly related to Hoffmeister's (1948) Scorpiid-Sagittariid complex, is
associated with Adonis.   We note that both the June nighttime stream and its twin
shower, the Capricornids-Sagittariids appearing in January and February, are in
terms of D within 0.2 from the asteroid's orbit, and that a minor stream, the
X Sagittariids, closely related to the Scorpiids-Sagittariids (actually its component),
is within 0.09 of the asteroid's orbit.   Hoffmeister did notice a resemblance between
the orbits of Adonis and his Scorpiid-Sagittariid system, but left open the possibility
of a real association between both.   This was the correct approach because his results
were based on inaccurate visual observations; also, he found a discouraging difference
of almost 25° between the longitudes of perihelion of the asteroid and of the middle
of the meteor complex.   Our radio meteor samples suggest that the difference is

Table 10-1. Possible comet–meteor, asteroid–meteor, and meteorite/fireball–meteor associations.

Possible parent object	Possible associated streams	Stream-to-parent D-test
P/Encke	β Taurids	0.247
	Taurids	0.275
P/Honda-Mrkos-Pajdušáková	λ Capricornids	0.292
P/Pons-Winnecke (1921)	α Draconids	0.162
	Canes Venaticids	0.193
	Bootids-Draconids	0.195
	July Draconids	0.217
P/Giacobini-Zinner	October Herculids	0.150
P/Gale	Canes Venaticids	0.286
P/Halley	Orionids	0.209
P/Helfenzrieder	ψ Leonids	0.247
P/Blanpain	λ Capricornids	0.288
P/Schwassmann-Wachmann 3	α Draconids	0.185
	Canes Venaticids	0.206
	Bootids-Draconids	0.220
P/Lexell	μ Sagittariids	0.151
	Ophiuchids	0.191
P/Swift-Tuttle	Perseids	0.101
P/Mellish	Monocerids	0.225
(1566) Icarus	Arietids	0.286
	Taurids-Arietids	0.289

Possible parent object	Possible associated streams	Stream-to-parent D-test
1936 CA Adonis	χ Sagittariids	0.089
	Scorpiids-Sagittariids	0.135
	ε Aquarids	0.193
	Capricornids-Sagittariids	0.199
	σ Capricornids	0.252
	α Capricornids	0.286
1937 UB Hermes	ε Arietids	0.170
	δ Piscids	0.270
1932 HA Apollo	χ Scorpiids	0.204
(1685) Toro	January Aquarids	0.144
(1620) Geographos	March Virginids	0.220
	Leonids-Ursids	0.263
1950 DA	Leonids-Ursids	0.122
	μ Leonids	0.168
	April Ursids	0.208
(1627) Ivar	μ Draconids	0.292
(433) Eros	ξ Cygnids	0.263
Příbram Meteorite	τ Leonids	0.243
	γ Virginids	0.248
	ρ Leonids	0.296
Prairie Network fireball 40617	β Triangulids	0.181
	ζ Aurigids	0.182
	η Taurids	0.249

actually much less than that. In the synoptic-year sample, the Capricornids-Sagittariids indicate a difference of 13°, and the Scorpiids-Sagittariids, only 8°.

10.3 Possible Associations with Other Minor Planets of the Apollo and Amor Types and with Meteorites and Bright Fireballs

Besides Adonis, there is a definite possibility of the existence of associations of meteor streams with the minor planets Apollo, Hermes, Toro, and 1950 DA, and to a lesser degree also with Icarus and, surprisingly, Geographos and even Eros. The last two must, however, be taken with much caution: The would-be associated streams belong to the group of Cyclids. We know that these orbits have high probability of encounter with the earth, and detection of any well-established associations is most difficult if not impossible. Besides, the perihelion distance of Eros is 1.13 a.u., so that detectable meteors could only be fairly loosely related to the asteroid anyway.

Of the meteorites and bright fireballs, the Příbram meteorite and the Prairie Network fireball 40617 may be associated with some of the detected streams (see Table 10-1). No streams were found to move in the orbit of the Lost City meteorite, but the radar system was not operating at and around the node of that object. No streams seem to be associated with a few other fireballs, among them Prairie Network 40503 and Mt. Riffler (in the latter case, the radar was, however, again idle).
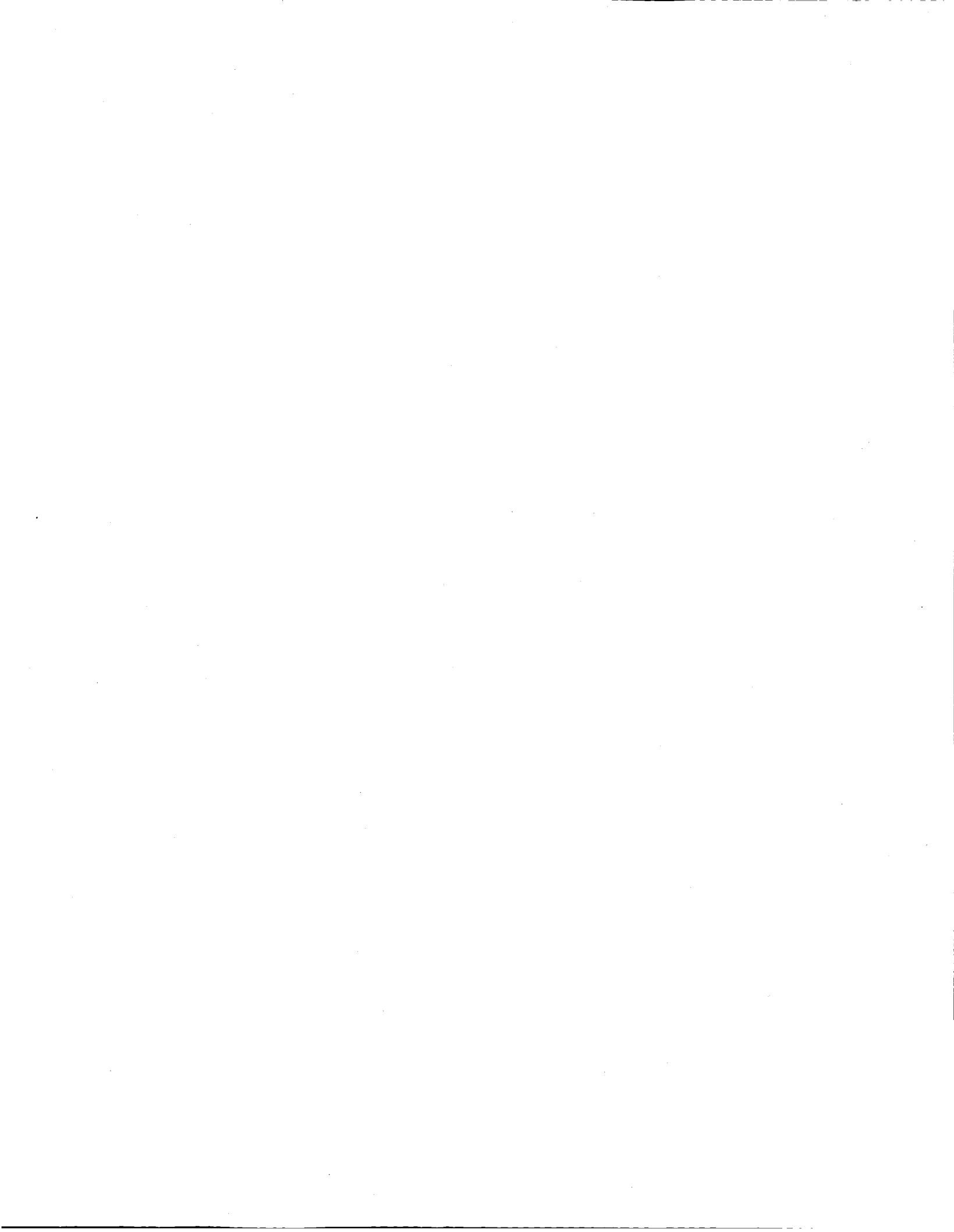
11. HEIGHT-VELOCITY DIAGRAM

11.1 Introduction

Ceplecha (1967, 1968) detected three discrete levels of beginning height on height-velocity plots of photographic meteors and interpreted them in terms of the composition and fragmentation of the meteoroids, thus suggesting that the bulk density of the latter is important. Cook (1970) applied Ceplecha's criterion to classify 25 photographic streams.

Height-velocity computer plots have been used in this study to search for the discrete height levels in the synoptic-year sample. Since for radio meteors the height at maximum ionization is much easier to define than the beginning height, we used essentially the former. A few check plots with the beginning height have confirmed that it makes little difference which of the two heights is used, except that the beginning height is subject to a larger dispersion.

11.2 Height-Velocity Plots for Individual Radio Meteors

The plot of 16,322 radio meteors of the synoptic year with zenith distance of radiant less than 60° (to eliminate a possible effect of nearly "tangential" meteors) has failed to show the discrete levels detected by Ceplecha among the photographic meteors (Figure 11-1). Nothing has been gained by dividing the whole sample into groups according to the meteor luminosity and perihelion distance (Figures 11-2 to 11-7). Dispersion seems to be large enough to mask completely the double-peak distribution in height. However, we have been able to detect some of the features of the height-velocity plots known for the photographic meteors.

First, there is a clear separation between the major concentration (at low V_∞) and the minor concentration (at high V_∞) in the velocity axis at $V_\infty \approx 48$ km sec^{-1}. The effect is obvious from all figures except Figure 11-4. In Ceplecha's terms, the gap separates the minor C_2 group from the major C_1 (plus A) group. The separation was originally recognized by Jacchia (1958).
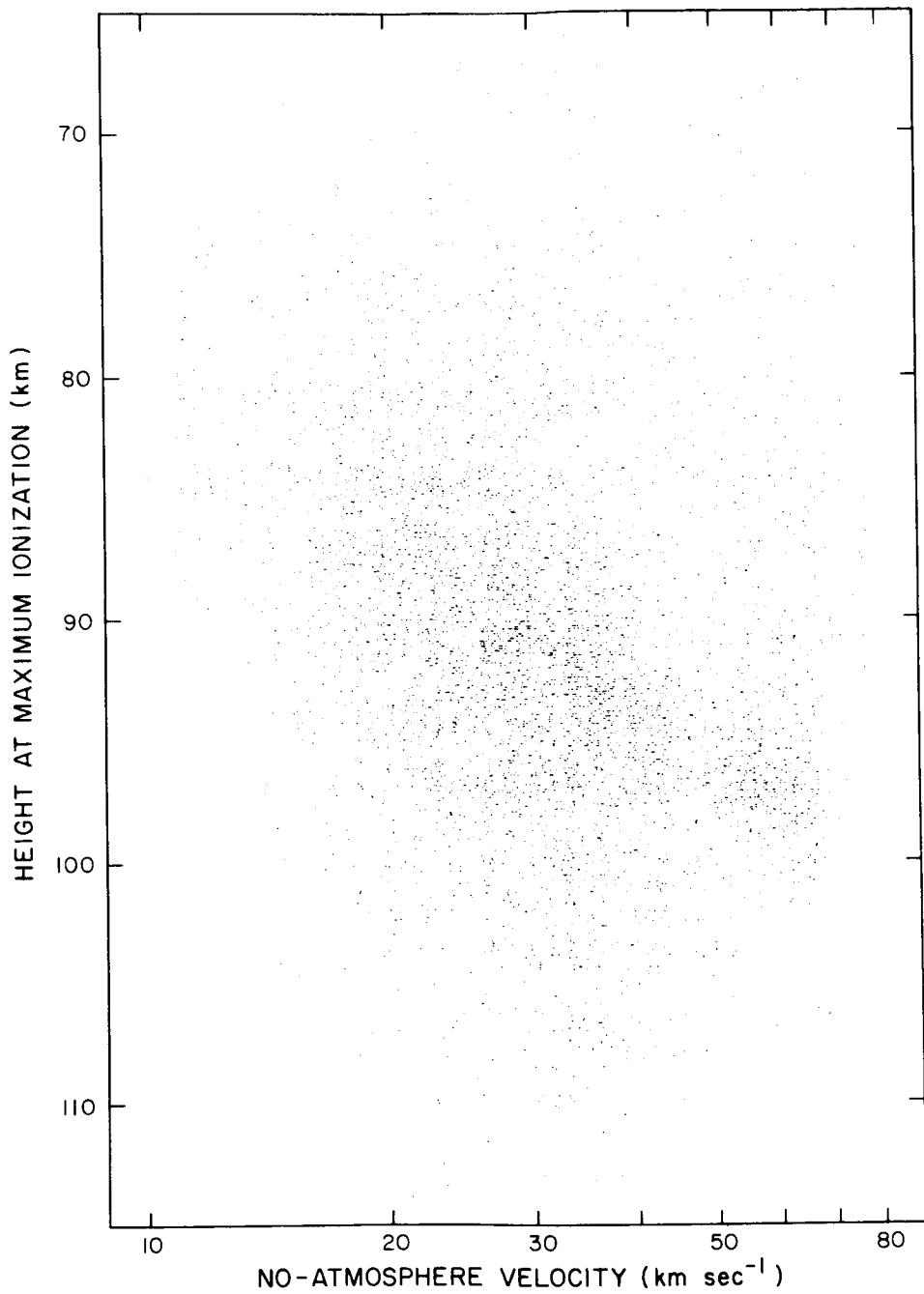
Figure 11-1. Height-velocity plot of 16,322 radio meteors of the synoptic year with zenith distances of radiant less than 60°.
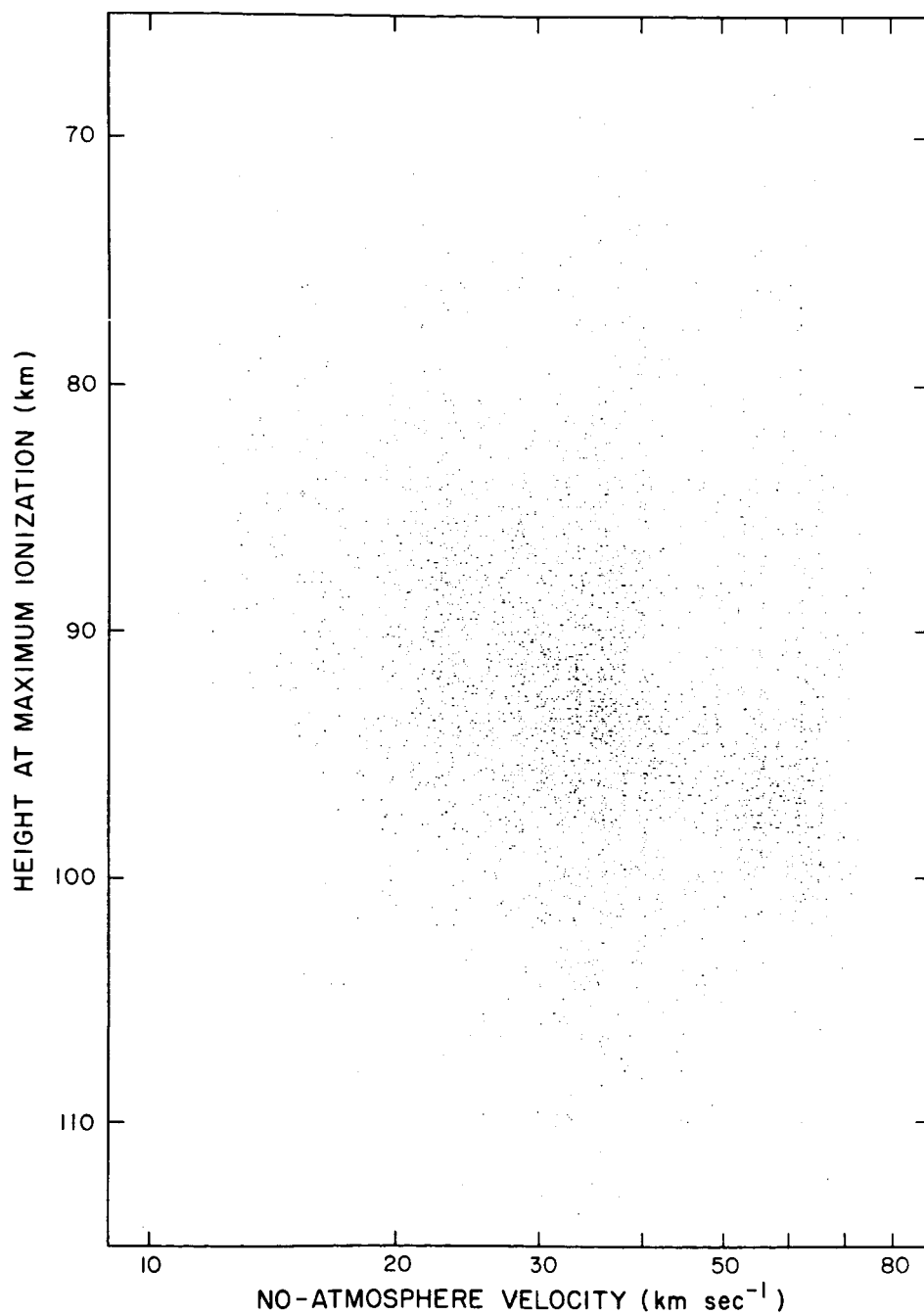
Figure 11-2. Height-velocity plot of 8487 radio meteors of the synoptic year with zenith distances less than 60° and "brighter" at maximum ionization than 11.5 mag.
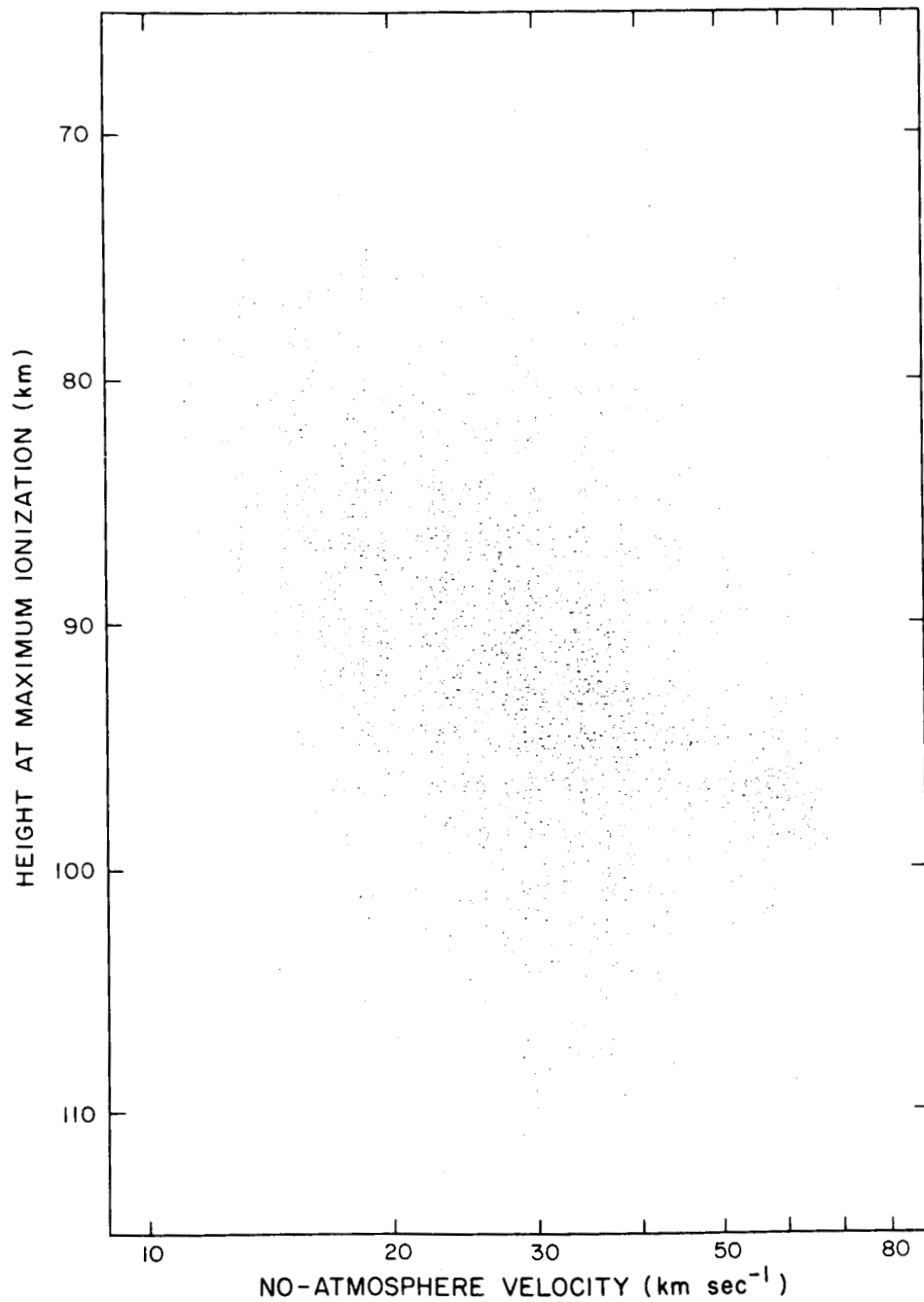
Figure 11-3. Height-velocity plot of 7835 radio meteors of the synoptic year with zenith distances less than 60° and "fainter" at maximum ionization than 11.5 mag.
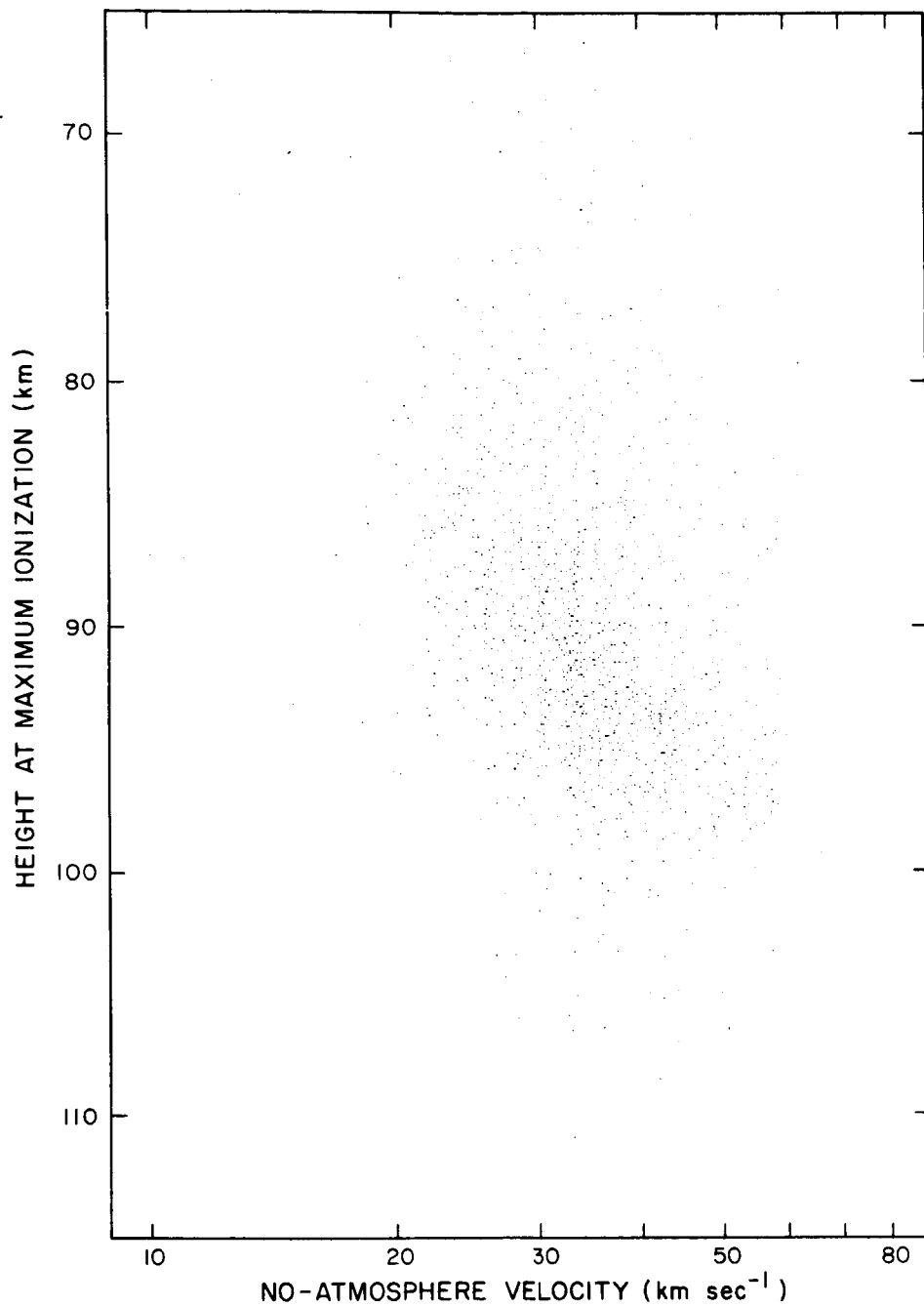
Figure 11-4.   Height-velocity plot of 2877 radio meteors of the synoptic year with zenith distances less than 60° and perihelion distances less than 0.25 a.u.

93
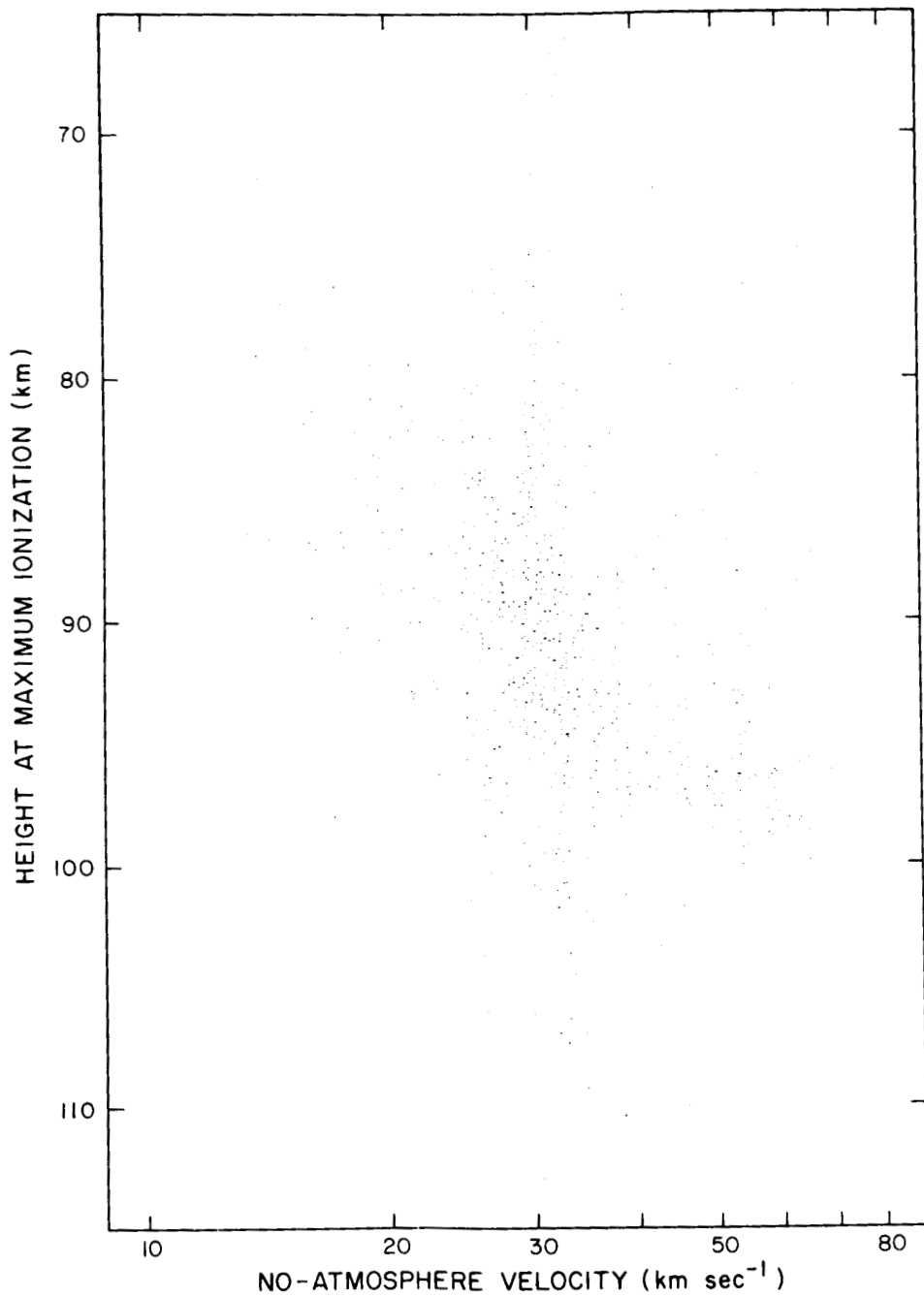
Figure 11-5. Height-velocity plot of 3008 radio meteors of the synoptic year with zenith distances less than 60° and perihelion distances between 0.25 and 0.50 a.u.

94
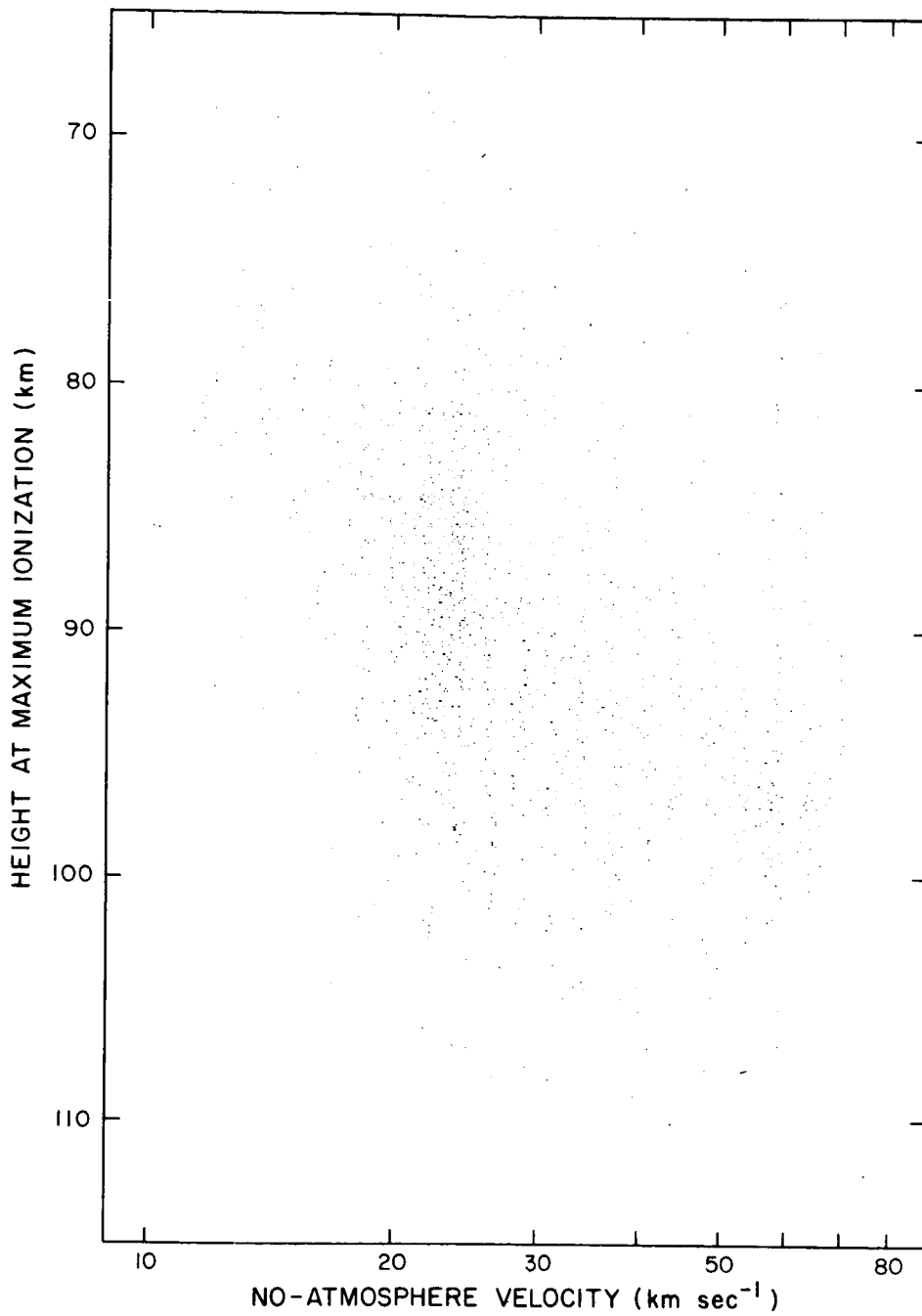
Figure 11-6. Height-velocity plot of 3256 radio meteors of the synoptic year with zenith distances less than 60° and perihelion distances between 0. 50 and 0. 75 a. u.
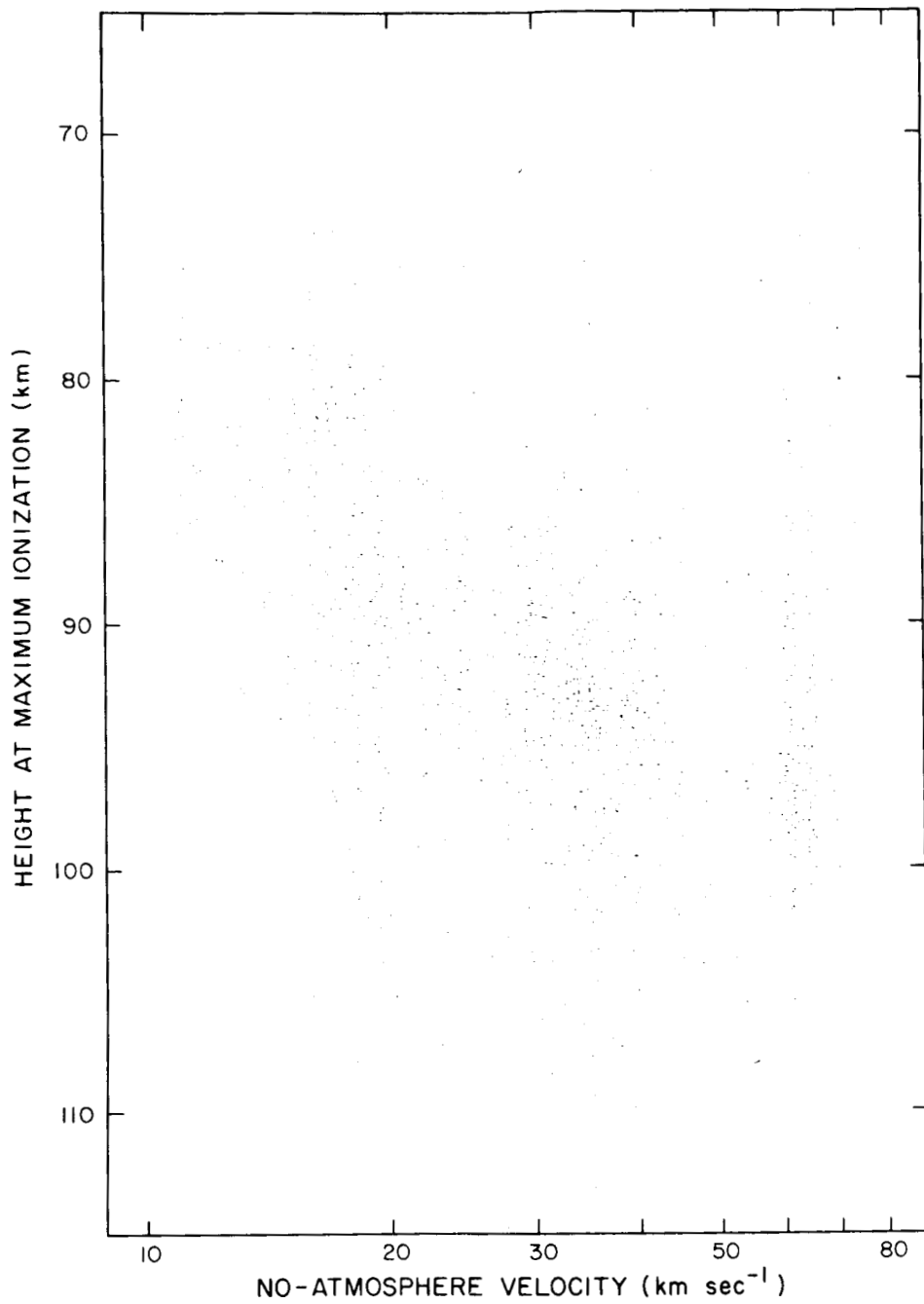
Figure 11-7.   Height-velocity plot of 7181 radio meteors of the synoptic year with zenith distances less than 60° and perihelion distances larger than 0.75 a.u.

Second, the vertical dispersion in the major concentration ($V_\infty < 48$ km sec^{-1}) is definitely larger than that in the minor concentration ($V_\infty > 48$ km sec^{-1}). From Ceplecha's results, we actually expect this, because the dispersion in the major concentration is a sum of the dispersions of the two groups ($A + C_1$) several kilometers apart, while the dispersion in the minor concentration represents that of the C_2 group alone.

Third, the minor concentration is more pronounced (relative to the major concentration) among the brighter meteors. Ceplecha found the same effect among the photographic meteors, although the magnitude scale was naturally shifted by about 10 mag.

Finally, Figure 11-4 (meteors with perihelion distances less than 0.25 a.u.) is the only one that shows but one cluster of meteors with the cutoff at $V_\infty \approx 60$ km sec^{-1} rather than 70 to 75 km sec^{-1} (as the other figures do). Among the photographic meteors, the group with $q < 0.25$ a.u. also indicated only one concentration; Ceplecha classified these meteors as forming an intermediate height level, which he called the B group.

11.3 A Height-Velocity Plot for Radio Streams

The last attempt to separate the discrete levels of radio meteor heights was a height-velocity plot for the meteor streams from the synoptic-year sample. Only streams with a mean error in height not exceeding $\pm$ 1 km were plotted. The idea was that with individual heights grouped into the stream heights, the dispersion within each of the two parallel levels A and C_1 may be lowered, so that the two levels show up. That did not, however, turn out to be the case, as can be seen from Figure 11-8. The major concentration remains structureless, despite a decrease in the overall dispersion along the height axis, as compared to the individual height-density plots. An interesting point, possibly worth pursuing further in the future, is a clear indication that the area of the main cluster with maximum heights (≈ 93 to 96 km at 25 km sec^{-1}, ≈ 95 to 98 km at 35 km sec^{-1}) is not populated by ecliptical high-eccentricity streams, as one might expect by analogy to Ceplecha's conclusions, but mostly by high-inclination, low-eccentricity streams. A question to be answered is whether a possible selection effect exists, since these streams consist of meteors whose radiants are most favorably located for the main beam of the radar system.
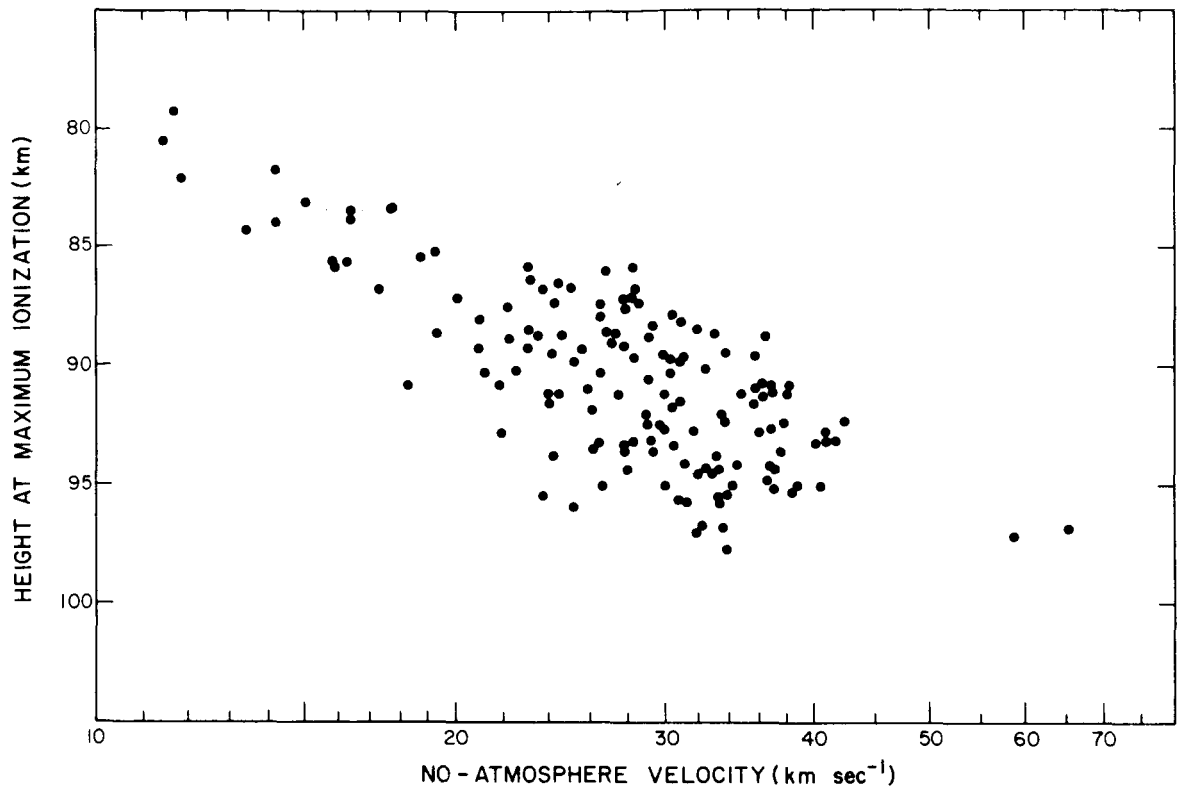
Figure 11-8. Height-velocity plot of 145 radio meteor streams with reliably deter-
mined mean heights (mean error in height not exceeding ±1.0 km).

Another feature of Figure 11-8 is a drastic drop in the height dispersion at
velocities below about 18 km sec^{-1}. At the other end of the velocity range, the C_2
group has reduced to only two points: the Orionids and the Perseids.

12. SPACE DENSITY IN RADIO METEOR STREAMS

12. 1 Mean Space Density in a Stream in Terms of the Sporadic Density

In Papers II and III, we derived the two parameters of the statistical model of meteor streams — the population coefficient Λ and the dispersion coefficient σ — for a number of streams from the 1961—1965 sample, and we commented that the population coefficient gives essentially the flux ratio of the stream meteors relative to the sporadic background in a limited vector space (i. e., the stream-to-background flux ratio of meteors from within a particular solid angle related to particular limits of the geocentric velocity). By varying the value of the D-test, we change the "volume" of the vector space and thereby can study the variations in the stream-to-background flux ratio along a given section of the earth's orbit. By extending the vector space to cover all directions and all velocities, we could derive the stream-to-background space-concentration ratio.

The parameters of the statistical model are derived from the cumulative D-distribution of meteors, not of meteor masses. This makes no difference within any stream, because the total range of D is then fairly narrow. Selection effects caused by both the observing conditions and the physical processes are, however, of considerable importance in assessing the overall concentration of meteoric matter in space, as shown elsewhere in this report.

The mean space density in a meteor stream, in units of the mean space density of the meteoric matter in the sporadic background, was derived by us with the use of the stream's population and dispersion coefficients and with the use of the overall distribution of the orbital elements of meteor masses from the synoptic year, corrected for all selection effects (see Figures 5-5 to 5-10). In Paper I, we defined the outer limit D_{II} of a stream by a condition of equal population of the stream and background meteors between $D = 0$ and $D = D_{II}$. The expression for D_{II} and its graph are also given in Paper I. Papers II and III list D_{II} for 83 streams of the 1961—1965 sample.

For each stream, a Monte Carlo method has been applied to simulate the distribution of 10,000 sporadic meteors of equal mass with orbital characteristics distributed as given in Figures 5-5 to 5-10. This distribution gives us the background noise for each stream in terms of the overall distribution of meteor masses. Specifically, for $D = D_{II}$, we can immediately find the fraction of the sporadic meteor masses that falls within D_{II} from the mean orbit of the stream. From the definition of D_{II}, this is also the fraction of the number of meteors (or meteor masses) of the stream that falls within D_{II}, which covers practically all the stream members. Since the space density is proportional to the total of meteor masses swept up by the earth within a certain period of time, this method gives us the space density in the meteor stream within D_{II} in terms of the overall space density of the sporadic background.

12.2 Space-Density Gradient in a Stream

In any meteor stream that can be distinguished from the sporadic background, there exists a measurable space-density gradient. The method described gives actually a lower limit for the space density in a stream, because D_{II} is much larger than the stream's characteristic dimension ($\approx \sigma\sqrt{2}$). We do not know the profiles of most streams, because there were gaps in the observing schedule, but we can estimate the density gradient from the shape of the D-distribution curves in the following way.

The number of meteors with $D < D_i$, $\mathcal{N}_s(D_i)$, swept by the earth during a pass through a stream is

$$\mathcal{N}_s(D_i) = \text{const} \cdot \rho(D_i) \, \frac{V_H}{V_E} \, W(D_i) \, \text{cosec} \, \epsilon \quad , \tag{12-1}$$

where $\rho(D_i)$ is the mean space density in the stream for $D \leq D_i$; $W(D_i)$ is the characteristic width of the stream for the same range in D; ϵ is the elongation of the corrected radiant from the apex of the earth's motion; and V_H and V_E are the comet's and earth's heliocentric velocities, respectively. For ρ independent of D, we would have from equation (12-1), $\mathcal{N}_s \sim W$. From Paper I, we know that the number of meteors would then vary as D^β (where $\beta \simeq 3.8$), so that $W \sim D^\beta$. In the case of a variable space density in the stream, equation (12-1) can be written thus:

$$\mathcal{H}_s(D_i) = \text{const} \cdot \rho(D_i) \ D_i^\beta \quad . \tag{12-2}$$

It is convenient to replace D_i as the argument by $E_i = D_i/(\sigma\sqrt{2})$ and to write, with the use of equation (6) of Paper I, the ratio of the mean space density in the stream within D_i to that within $\sigma\sqrt{2}$:

$$\frac{\rho(E_i)}{\rho(1)} = \frac{\mathcal{H}_s(E_i)}{\mathcal{H}_s(1)} \ E_i^{-3.8} = 2.34 \left[\text{erf}(E_i) - 1.13 \ E_i e^{-E_i^2} \right] E_i^{-3.8} \quad , \tag{12-3}$$

where

$$\text{erf}(E) = \frac{2}{\sqrt{\pi}} \int_0^E e^{-z^2} dz \quad . \tag{12-4}$$

The function $\rho(E)/\rho(1)$ is plotted in Figure 12-1. It can be shown that for $E \ll 1$, this expression simplifies to

$$\frac{\rho(E)}{\rho(1)} = 1.77 \ E^{-0.8} \quad , \tag{12-5}$$

and for $E \gg 1$, to

$$\frac{\rho(E)}{\rho(1)} = 2.34 \ E^{-3.8} \quad . \tag{12-6}$$

Also plotted in Figure 12-1 is the relative number of meteors in a stream as a function of E. We note that the statistical model predicts that only 0.1% of the total mass of a stream move in orbits with $D \lesssim 0.15 \ \sigma$, so that the mean density within $E \approx 0.1$ is perhaps a realistic estimate for the actual maximum central space density in meteor streams.

12.3 Numerical Results

The results of the Monte Carlo simulation, described earlier in this section, and those of the subsequent space-density calculations are summarized in Table 12-1 for several of the more important streams of the 1961-1965 sample.

We conclude that mean space densities in meteor streams are small compared with the space density of the surrounding sporadic background, but that central densities in some major streams can significantly exceed the background density.
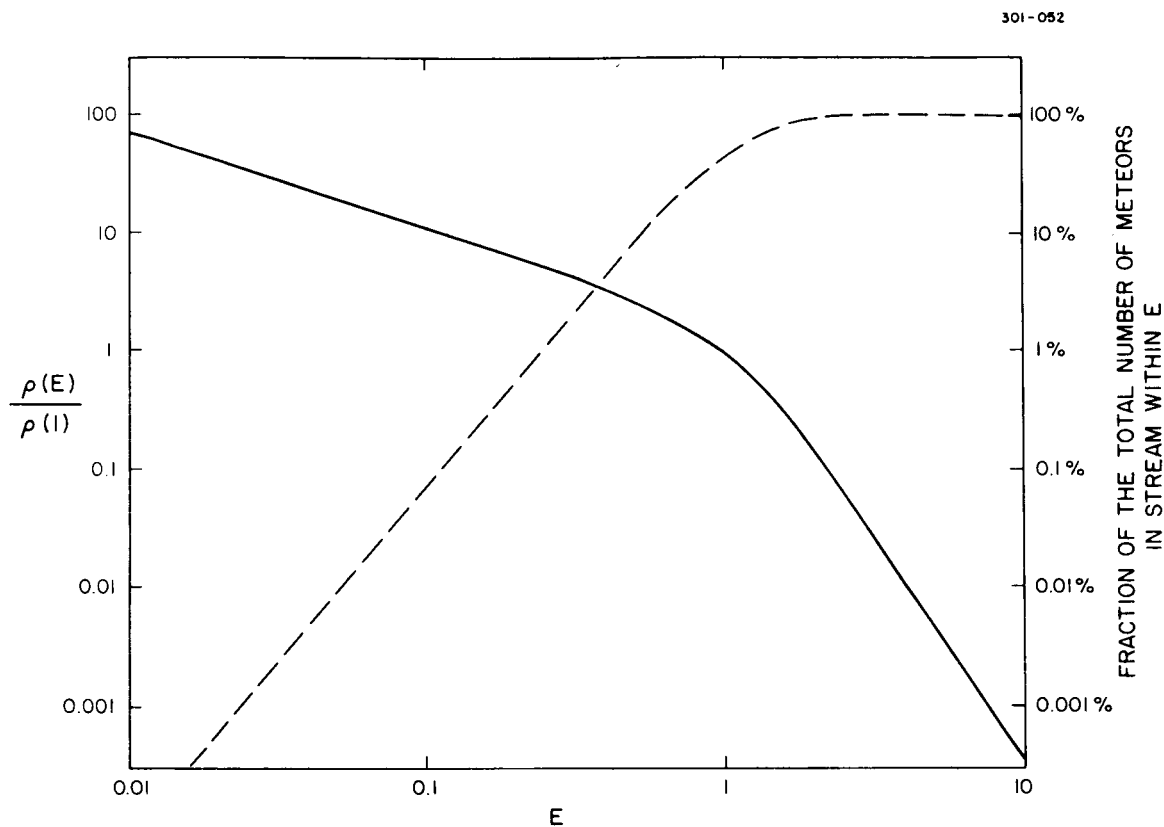
Figure 12-1. Space-density variation (solid curve, left-hand scale) in meteor streams versus $E = D/(\sigma\sqrt{2})$ (σ is the dispersion coefficient) predicted from the statistical model, and a relative cumulative number of a stream's members (dashed curve, right-hand scale) as a function of E.

With an average overall space density of 4×10^{-22} g cm^{-3} in the vicinity of the earth (see Section 7.3), the results of Table 12-1 suggest that mean densities in meteor streams are typically several times 10^{-24} g cm^{-3} and that the central density in some streams could be as high as almost 10^{-20} g cm^{-3}. In meteoric storms, the density must be still at least 1 to 2 orders of magnitude higher, i.e., some 10^{-19} to 10^{-18} g cm^{-3}.

Table 12-1. Mean and central space densities in radio meteor streams.

Stream	Space density in stream (in units of sporadic density $\simeq 4 \times 10^{-22}$ g cm^{-3})	
	mean (at $D \leqq D_{II}$)	central (at $D \lesssim 0.15\ \sigma$)
Scorpiids-Sagittariids	0.06	30
Geminids	0.005	10
σ Capricornids	0.05	8
Piscids	0.03	3
Monocerids	0.01	3
Taurids	0.02	2
Southern Arietids	0.02	2
July Draconids	0.006	2
Triangulids	0.02	1
o Cetids	0.006	1
Southern δ Aquarids	0.003	1
Lyrids	0.0002	0.4
Arietids (Daytime)	0.002	0.3
χ Orionids	0.003	0.2
ζ Perseids	0.002	0.2
β Taurids	0.002	0.1
α Leonids	0.002	0.1
Southern Virginids	0.001	0.05
Quadrantids	0.00002:	0.01:
Orionids	0.000002:	0.005:

12.4 Space Density from Cometary Production Rates of Solid Material; Comparison of the Two Methods

It is of interest to compare the above conclusions with independent evidence available from the study of cometary type II tails. Finson and Probstein's (1968a) model of dust comets makes it possible to estimate the total mass of the solid material lost

by a comet during an approach to the sun. The results from the regular dust tails are unfortunately inconclusive for the particle sizes that produce radio meteors ($\approx$ 0.1 cm in diameter), since the method is based on photometric considerations and the effect from heavy particles is always masked by the much stronger light-scattering power of micron and submicron particles. Consequently, the size-distribution function, which is also determined by the Finson-Probstein model, is uncertain for large masses. However, the "spike" tail of comet Arend-Roland 1957 III, studied by Finson and Probstein (1968b), appeared to be composed of only heavy particles ($\gtrsim$ 0.01 cm in diameter). The two authors showed that the spike had been formed as a result of an outburst about 2 months before the comet reached the perihelion point and that the total mass ejected during the outburst had been of the order of 10^{13} to 10^{14} g. It seems that this is the only quantitative estimate to date of the emission rate of dust particles approaching the radio meteor range of masses.

With a characteristic dispersion in their velocity distribution along the orbit of some 10 m $\sec^{-1}$, the particles ejected from a short-period comet in an isolated outburst would form, after one revolution around the sun, a filament some 0.2 a.u. long. With a width of $\approx$ 0.001 a.u. (corresponding to the duration of less than 0.1 day, typical for meteoric storms), the volume of the filament is $\approx 5 \times 10^{32}$ cm^3, and with the mass of $\approx 10^{14}$ g, its space density comes out to exceed 10^{-19} g cm^{-3}, in total agreement with the estimate given in the previous section.

To estimate the space density in old streams dispersed along the whole arc of orbit around the sun, we can adopt the orbital length $\approx$ 15 a.u. and the width $\approx$ 0.5 a.u., so that the volume of the stream is $\approx 10^{40}$ cm^3. The total mass involved can be inferred either from the order-of-magnitude estimate of the age ($\approx 10^3$ revolutions), assuming that the comet is ejecting meteoroids at a more or less constant rate, or from the total mass of the parent comet (if the latter is presumed defunct), assuming that a significant fraction of the comet disintegrated into the stream. Both estimates give fairly consistently a mass of $\approx 10^{16}$ to 10^{17} g and a space density $\approx 10^{-23}$ to 10^{-24} g cm^{-3}, again consistent with the results of Section 12.3.

13. REFERENCES

Baggaley, W. J., 1970, The determination of the initial radius of meteor trains. Monthly Notices Roy. Astron. Soc., vol. 147, pp. 231-243.

Briggs, R. E., 1962, Steady-state distribution of meteoric particles under the operation of the Poynting-Robertson effect. Astron. Journ., vol. 67, pp. 710-723.

Ceplecha, Z., 1967, Classification of meteor orbits. Smithsonian Contr. Astrophys., vol. 11, pp. 35-60.

Ceplecha, Z., 1968, Discrete levels of meteor beginning height. Smithsonian Astrophys. Obs. Spec. Rep. No. 279, 54 pp.

Cook, A. F., 1970, Discrete levels of beginning height of meteors in streams. Smithsonian Astrophys. Obs. Spec. Rep. No. 324, 22 pp.

Cook, A. F., 1972, A working list of meteor streams. In Meteor Research Program, Final Report on Contract NSR 09-015-033, NASA CR-2109, pp. 153-166.

Cook, A. F., Flannery, M. R., Levy II, H., McCrosky, R. E., Sekanina, Z., Shao, C.-Y., Southworth, R. B., and Williams, J. T., 1972, Meteor Research Program. Final Report on Contract NSR 09-015-033, NASA CR-2109, 166 pp.

Elford, W. G., 1964, Calculation of the response function of the Harvard Radio Meteor Project radar system. Harvard-Smithsonian Radio Meteor Project Res. Rep. No. 8, 51 pp.

Finson, M. L., and Probstein, R. F., 1968a, A theory of dust comets. I. Model and equations. Astrophys. Journ., vol. 154, pp. 327-352.

Finson, M. L., and Probstein, R. F., 1968b, A theory of dust comets. II. Results for comet Arend-Roland. Astrophys. Journ., vol. 154, pp. 353-380.

Hawkins, G. S., 1963, The Harvard Radio Meteor Project. Smithsonian Contr. Astrophys., vol. 7, pp. 53-62.

Hoffmeister, C., 1948, Meteorströme. Werden & Wirken, Weimar.

Jacchia, L. G., 1958, On two parameters used in the physical theory of meteors. Smithsonian Contr. Astrophys., vol. 2, pp. 181-187.

Kinard, W. H., and Soberman, R. K., 1972, Sci. News, vol. 101, p. 391.

Kolomiets, G. I., 1971, The measurements of the initial radii of meteor trails. Astron. Tsirk., no. 625, pp. 7-8.

Lindblad, B. A., 1971, A computer stream search among 2401 photographic meteor orbits. Smithsonian Contr. Astrophys., vol. 12, pp. 14-24.

Manning, L. A., 1958, The initial radius of meteoritic ionization trails. Journ. Geophys. Res., vol. 63, pp. 181-196.

Moisya, R. I., Melnik, V. J., and Kolomiets, G. I., 1970, Some results of meteor observations on three wavelengths. Vestnik Kiev, Univ. Ser. Astron. No. 12, pp. 57-60.

Öpik, E. J., 1955, Meteors and the upper atmosphere. Irish Astron. Journ., vol. 3, pp. 165-181.

Roosen, R. G., 1970, The gegenschein and interplanetary dust outside the earth's orbit. Icarus, vol. 13, pp. 184-201.

Sekanina, Z., 1970a, Statistical model of meteor streams. I. Analysis of the model. Icarus, vol. 13, pp. 459-474.

Sekanina, Z., 1970b, Statistical model of meteor streams. II. Major showers. Icarus, vol. 13, pp. 475-493.

Sekanina, Z., 1973, Statistical model of meteor streams. III. Stream search among 19303 radio meteors. Icarus, vol. 18, pp. 253-284.

Southworth, R. B., 1967, Space density of radio meteors. In The Zodiacal Light and the Interplanetary Medium, ed. by J. L. Weinberg, NASA SP-150, pp. 179-188.

Southworth, R. B., 1973, Recombination in radar meteors. In The Evolutionary and Physical Properties of Meteoroids, Proc. IAU Colloq. No. 13, ed. by A. F. Cook, C. L. Hemenway, and P. M. Millman, NASA SP-319, in press.

Southworth, R. B., and Hawkins, G. S., 1963, Statistics of meteor streams. Smithsonian Contr. Astrophys., vol. 7, pp. 261-285.

Whipple, F. L., 1940, Photographic meteor studies. III. The Taurid meteor shower. Proc. Amer. Phil. Soc., vol. 83, pp. 711-745.

Whipple, F. L., 1967, On maintaining the meteoritic complex. In The Zodiacal Light and the Interplanetary Medium, ed. by J. L. Weinberg, NASA SP-150, pp. 409-426.